



UNIVERSIDADE ESTADUAL DE CAMPINAS
FACULDADE DE CIÊNCIAS MÉDICAS

BRUNNO MACHADO DE CAMPOS

CONECTIVIDADE FUNCIONAL E ESTRUTURAL EM PACIENTES COM
EPILEPSIA FOCAL

*FUNCTIONAL AND STRUCTURAL CONNECTIVITY IN PATIENTS WITH FOCAL
EPILEPSY*

CAMPINAS

2016

BRUNNO MACHADO DE CAMPOS

CONECTIVIDADE FUNCIONAL E ESTRUTURAL EM PACIENTES COM
EPILEPSIA FOCAL

*FUNCTIONAL AND STRUCTURAL CONNECTIVITY IN PATIENTS WITH FOCAL
EPILEPSY*

Tese apresentada à Faculdade de Ciências
Médicas da Universidade Estadual de Campinas
como parte dos requisitos exigidos para a
obtenção do título de Doutor em Ciências.

*Thesis presented to the Health Science School of
the University of Campinas as a part of the
required requisites to obtain the title of Doctor of
Science.*

ORIENTADOR: PROF. DR. FERNANDO CENDES
COORIENTADORA: PROFA. DRA. ANA CAROLINA COAN

ESTE EXEMPLAR CORRESPONDE À VERSÃO
FINAL DA TESE DEFENDIDA PELO
ALUNO BRUNNO MACHADO DE CAMPOS, ORIENTADO PELO
PROF. DR. FERNANDO CENDES.

CAMPINAS

2016

Agência(s) de fomento e nº(s) de processo(s): Não se aplica.

Ficha catalográfica
Universidade Estadual de Campinas
Biblioteca da Faculdade de Ciências Médicas
Maristella Soares dos Santos - CRB 8/8402

C157c Campos, Brunno Machado de, 1988-
Conectividade funcional e estrutural em pacientes com epilepsia focal /
Brunno Machado de Campos. – Campinas, SP : [s.n.], 2016.

Orientador: Fernando Cendes.
Coorientador: Ana Carolina Coan.
Tese (doutorado) – Universidade Estadual de Campinas, Faculdade de
Ciências Médicas.

1. Epilepsia. 2. Imagem de difusão por ressonância magnética. 3.
Mapeamento encefálico. I. Cendes, Fernando, 1962-. II. Coan, Ana
Carolina, 1980-. III. Universidade Estadual de Campinas. Faculdade de
Ciências Médicas. IV. Título.

Informações para Biblioteca Digital

Título em outro idioma: Functional and structural connectivity in patients with focal epilepsy

Palavras-chave em inglês:

Epilepsy

Diffusion magnetic resonance imaging

Brain mapping

Área de concentração: Fisiopatologia Médica

Titulação: Doutor em Ciências

Banca examinadora:

Fernando Cendes [Orientador]

Luiz Eduardo Gomes Garcia Betting

Carlos Eduardo Soares Silvado

Roberto Jose Maria Covolan

Rickson Coelho Mesquita

Data de defesa: 01-11-2016

Programa de Pós-Graduação: Fisiopatologia Médica

BANCA EXAMINADORA DA DEFESA DE DOUTORADO

BRUNNO MACHADO DE CAMPOS

ORIENTADOR: PROF. DR. FERNANDO CENDES

COORIENTADORA: PROFA. DRA. ANA CAROLINA COAN

MEMBROS:

1. PROF. DR. FERNANDO CENDES

2. PROF. DR. LUIZ EDUARDO GOMES GARCIA BETTING

3. PROF. DR. CARLOS EDUARDO SOARES SILVADO

4. PROF. DR. ROBERTO JOSE MARIA COVOLAN

5. PROF. DR. RICKSON COELHO MESQUITA

Programa de Pós-Graduação em Fisiopatologia Médica da Faculdade de Ciências Médicas da Universidade Estadual de Campinas.

A ata de defesa com as respectivas assinaturas dos membros da banca examinadora encontra-se no processo de vida acadêmica do aluno.

Data: DATA DA DEFESA 01/11/2016

AGRADECIMENTOS

Durante a realização deste trabalho, ao longo dos últimos três anos e meio, inúmeras pessoas foram importantes e me auxiliaram direta ou indiretamente. Ao término desta importante etapa, não posso deixar de mencionar nomes essenciais na construção de minhas bases educacionais e éticas, pessoas às quais sou profundamente grato e para as quais vou sempre manter profundo sentimento de gratidão:

Minha família, minha esposa Gabriela K.F. Castanho, que nos últimos anos me apoiou e estimulou de forma continuada e intensiva e que sempre me dá força para crescer, com apoio, compreensão e carinho. Meu filho Breno C. M de Campos, que ao longo deste ano decisivo, ainda na barriga da mãe e agora recém-nascido, foi grande estímulo e enorme motivo de alegria, me impulsionando na execução de minhas tarefas com ainda mais esmero e energia. Meus pais, Walter M. de Campos Jr. e Maria Cristina H. M. de Campos como os grandes responsáveis pela minha formação educacional e pessoal, foram os exemplos e os guias que formaram com carinho e orientação o ser humano que sou hoje. Minha irmã Maria Paula M. de Campos que é exemplo de determinação, ética e caráter.

Em minha vida acadêmica, existem pessoas de grande importância que me auxiliaram e orientaram. Pessoas que respeitarei por toda a minha vida e que terão para sempre minha gratidão, '*o Brunno nunca esquece*': O prof. Fernando Cendes, com o qual tenho o prazer e a oportunidade de trabalhar e conviver já há 7 anos, e que é exemplo pessoal e profissional, como orientador atencioso e preciso e como chefe humano e justo que me possibilita enormes oportunidades que veem mudando minha vida de maneira inimaginável. A profa. Ana Carolina Coan que no último semestre de graduação acreditou em mim, e desde então é modelo ético e profissional, me guiando e direcionando nas atitudes do cotidiano e da prática acadêmica e que ainda, neste trabalho, exerceu papel indispensável e decisivo como co-orientadora.

Aos colegas de laboratório, que dia-a-dia, ao longo de todos estes anos, foram estímulo e escape, além de intermináveis fontes de ajudas e ensinamentos.

Por fim, agradeço a Universidade Estadual de Campinas, representando toda a estrutura de pessoal e física que me possibilitou exercer com tranquilidade e eficiência meu trabalho.

RESUMO

Introdução: Estudos recentes demonstram que as epilepsias são doenças relacionadas a alterações de redes neuronais. Técnicas de neuroimagem funcional e de difusão aliadas a avançados métodos de pós-processamento computacional permitem avaliações de conectividade funcional e estrutural do cérebro fornecendo informações sobre os padrões organizacionais das redes associadas. Este estudo visa avaliar a conectividade estrutural e funcional em pacientes com epilepsias focais, caracterizando as alterações de pacientes com epilepsia de lobo temporal mesial (ELTM) associada à esclerose hipocampal (EH) e comparando com outras epilepsias focais.

Métodos: Instrumentações de software foram desenvolvidas para as análises realizadas: 1- de conectividade estrutural e 2- de conectividade funcional. Para avaliação da conectividade estrutural, foram selecionados três grupos de pacientes (ELTM-EH, ELT-não lesional [NL] e epilepsia de lobo frontal associada a displasia cortical focal [ELF-DCF]) e um grupo controle. Metodologia de tractografia semiautomática avaliou a anisotropia fracionada (FA), difusividade radial (RD) e axial (AD) de quatro fascículos: 1-uncinado; 2-fórnix; 3-fronto-occipital inferior; 4-cíngulo. As análises de conectividade funcional foram realizadas comparando pacientes de ELTM-EH com lateralização à direita (D-ELTM) e à esquerda (E-ELTM) e um grupo controle. Setenta regiões de interesse representando 12 redes funcionais foram usadas para análise de criação das matrizes de adjacência. O segundo nível foi realizado comparando pacientes e controles.

Resultados: Análise macroestrutural de substância branca (SB) mostrou alterações (principalmente ipsilaterais) para ELTM-EH e ELF-DCF. A análise microestrutural mostrou alterações em parâmetros de difusão para os mesmos grupos. Os pacientes ELT-NL não apresentaram alterações em nenhuma das análises de integridade estrutural. Comparados ao grupo controle, os grupos D-ELTM e E-ELTM apresentaram alterações de conectividade funcional. Das 12 redes, apenas *auditory* e *visual* não apresentaram alterações em ambos os grupos. Para D-ELTM, a anterior salience e a *sensorimotor* também foram preservadas. Pacientes de E-ELTM apresentaram alterações mais difusas, afetando os dois hemisférios de forma mais evidente.

Discussão e conclusão: Pacientes com epilepsias focais apresentam alterações de conectividade funcional e estrutural. Pacientes com ELTM-EH apresentaram piores resultados de alterações estruturais e vasta rede de alterações quando comparados a frontais ou não lesionais. Adicionalmente, apresentam complexa rede de alterações funcionais. Pacientes com E-ELTM apresentaram de alterações funcionais mais complexo quando comparados aos com D-ELTM. O desenvolvimento de toolboxes para as modalidades metodológicas propostas possibilitaram padronização e eficiência na análise dos dados.

Palavras-chave: Epilepsia. MRI de Difusão. Mapeamento Cerebral Funcional.

ABSTRACT

Introduction: Recent studies has shown that epilepsies are diseases related to neuro networks alterations. Functional and diffusion neuroimaging techniques explored by advanced computational methodologies, allows the functional and structural brain connectivity evaluation providing information regarding the brain networks behavior. This project aim to evaluate the functional and the structural connectivity in patients with temporal lobe epilepsy comparing its alteration patterns with other focal epilepsies.

Methods: We developed software resources to perform the analysis: 1- Structural connectivity and 2- functional connectivity. For structural evaluations, three groups of patients were included (mesial temporal lobe epilepsy [MTLE] associated to hippocampal sclerosis [HS], non-lesional temporal lobe epilepsy [TLE-NL] and frontal lobe epilepsy associated to focal cortical dysplasia [FLE-FCD]) and a control group. We performed a semi-automatic tractography procedure to evaluate the fractional anisotropy (FA), the radial diffusivity (RD) and the axial diffusivity (AD) of four anatomic relevant fasciculi: uncinata, body of fornix, inferior fronto-occipital and body of cingulum. We performed functional connectivity analysis comparing patients with left and right MTLE-HS and controls. We used 70 regions of interest (ROIs) from 12 functional networks to compute the connectivity adjacency matrices and performed a second level analysis to compare patients and controls groups.

Results: The macrostructural white matter (WM) analysis showed alterations (manly ipsilateral) on MTLE-HS and FLE-FCD. The microstructural WM analysis presented alterations on diffusion parameters for the same groups. Patients with TLE-NL showed no changes for both structural analysis. Compared to the control group, the R-MTLE and L-MTLE groups showed functional connectivity alterations. From the 12 studied networks, only the auditory and the visual networks were preserved on both groups. For the R-MTLE patients, the anterior salience and the sensorimotor networks were also not affected. Patients with L-MTLE showed more diffuse alterations, more evidently affecting both hemispheres.

Discussion and conclusion: The study and the proposal methodology were effective for the identifications and characterization of functional and structural connectivity alterations in patients with focal epilepsies. The MTLE-HS showed worse widespread

structural alterations compared to the FLE and TLE-NL. Additionally, they presented complex and widespread functional networks abnormalities. Patients with L-MTLE demonstrated worse and more bilaterally affected pattern of alterations when compared to R-MTLE. The development of toolboxes to perform the proposal methodology enabled the standardization and high data analysis efficiency, throughout clear procedures.

Key words: Epilepsy. MRI. Diffusion Magnetic Resonance Imaging. MRI. Brain Mapping.

LISTA DE ILUSTRAÇÕES

Fig. 1: reconstrução tridimensional do cérebro. Destacado em azul claro, o lobo temporal; em azul escuro porção mesial do lobo temporal; em vermelho os hipocampi.	17
Fig. 2: Fluxograma da resposta hemodinâmica do cérebro mediante a um estímulo pontual.	20
Fig. 3: Exemplo de series temporais correlacionadas. As regiões do exemplo, representadas pelas séries temporais destacadas com os quadros vermelhos, estariam funcionalmente conectadas.	21
Fig. 4: Representação real de um resultado de conectividade funcional. No exemplo, identificam-se as regiões que caracterizam a DMN.	23
Fig. 5: Exemplos de imagens com técnicas de difusão. Na esquerda, extensa tractografia cerebral e na direita imagem de difusão com codificação direcional de cor.	24
Fig. 6: Representação esquemática dos conceitos básicos em difusão. Na esquerda, representação do corpo do neurônio e indicação da região do cérebro que constitui, a SC. Na direita, representação artística do axônio, com indicação da região do cérebro que constitui, a SB.	25
Fig. 7: Duas representações esquemáticas para o cálculo do FA. A da esquerda ilustra os vetores de uma região com grande anisotropia. Na direita, ilustração dos vetores de região com difusão praticamente isotrópica. λ_1 representam o deslocamento na direção preferencial, portanto o maior deslocamento. λ_2 e λ_3 representam os deslocamentos perpendiculares ao deslocamento preferencial.	26
Fig. 8: Interface gráfica do software NCA. No topo janela principal, e na parte inferior, interface da modalidade de processamento e tractografia de DTIs.	33
Fig. 9: Template brasileiro desenvolvido no projeto. Na esquerda imagem de não-difusão associada e na direita, o template com a codificação direcional em cores.	34
Fig. 10: Exemplo real de estratégia normalizada para tractografia. No exemplo, estratégia bilateral para o fascículo uncinado.	34
Fig. 11: Fluxograma do pré-processamento e das etapas do método semiautomático de tractografia.	35
Fig. 12: Interface gráfica do software UF ² C, demonstrando a janela principal, de boas-vindas, do programa.	36

Fig. 13: Imagem do website do UF ² C: http://www.lni.hc.unicamp.br/app/uf2c/	40
Fig. 14: Dados geográficos rastreáveis dos downloads realizados no site. O procedimento exclui downloads automáticos realizados por repositórios de arquivos e ainda downloads consecutivos de um mesmo usuário.	41

LISTA DE ABREVIATURAS E SIGLAS

AD: do inglês, *axial diffusivity* ou difusividade axial

AED: do inglês, *antiepileptic drug* ou droga antiepiléptica

ATP: adenosina trifosfato

BoC: do inglês, *body of cingulum* ou corpo do cíngulo

BoF: do inglês, *body of fornix* ou corpo de fórnix

BOLD: do inglês, *Blood-Oxygenation-Level Dependent* ou dependente do nível de oxigênio no sangue

DCF: displasia cortical focal

DTI: do inglês, *diffusion tensor image* ou imagem por tensores de difusão

EEG: eletroencefalografia

EH: esclerose hipocampal

ELF: epilepsia de lobo frontal

ELT: epilepsia de lobo temporal

ELTM: epilepsia de lobo temporal mesial

EPI: do inglês, *echo planar image* ou imagem eco planar

FA: do inglês, *fractional anisotropy* ou anisotropia fracionada

FCD: do inglês, *focal cortical dysplasia* ou displasia cortical focal

FDG: Fluorodesoxiglicose

FLE: do inglês, *frontal lobe epilepsy* ou epilepsia de lobo frontal

FOV: do inglês, *field of view* ou campo de visão

HS: do inglês, *hippocampal sclerosis* ou esclerose hipocampal

IFO: do inglês, *inferior frontal occipital* ou fascículo fronto-occipital

IRM: imagem por ressonância magnética

MRI: do inglês, *magnetic resonance image* ou imagem por ressonância magnética

NCA: do inglês, Neuroimaging Computational Analysis

NL: do inglês, *non-lesional* ou não-lesional

PET: do inglês, *positron emission tomography* ou tomografia por emissão de pósitron

RD: do inglês, *radial diffusivity* ou difusividade radial

RF: radiofrequência

RM: ressonância Magnética

RMf: ressonância magnética funcional

SB: substância branca

SC: substância cinzenta

SPECT: do inglês, *single-proton emission computed tomography* ou tomografia computadorizada por emissão de fóton único

SPM: do inglês, Statistical Parametric Mapping©

TE: tempo ao eco

TLE: do inglês, *temporal lobe epilepsy* ou epilepsia de lobo temporal

TR: tempo de repetição

UF: do inglês, *uncinate fasciculus* ou fascículo uncinado

UF²C: do inglês, User Friendly Functional Connectivity

VBM: do inglês, *voxel-based morphometry* ou morfometria baseada em voxel

WM: do inglês, *white matter* ou substância branca

Sumário

1. INTRODUÇÃO	16
1.1 EPILEPSIA	16
1.2 RESSONÂNCIA MAGNÉTICA	18
1.3 RESSONÂNCIA MAGNÉTICA FUNCIONAL	19
1.4 CONECTIVIDADE FUNCIONAL	21
1.5 TENSORES DE DIFUSÃO E CONECTIVIDADE ESTRUTURAL	24
2. OBJETIVOS	29
3. METODOLOGIA	30
3.1 SELEÇÃO DOS SUJEITOS DA PESQUISA	30
3.2 PROTOCOLOS DE IMAGENS	31
3.3 DESENVOLVIMENTO DE SOFTWARES	32
3.3.1 NCA: NEUROIMAGING COMPUTATIONAL ANALYSIS	33
3.3.2 UF²C: USER FRIENDLY FUNCTIONAL CONNECTIVITY	36
4. RESULTADOS	39
4.1 DESENVOLVIMENTO DE SOFTWARE	39
4.1.1 NCA - NEUROIMAGING COMPUTATIONAL ANALYSIS	39
4.1.2 UF²C – USER FRIENDLY FUNCTIONAL CONNECTIVITY	40
4.2 ARTIGOS	42
4.2.1 ARTIGO 1: ANÁLISE DE CONECTIVIDADE ESTRUTURAL	42
4.2.2 ARTIGO 2: ANÁLISE DE CONECTIVIDADE FUNCIONAL	62
5. DISCUSSÃO GERAL	95
6. CONCLUSÃO	98
REFERÊNCIAS	99
APÊNDICES	103

APÊNDICE 1: TUTORIAL DO UF²C	103
ANEXO 1: OS DOCUMENTOS DE APROVAÇÃO NO COMITÊ DE ÉTICA DA UNICAMP	146
ANEXO 2: TERMO DE CONSENTIMENTO LIVRE ESCLARECIDO	149
ANEXO 3: PERMISSÕES EDITORIAIS	152
ARTIGO 1	152
ARTIGO 2	156
ANEXO 4: DECLARAÇÃO	157

1. INTRODUÇÃO

A neurociência é a área da ciência interdisciplinar que estuda o sistema nervoso em diferentes aspectos através de diversas opções metodológicas e ferramentas investigatórias. Nas últimas décadas, com o aperfeiçoamento das técnicas de imagem *in vivo*, como PET (Tomografia por Emissão de Póstron) e IRM (imagem por ressonância magnética), tornou-se possível a utilização destas ferramentas como instrumentos diagnósticos e de pesquisa clínica, capazes de quantificar em diferentes aspectos o tecido e as funções nervosas com alta precisão, de forma não invasiva.

1.1 EPILEPSIA

Dentre as doenças mais estudadas por estes avanços, os estudos da epilepsia destacam-se devido à relevância social da doença, e aos riscos associados a ela. Epilepsia é um distúrbio cerebral caracterizado por uma predisposição persistente a gerar crises epilépticas e pelas consequências neurobiológicas, cognitivas, psicológicas e sociais dessa condição^{1,2}. As epilepsias englobam uma ampla variedade de sintomas decorrentes de funções cerebrais alteradas em decorrência de um grande número de processos patológicos^{2,3}.

Crise epiléptica é a manifestação clínica ou eletrográfica oriunda de disfunção temporária e sincronizada de uma rede de neurônios causada por malformações celulares ou disfunções das células nervosas nas ações excitatórias ou inibitórias. A crise epiléptica ocorre quando há descarga elétrica anormal excessiva e transitória das células nervosas, decorrente das correntes iônicas através da membrana celular. A atividade elétrica pode ser registrada com equipamento de eletroencefalografia (EEG), com o qual é possível identificar padrões de onda (em amplitude, forma e frequência) característicos desta patologia e denominados de atividade epileptiforme^{4,5,6}. Por definição, as crises podem ser focais, quando envolvem parte do córtex ou generalizadas, quando acometem áreas extensas que envolvem os dois hemisférios cerebrais.

Dentre os subtipos, a epilepsia de lobo temporal mesial associada a esclerose hipocampal (ELTM-EH) é o mais prevalente em pacientes adultos, sendo que ~70% dos casos são refratários ao tratamento medicamentoso com elevada prevalência de comorbidades. O bom encaminhamento do tratamento e a eficácia da intervenção

médica, dependem da análise clínica e eletrográfica, além de conhecimento das redes neurais e regiões cerebrais envolvidas no processo patológico em cada caso.

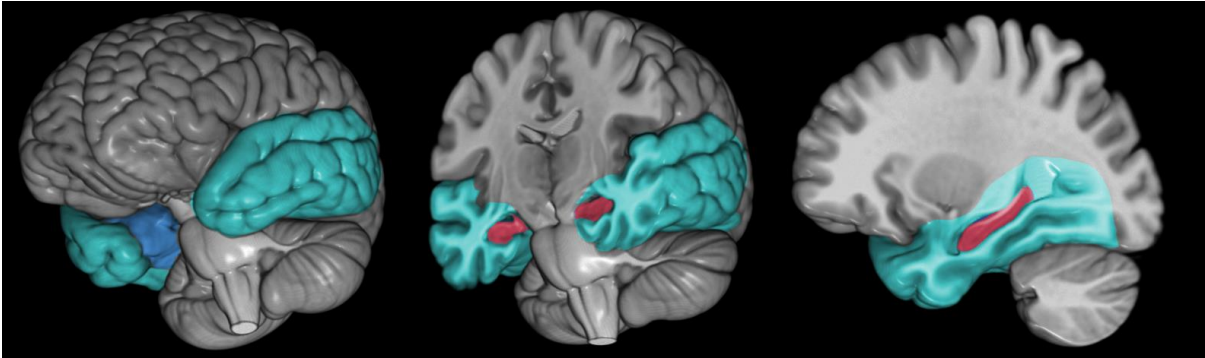


Fig. 1: Reconstrução tridimensional do cérebro. Destacado em azul claro, o lobo temporal; em azul escuro porção mesial do lobo temporal; em vermelho os hipocampos.

Classificações recentes definem a epilepsia como doença de redes⁷. Embora possa ter origem focal, gera distúrbios estruturais e funcionais abrangentes, comumente associados ao recrutamento anormal de redes funcionais, relacionadas ou não a redes de alterações estruturais. Estas anormalidades poderiam estar associadas aos fenômenos ictais (evento de crise) e interictais (eventos eletrográficos em períodos entre crises), ocasionando alteração de memória, depressão e ansiedade^{7,8}.

1.2 RESSONÂNCIA MAGNÉTICA

Modernos métodos de obtenção imagens tomográficas também são utilizados como ferramenta de auxílio nas definições das síndromes epiléticas, uma vez que possibilitam a localização de lesões ou malformações estruturais que possam ser visíveis a olho nu e às quais a síndrome epilética pode estar associada. As imagens por RM possibilitam aquisição de cortes anatômicos através de informações geradas a partir da resposta energética emitida pelos núcleos do hidrogênio do corpo humano, após serem excitados por um sistema emissor de radiofrequência (RF). Na década de 1980, os primeiros escâneres comerciais com capacidade de realizar exames de todo o corpo começaram a ser comercializados, viabilizando também o uso dos equipamentos na clínica experimental.

1.3 RESSONÂNCIA MAGNÉTICA FUNCIONAL

A partir de 1990, dentre os métodos aplicados à neurociência, destacam-se as pesquisas científicas aplicadas às funções cerebrais com a técnica de ressonância magnética funcional (RMf). Desde então, a técnica tem sido aprimorada e realizada de forma satisfatória em vários centros do mundo, tornando-se atualmente uma das mais importantes ferramentas da neurologia experimental uma vez que possibilita estimar e mapear da atividade metabólica do cérebro de forma não invasiva⁹. Para inferir mudanças locais na atividade neural, a RMf utiliza a resposta metabólica e hemodinâmica do organismo a estímulos pré-definidos ou inclusive às atividades espontâneas do córtex. O objetivo do estudo de imagens funcionais é obter dados que sejam sensíveis ao funcionamento do cérebro. Existem métodos eletrofisiológicos invasivos que medem a atividade neural diretamente, entretanto, a RMf, através de efeitos relacionados à atividade neural, pode quantificá-la e localizá-la de forma não invasiva e sem uso de radiação ionizante ou contrastes intravenosos¹⁰. O sinal contrastante em RMf é dependente do nível de oxigenação do sangue e é chamado sinal BOLD (*Blood-Oxygenation-Level Dependent*).

O sinal BOLD está associado à reação hemodinâmica do organismo, mediante a ativação cortical e baseia-se em princípios fisiológicos e físicos. O cérebro não armazena energia, o ATP (adenosina trifosfato), precisa ser formado a partir da oxidação da glicose presente no sangue e estudos mostram que este consumo se concentra em regiões com atividade neural aumentada. O aumento do fluxo sanguíneo em regiões ativas do cérebro acarreta em aumento do transporte de glicose e oxigênio a fim de suprir as necessidades energéticas das células. Neste processo, há um atraso entre o início na demanda energética e a efetivo suprimento às células ativadas, gerando consumo local de glicose e oxigênio causando a desoxigenação relativa do volume local sangue. Esta depressão inicial ocorre até que o organismo supra as demandas aumentando o fluxo sanguíneo na região, implicando na diminuição relativa da concentração de desoxi-hemoglobina (hemoglobina desoxigenada) e no aumento da concentração de oxi-hemoglobina (hemoglobina oxigenada).

A oxi-hemoglobina é diamagnética (exibe fraca interação com um campo magnético) e a desoxi-hemoglobina, paramagnética (alinha-se a campo magnético externo). Quando expostas a campo magnético, as moléculas de desoxi-hemoglobina,

criam gradientes próprios no campo magnético dentro dos vasos que irrigam o tecido, gerando uma defasagem dos spins das moléculas de água, reduzindo T_2^* e qualquer sinal de RM que dependa desse fator em até 20% em relação ao sangue totalmente oxigenado¹¹. A oxigenação do sangue gera aumento do sinal de RM, pois diminui a interferência gerada por campos locais associados à desoxi-hemoglobina. O sinal BOLD permite desta forma estudar a atividade cerebral de forma indireta, uma vez que esta causa variações locais na taxa de consumo de oxigênio e no fluxo sanguíneo de regiões ativas.

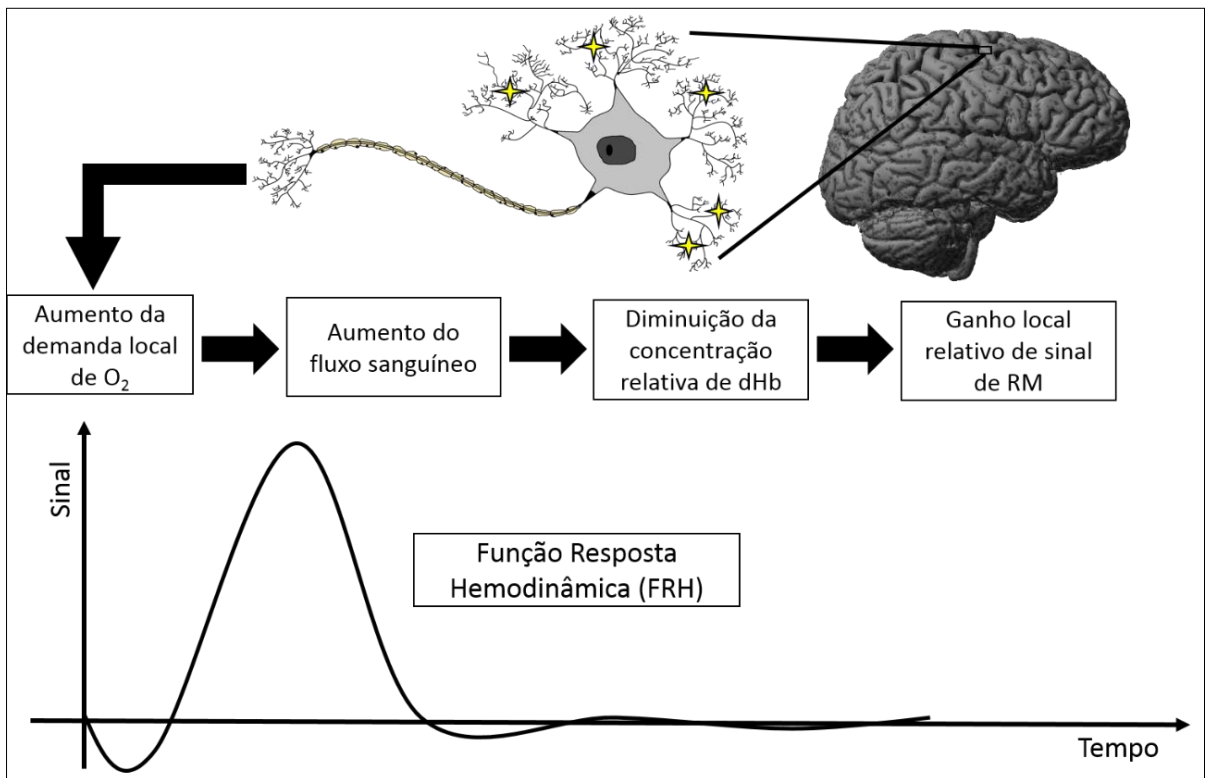


Fig. 2: Fluxograma da resposta hemodinâmica do cérebro mediante a um estímulo pontual.

1.4 CONECTIVIDADE FUNCIONAL

A flutuação do sinal BOLD pode ocorrer de forma relacionadas a uma tarefa específica como o mexer da mão direita quando se espera que a região do córtex associada à função executiva desde movimento tenha aumento de sinal de RM. Estas variações são inerentes ao funcionamento do cérebro: são permanentes e não aleatórias ocorrendo mesmo em repouso, quando as RSN (do inglês, *resting state networks* ou redes funcionais de repouso) estão eloquentes^{12,13}.

Conectividade funcional (CF) é uma técnica que possibilita encontrar regiões distintas no cérebro que variam a atividade metabólica ou as taxas de consumo de oxigênio em sincronia temporal. A CF é a medida da correlação entre duas regiões corticais durante uma tarefa ou até mesmo no repouso e avalia o sincronismo entre a oscilação do sinal BOLD nestas regiões. É importante ressaltar que CF não exige conexão estrutural direta (anatômica) entre as partes avaliadas e não permite inferências de causa-efeito ou direcionalidade^{12,13}.

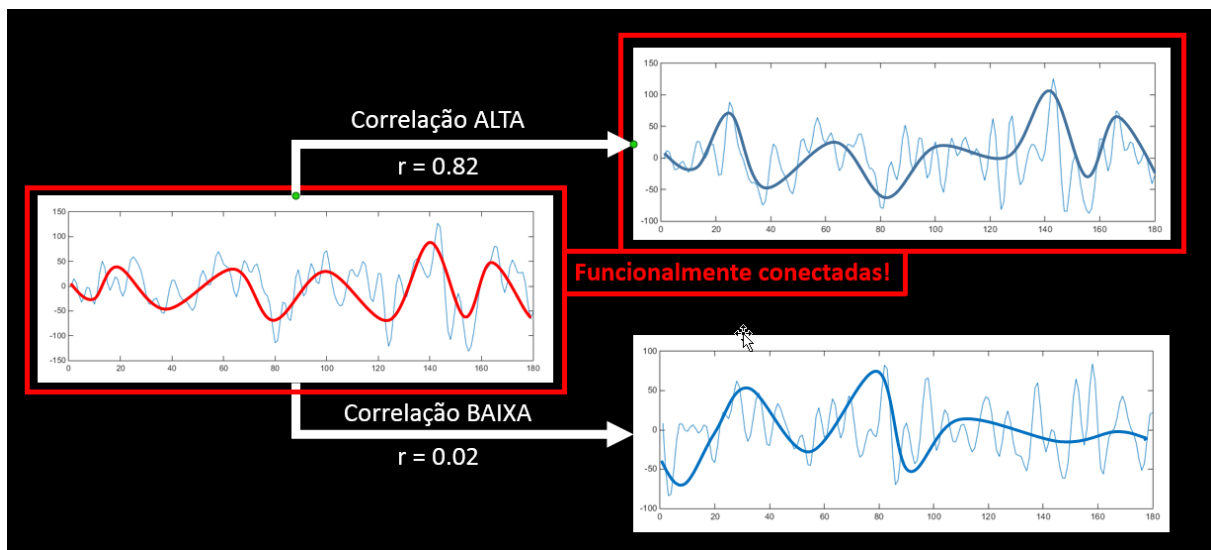


Fig. 3: Exemplo de series temporais correlacionadas. As regiões do exemplo, representadas pelas séries temporais destacadas com os quadros vermelhos, estariam funcionalmente conectadas.

Existem diferentes metodologias para avaliação da conectividade funcional que vão além da correlação entre regiões sementes. Métodos guiados pelos dados (*data-driven*) oferecem possibilidades que não exigem fortes suposições iniciais ou espacialmente enviesadas, tendo como principal exemplo as análises de componentes independentes (ICA). O ICA busca definir componentes do sinal que são estatisticamente independentes sob diversos aspectos, resultando em mapas

relacionados desde fatores de interferência (movimento, respiração e balistocardiograma) até os mapas de redes funcionais^{12,13}. Embora métodos guiados pelos dados sejam inicialmente vantajosos em relação a métodos baseados no modelo, devido ao viés inicial, podemos compreender que para análises populacionais e comparações de grupos a interferência do pesquisador sempre entrará no desenho experimental de uma forma ou outra. Livre das inferências espaciais iniciais o ICA demandará árduo procedimento de separação e tipificação das componentes, sejam elas do nível individual ou de grupo uma vez que não há métodos eficazes que não dependam do analisador em alguma etapa. A escolha da melhor metodologia dependerá da natureza dos dados assim como do perfil do analisador^{12,13}.

Redes funcionais são formadas por grupos de regiões funcionalmente conectadas, síncronas temporalmente (em relação ao sinal BOLD) e que compartilham ou desenvolvem processos cognitivos específicos. O grau de “conexão” pode ser avaliado entre as redes (inter-redes) ou dentre regiões de uma mesma rede (intra-rede), podendo naturalmente estabelecer uma relação direta, indireta ou desprezível^{14,15}.

Estudos em conectividade funcional em pacientes com epilepsia exaltam a necessidade da homogeneização dos grupos e revelam dificuldades em representar virtualmente a conectividade funcional devido a possíveis alterações das redes funcionais, ocasionadas pela síndrome epiléptica¹⁶. Liao *et al.*, descreveram os padrões de conectividade funcional em pacientes com epilepsia de lobo temporal mesial como completamente alteradas em relação aos padrões funcionais normais¹⁷. Também neste estudo foi descrito a relação entre tempo a partir do início da síndrome epiléptica e os valores absolutos de conectividade, revelando correlação negativa entre estes parâmetros.

A grande parte dos estudos avaliam redes funcionais isoladamente e reportam redução generalizada na conectividade da DMN (do inglês, *default mode network* ou rede de modo padrão) e da *salience network*, relacionando os achados ao desempenho inferior em testes de linguagem e memória com sincronia anormal entre regiões das redes da percepção. Não há estudos comparando de forma abrangente a interação direta entre redes (inter-redes) em pacientes com epilepsias¹⁵.

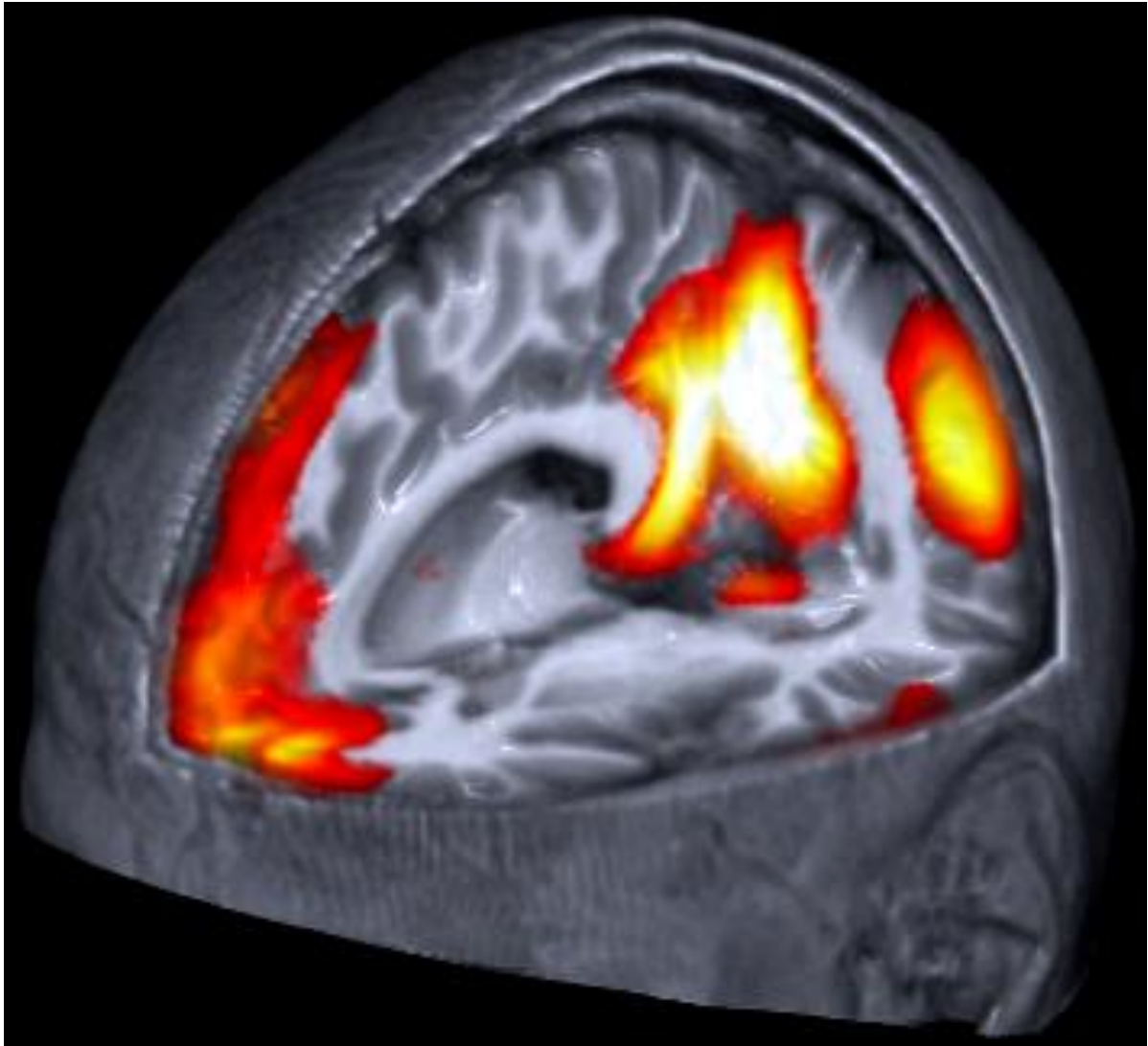


Fig. 4: Representação real de um resultado de conectividade funcional. No exemplo, identificam-se as regiões que caracterizam a DMN.

A bibliografia demonstra que a conectividade funcional pode medir distúrbios sutis nas funções cognitivas superiores. O método vem destacando-se como importante ferramenta na investigação de redes neurais associadas a diferentes aspectos funcionais, sendo sensível a alterações não facilmente mensuráveis através de paradigmas funcionais convencionais^{12,13}.

1.5 TENSORES DE DIFUSÃO E CONECTIVIDADE ESTRUTURAL

Conectividade estrutural, por definição, é a técnica que avalia a conexão entre duas áreas, considerando-se a estrutura cerebral real, os fascículos axonais. Estes tratos são feixes axonais coerentes responsáveis por transmitir as informações entre um neurônio e outro, e caracterizam-se como a substância branca (SB) do córtex.

O conceito de conectividade estrutural na Neuroimagem é representado pelas DTIs (do inglês, *diffusion tensor images* ou imagens por tensores de difusão). Estas aquisições são ponderadas pela difusão das moléculas de água no cérebro e seus padrões de deslocamento. O equipamento de RM supõe resultante nula, imobilidade dos prótons da água entre os “pulsos” de gradientes do equipamento de RM. O deslocamento de moléculas de água gera atenuação do sinal de RM local, causando “falha” no processo de ‘*refasagem*’ para regiões onde uma quantidade considerável de moléculas de água se deslocaram. Esta “falha” de ‘*refasagem*’ é proporcional à difusão local e é usada como medida quantitativa de difusão de água¹⁹.

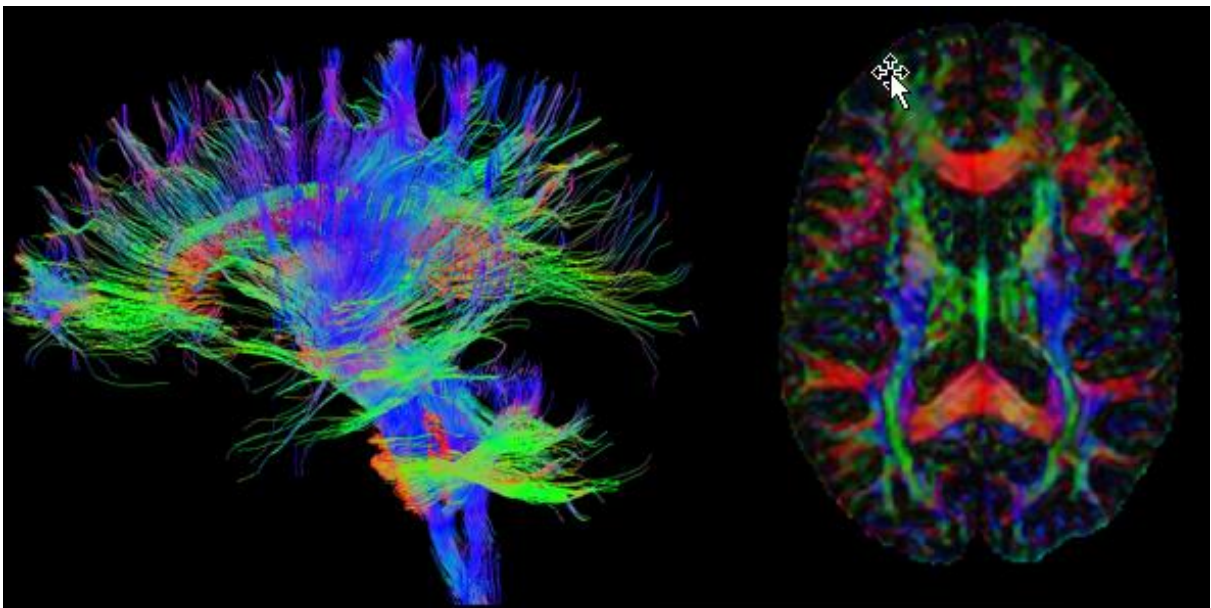


Fig. 5: Exemplos de imagens com técnicas de difusão. Na esquerda, extensa tractografia cerebral e na direita imagem de difusão com codificação direcional de cor.

Movimento browniano é o movimento aleatório de partículas suspensas em um fluido simetricamente limitado (ou ilimitado). Pode ser representado como movimento errático, com resultante nula, isotrópico. Este conceito é fundamental na interpretação dos dados de difusão em Neuroimagem, pois diferentes estruturas do córtex, ou ainda mais especificamente, do neurônio, apresentam padrões distintos de difusão. A

substância cinzenta (SC) do cérebro é basicamente constituída de corpos neuronais, estruturas com geometria de tenência esférica, tridimensional. Por outro lado, a substância branca é constituída principalmente por feixes axonais, estruturas alongadas, delimitadas linearmente pelas bainhas de mielina.

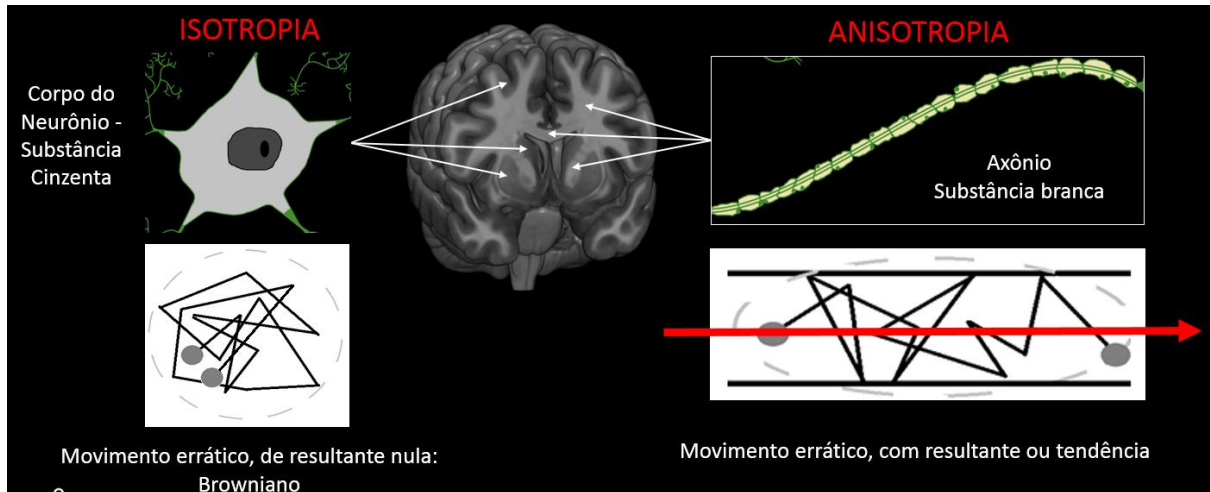


Fig. 6: Representação esquemática dos conceitos básicos em difusão. Na esquerda, representação do corpo do neurônio e indicação da região do cérebro que constitui, a SC. Na direita, representação artística do axônio, com indicação da região do cérebro que constitui, a SB.

Em parâmetros de difusão, podemos afirmar que o corpo do neurônio possui difusão com tendência isotrópica (igual em todas as direções), enquanto o axônio, difusão com tendência anisotrópica (reduzida perpendicularmente e aumentada paralelamente à estrutura)²⁰. O FA (do inglês, *fractional anisotropy* ou anisotropia fracionada) é um parâmetro quantitativo, adimensional, de valor entre 0 e 1 e que indica se há ou não uma direção na qual o deslocamento das moléculas de água é preferencial (grau de anisotropia):

$$FA = \sqrt{\frac{3}{2}} \times \frac{\sqrt{(\lambda_1 - \hat{\lambda})^2 + (\lambda_2 - \hat{\lambda})^2 + (\lambda_3 - \hat{\lambda})^2}}{\sqrt{\lambda_1^2 + \lambda_2^2 + \lambda_3^2}},$$

onde os λ representam os autovalores dos autovetores do elipsoide que melhor descreve o deslocamento das moléculas no meio (Fig. 7).

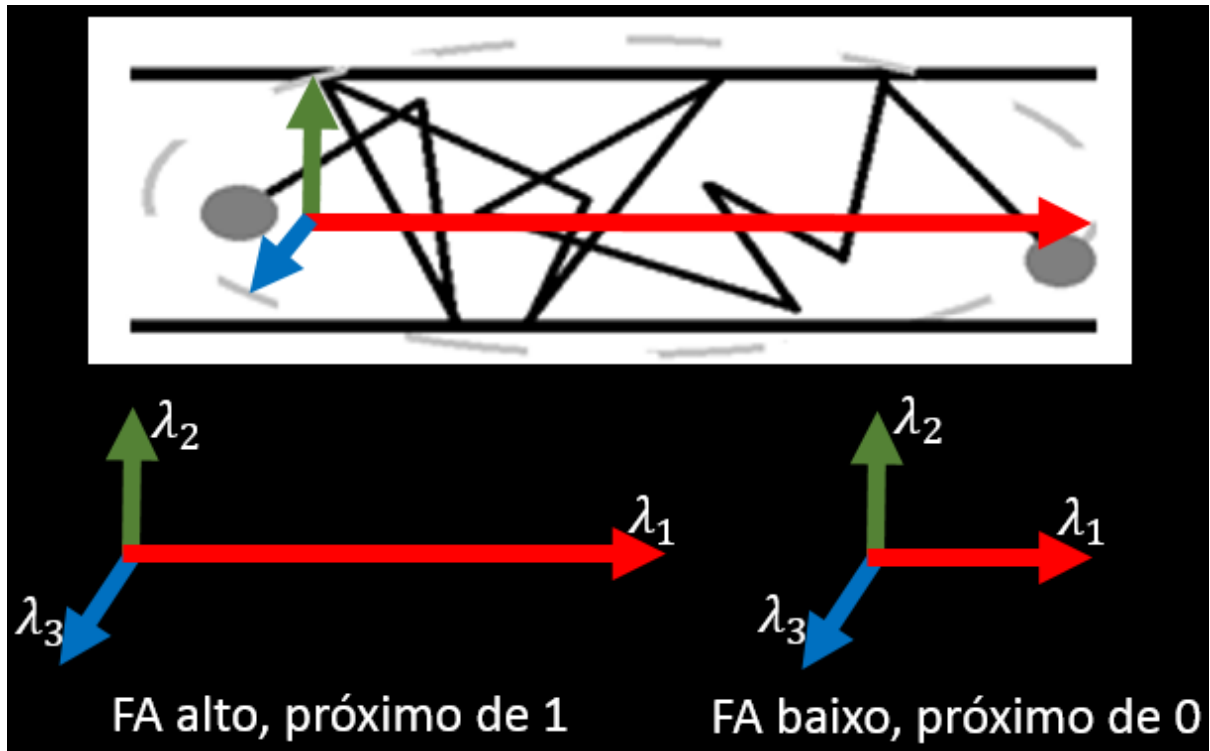


Fig. 7: Duas representações esquemáticas para o cálculo do FA. A da esquerda ilustra os vetores de uma região com grande anisotropia. Na direita, ilustração dos vetores de região com difusão praticamente isotrópica. λ_1 representa o deslocamento na direção preferencial, portanto o maior deslocamento. λ_2 e λ_3 representam os deslocamentos perpendiculares ao deslocamento preferencial.

O FA, de forma indireta, reflete densidade de tratos, coerência dos fascículos, e suas alterações podem indicar desmielinização e ruptura axonal. De forma não específica, aponta se existe ou não alterações de SB. Outros parâmetros são quantificados a fim de auxiliar na caracterização das alterações de SB: A MD (do inglês, *mean diffusivity* ou difusividade média), expressa em unidades de área por tempo ($\frac{mm^2}{seg}$):

$$MD = \frac{\lambda_1 + \lambda_2 + \lambda_3}{3}.$$

A MD é a média total do deslocamento das moléculas de água, em todas as direções. Demonstra de forma geral o grau de deslocamento das moléculas de água e, comparativamente, pode indicar alterações no volume água intersticial, degeneração axonal e interrupção dos tratos²⁰. A AD (do inglês, *axial diffusivity* ou

difusividade axial), é a representação da difusão apenas na direção de maior deslocamento (paralela ao eixo principal):

$$AD = \lambda_1.$$

A AD demonstra de forma mais sensível, o grau de deslocamento das moléculas de água ao longo do trato. Comparativamente, pode indicar degeneração axonal, interrupção dos tratos, coerência do fascículo e densidade de tratos. Por fim, o RD (do inglês, *radial diffusivity* ou difusividade radial) é quantificado pela média do deslocamento das moléculas de água nas direções perpendiculares à direção preferencial:

$$RD = \frac{\lambda_2 + \lambda_3}{2}.$$

A RD demonstra de forma mais sensível, o grau de deslocamento das moléculas de água, perpendicular à direção anatômica do trato. Comparativamente, é o melhor indicador de desmielinização.

Epilepsia é certamente uma desordem cortical e embora a grande parte das investigações sobre a patogênese da epilepsia centrem-se na SC, os avanços recentes em neuroimagem quantitativa demonstram extensas alterações na substância branca²⁰. De acordo com estudos anteriores, diferentes subgrupos de epilepsia podem apresentar maiores ou menores anormalidades de substância branca em regiões relevantes a estas patologias. A epilepsia de lobo temporal mesial tem sido a síndrome mais estudada dentre os subgrupos de epilepsia, e as tractografias de regiões como cíngulo, fórnix e fascículos anatomicamente relacionados têm demonstrado achados significantes que caracterizam este subgrupo quanto à integridade estrutural da substância branca²⁰.

Estudos anteriores reportaram anormalidade de SB em várias epilepsias. Na ELTM com EH, estes estudos demonstram anomalias difusas e bilateralmente distribuídas. Por outro lado, para outros subtipos, a análise de DTIs é descrita como técnica que pode ajudar a identificar lesões sutis, porém, com resultados discordantes. A definição dos padrões de anormalidade estruturais e funcionais em subtipos da epilepsia pode acrescentar informações específicas a cada síndrome melhorando entendimento de suas origens e dinâmicas. Aperfeiçoando o entendimento e a

caracterização destes subtipos, podemos trazer novas perspectivas ao tratamento clínico, neuropsicológico e cirúrgico.

2. OBJETIVOS

- Geral:
 - Avaliar a conectividade estrutural e funcional em pacientes com epilepsias focais
- Específicos
 - Avaliar alterações de conectividade estrutural em ELTM-EH e compará-las com alterações em outras epilepsias focais
 - Avaliar alterações de conectividade funcional em ELTM-EH
 - Desenvolver e aperfeiçoar softwares que padronizem e forneçam novas perspectivas metodológicas para os estudos de alterações de conectividade estrutural e funcional

3. METODOLOGIA

3.1 SELEÇÃO DOS SUJEITOS DA PESQUISA

As imagens de RM utilizadas neste projeto estavam no banco de dados do Laboratório de Neuroimagem e foram obtidas em projetos aprovados pelo comitê de ética da Unicamp. Os sujeitos da pesquisa foram selecionados através de análise de histórico e caracterização clínica realizadas através do ambulatório de epilepsia da UNICAMP. Todos assinaram termo de consentimento livre esclarecido.

Os pacientes com ELTM-EH e ELT-NL foram selecionados a partir de estudo anterior realizado por Coan *et al.*²¹. Neste estudo prévio, foram incluídos pacientes consecutivos acompanhados no Ambulatório de Epilepsia do Hospital de Clinicas da Unicamp, com diagnóstico clínico e eletroencefalográfico de ELT, de acordo com os critérios da Liga Internacional Contra a Epilepsia (*International League Against Epilepsy – ILAE*)²². A presença de sinais de EH nas imagens de RM foi determinada por análise visual associada à quantificação de sinal e volume da estrutura hipocampal. No presente estudo, foram incluídos o subgrupo de pacientes com ELTM que apresentavam exames de RM com protocolo adequado para as análises propostas.

Para o presente estudo, foram ainda selecionados pacientes consecutivos acompanhados no Ambulatório de Epilepsia do Hospital de Clinicas da Unicamp com diagnóstico clínico e eletroencefalográfico de epilepsia de lobo frontal (ELF), de acordo com os critérios da ILAE²² e que possuíam exames de RM de crânio revisada por especialista evidenciando sinais sugestivos de displasia cortical focal (DCF). Foram incluídos todos os pacientes com exames de RM com protocolo adequado para as análises propostas.

3.2 PROTOCOLOS DE IMAGENS

Para todos os protocolos foi utilizado equipamento de RM Philips Achieva 3 de tesla:

1. Imagem estrutural: ponderadas T1, voxel isotrópico de 1mm^3 , sem *gap*, ângulo de *flip* de 8° , TR (tempo de repetição) de 7 ms, TE (tempo ao eco) de 3.2 ms, 180 fatias sagitais e FOV (do inglês: *field of view*) de 240×240 mm
2. Imagens funcionais:
 - a) Imagens eco planares (EPIs), ponderadas por T2*, voxel de $3 \times 3 \times 3 \text{mm}^3$, *gap* entre fatias de 0.3 mm, ângulo de *flip* de 75° , TR de 2000 ms, TE de 30 ms, 32 fatias axiais e FOV de 240×240 mm e 180 volumes
 - b) EPIs, T2*, voxel $3 \times 3 \times 3 \text{mm}^3$, sem *gap*, ângulo de *flip* de 90° , TR de 2000 ms, TE de 30 ms, 40 fatias axiais e FOV de 240×240 mm e 180 volumes
3. DTI: Spin-eco single shoot EPI, voxel adquirido com $2 \times 2 \times 2 \text{mm}^3$, re-amostrado para $1 \times 1 \times 2 \text{mm}^3$, sem *gap*, ângulo de *flip* de 90° , TR de 8500 ms, TE de 61 ms, 70 fatias axiais, 32 direções de gradiente, b-fator máximo de 1000 s/mm^2 e FOV de 240×240 mm

3.3 DESENVOLVIMENTO DE SOFTWARES

Visando maior flexibilidade, compatibilidade e padronização, as principais ferramentas utilizadas nas metodologias foram desenvolvidas no Laboratório de Neuroimagem, utilizando como base a plataforma Matlab e ferramentas já existentes como SPM (*Statistical Parametric Mapping*) versões 8 e 12, e ExploreDTI. O desenvolvimento instrumental possibilita profunda imersão nos conceitos teóricos e metodológicos além do claro conhecimento de cada passo e etapa realizada, evitando os chamados processos “caixa-preta”.

3.3.1 NCA: NEUROIMAGING COMPUTATIONAL ANALYSIS

O NCA (do inglês: *Neuroimaging Computational Analysis*) foi desenvolvido em parceria com Guilherme Côco Beltramini para oferecer de forma simplificada e organizada, ferramentas computacionais disponíveis na área de neuroimagem. A *toolbox* (inglês para caixa de ferramentas), inclui entre outras modalidades de análise, um conjunto de metodologias que possibilitam o processamento de imagens de DTI, a *tractografia* de diversos fascículos axônais e a quantificação dos parâmetros de difusão resultantes.

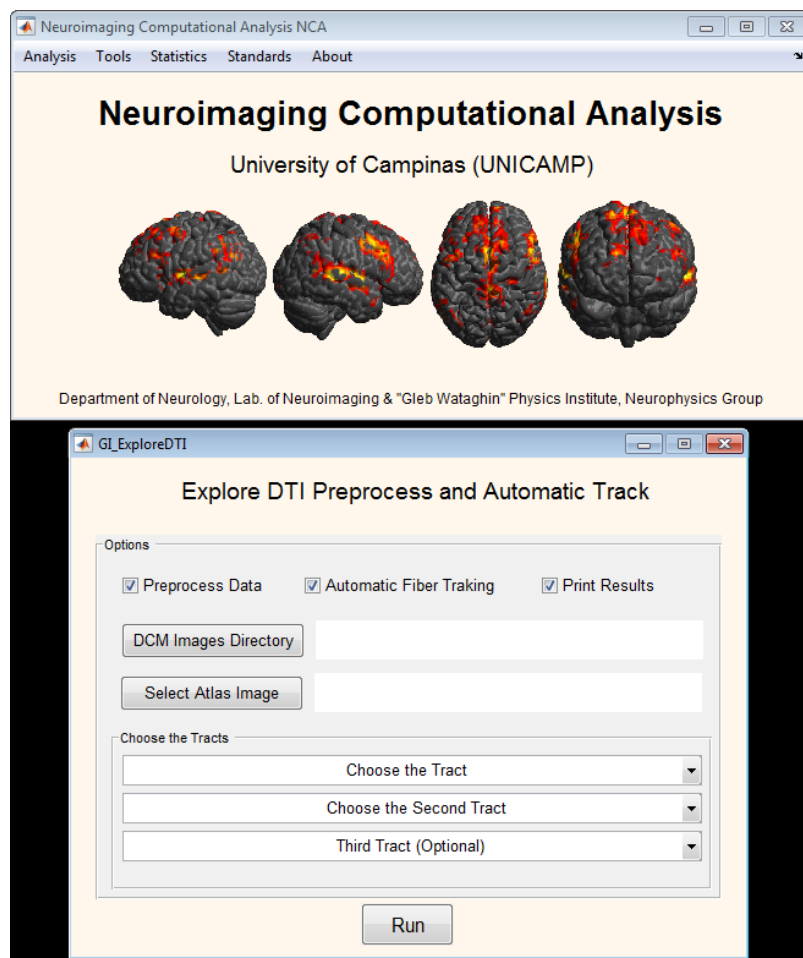


Fig. 8: Interface gráfica do software NCA. No topo janela principal, e na parte inferior, interface da modalidade de processamento e tractografia de DTIs.

O processamento das imagens é realizado, seguindo método adaptado e aperfeiçoado, previamente descrito por Lebel *et al.*, 2008^{23,24}. Inicialmente, desenvolvemos a imagem de referência (*template*) normalizada. Este *template* foi obtido com imagens de 10 indivíduos controles, cinco homens e cinco mulheres, com idade entre 22 e 47 anos. As imagens destes indivíduos foram registradas,

normalizadas e suavizadas. A média entre elas (o *template*) seria então utilizada como referência na elaboração de estratégias de tractografia.

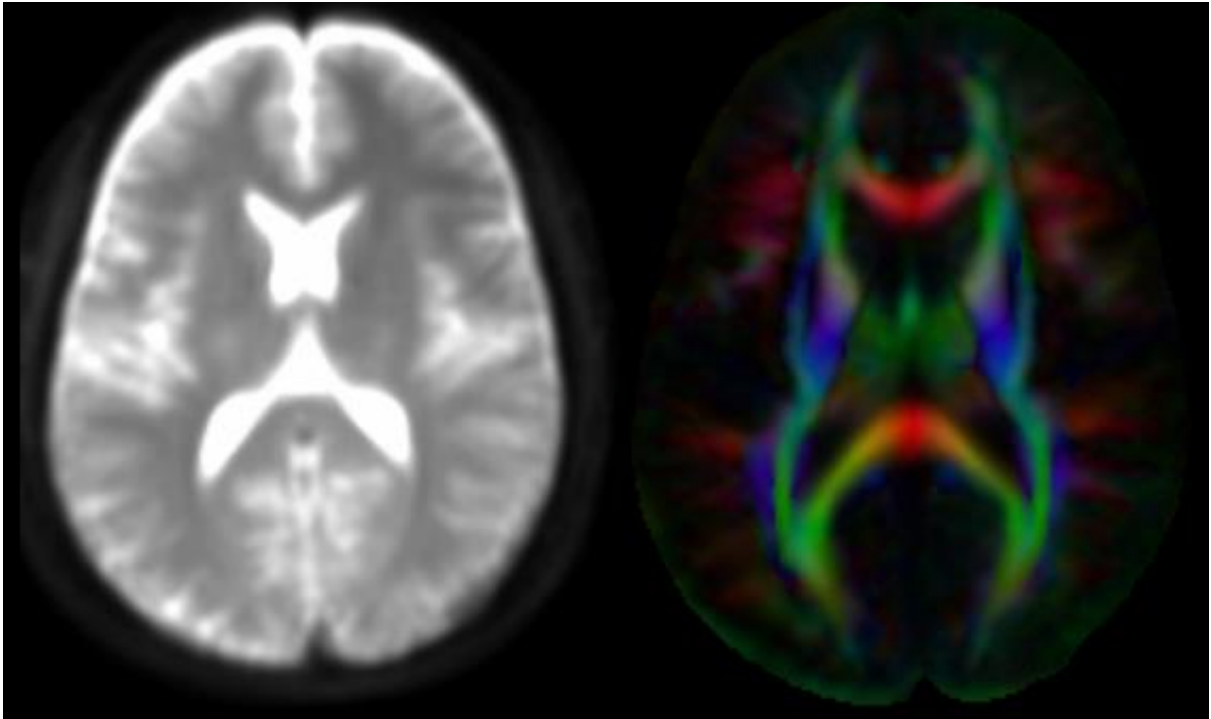


Fig. 9: *Template* brasileiro desenvolvido no projeto. Na esquerda imagem de não-difusão associada e na direita, o *template* com a codificação direcional em cores.

O método é considerado semiautomático, pois exige a elaboração das estratégias de tractografia uma única vez, utilizando o *template* como base.

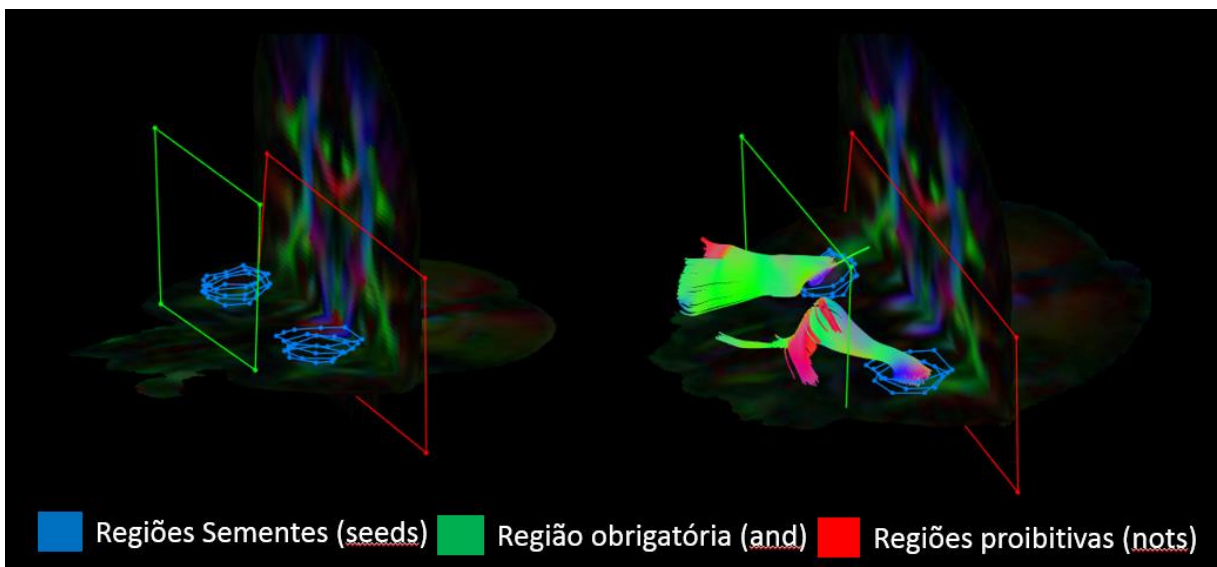


Fig. 10: Exemplo real de estratégia normalizada para tractografia. No exemplo, estratégia bilateral para o fascículo uncinado.

Até o momento, o NCA possui em sua interface, oito tratos com estratégias definidas: Fascículo Uncinado; Fascículo Fronto-ocipital inferior; Corpo do Fórnix; Fascículo do Cíngulo; Corpo do Corpo Caloso; Radiação Óptica; Tronco cerebral; Trato piramidal.

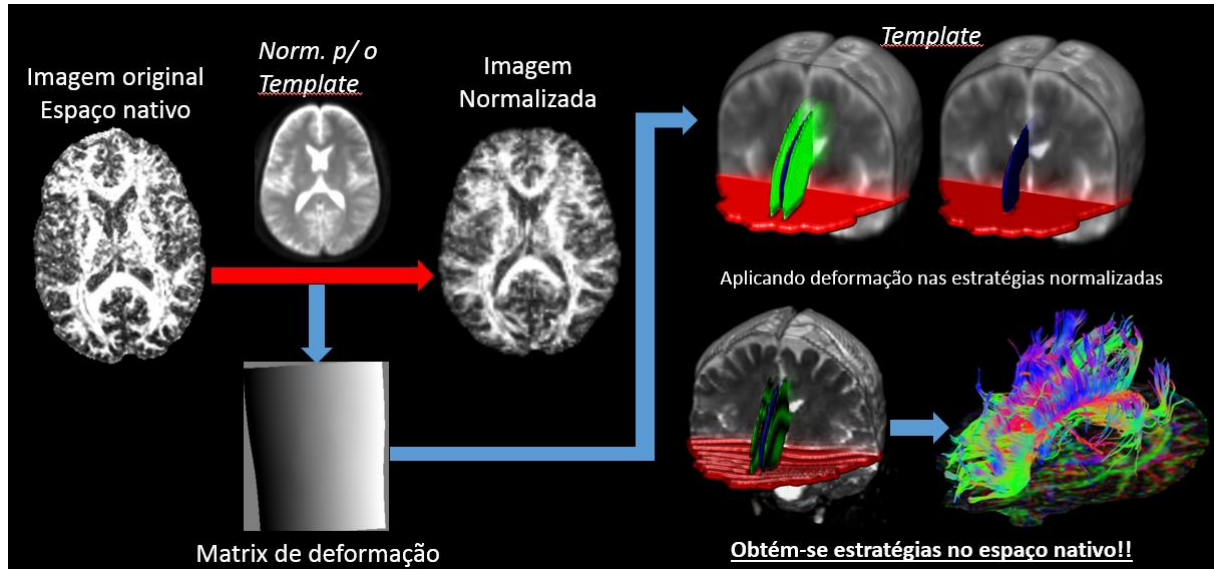


Fig. 11: Fluxograma do pré-processamento e das etapas do método semiautomático de tractografia.

A tractografia semiautomática determinística utiliza parâmetros estimados e estratégias desenvolvidas manualmente uma única vez. Mais detalhadamente, o procedimento é descrito na sequência:

1. A imagem no espaço nativo do voluntário é normalizada para o espaço padrão, utilizando o *template* desenvolvido.
2. Este processo estima e armazena as matrizes de deformação: matrizes que contém informações sobre as transformações espaciais aplicadas à imagem no espaço nativo, para se tornar normalizada (espaço padrão do *template*). A imagem normalizada do sujeito pode ser descartada.
3. Uma operação inversa é aplicada sobre as estratégias de tractografia normalizadas do NCA: aplicando a inversa da matriz de deformação individual estimada, fazemos com que as estratégias normalizadas criadas sobre o *template* passem ao espaço nativo e peculiar do voluntário.
4. As estratégias individualizadas são então utilizadas para gerar o trato em questão.
5. A região delimitada pelo trato é quantificada e os parâmetros de difusão tabulados.

3.3.2 UF²C: USER FRIENDLY FUNCTIONAL CONNECTIVITY

O UF²C é um software de código aberto, desenvolvido em m-code (linguagem da plataforma Matlab). Funciona como ferramenta para o SPM12 (*Statistical Parametric Mapping 12*) mas possui inúmeras funções independentes. O *software* está disponível para *download* e objetiva simplificar e organizar estudos de conectividade funcional, através de uma metodologia simplificada e validada, sem sacrificar a qualidade.

O *software* possui rotinas completas, que incluem desde o processamento das imagens brutas até avançados métodos de análises estatísticas e quantitativas. A interface amigável faz as etapas de pré-processamento e análise, geralmente complexas, serem acessíveis a neurocientistas de diversas áreas do conhecimento.

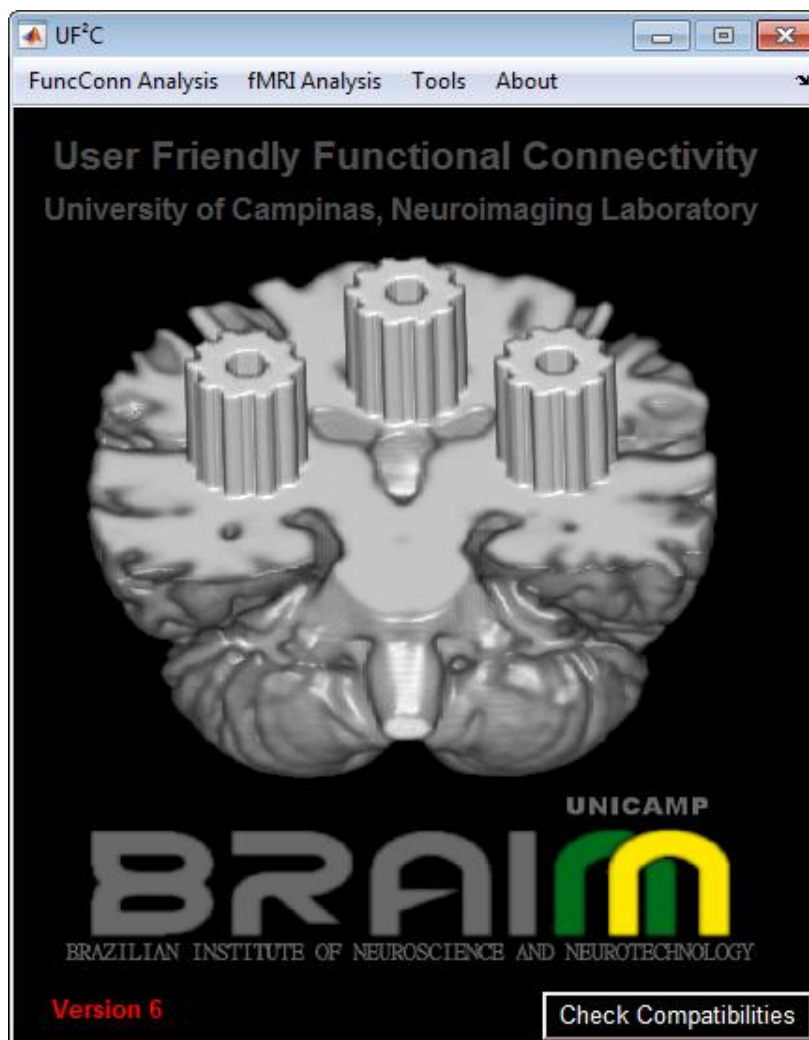


Fig. 12: Interface gráfica do *software* UF²C, demonstrando a janela principal, de boas-vindas, do programa.

Atualmente o UF²C conta com quatro modalidades distintas de análise de conectividade funcional, uma interface para análise de aquisições funcionais padrão (interface desenvolvida em parceria com Raphael Fernandes Casseb) e nove ferramentas complementares que auxiliam no dia a dia de neurocientistas que trabalham com imagens médicas.

As modalidades disponíveis para análise de conectividade funcional são:

1. Rotina exclusiva para pré-processamento: habilita todas as seguintes análises, gerando imagens prontas para inferências estatísticas.
2. Conectividade baseada em semente única: gera mapas estatísticos, comparando a região semente com todos os voxels do córtex.
3. Interatividade funcional: Análise com múltiplas sementes, automaticamente posicionadas, de forma a abranger todas as áreas possíveis do córtex. Os múltiplos mapas resultantes são integrados, formando a ideia conceito de interatividade funcional.
4. Análise ROI-a-ROI:
 - a. Primeiro nível estatístico (Individual): computa a correlação direta entre várias regiões de interesse, resultando em matrizes de adjacência individuais.
 - b. Segundo nível estatístico (inferências de grupo): Possibilita sob diversos aspectos comparar grupos, utilizando como entrada, os dados gerados na modalidade anterior.
5. Conectividade baseada em semente única, com janela temporal variante: possibilita a análise dinâmica, definindo mapas estatísticos de todo o cérebro que diferem temporalmente.

Para estudos de ressonância magnética funcional, com paradigmas de estímulo em bloco, o software disponibiliza as seguintes modalidades:

1. Pré-processamento de RMf: processamento de imagens funcionais e estruturais/anatômicas, otimizado para estudos com paradigma em bloco.
2. Análise de paradigmas em bloco: rotina simplificada para desenho e análise de aquisições com paradigma em bloco. As imagens resultantes da modalidade anterior são usadas como dados de entrada.

Complementarmente, nove ferramentas gerais são disponibilizadas, visando auxiliar em problemas cotidianos da Neuroimagem:

1. Visualizador de movimento da cabeça: auxilia no controle de qualidade de dados de RMf
2. Análise de movimento da cabeça: quantifica, sob diversos aspectos o movimento da cabeça de vários sujeitos simultaneamente. Possibilita avaliar possíveis interferências do movimento entre os grupos estudados.
3. Editor de imagem: Possibilita corrigir erros de reconstrução, remover intervalos temporais em IRMf ou ainda um volume específico.
4. '*Renomeador*' de arquivos em massa: possibilita renomear quaisquer arquivos, incluindo sufixo, prefixo, prefixo de contagem e ainda remover e substituir trechos dos nomes dos arquivos. Importante e útil na organização dos grupos estudados.
5. Ferramenta para segmentação de imagens estruturais em diversos tecidos (ex: SB, SC, líquido, osso, pele e etc...)
6. Volumetria: ferramenta que quantifica o volume real de imagens e ROIs, possibilita ainda quantificar valores relativos de volume intracraniano e tecidos corticais específicos.
7. Ferramenta de interpolação de imagens.
8. Conversor de r-score para z-score: Converte imagens ou variáveis de Matlab, utilizando a transformada de Fisher.
9. '*Anonimizador*' de arquivos DICOM.

Os métodos específicos utilizados pelo software no processamento e análise de imagens são descritos na seção **Artigo 2** (pág. 62).

4. RESULTADOS

4.1 DESENVOLVIMENTO DE SOFTWARE

4.1.1 NCA - NEUROIMAGING COMPUTATIONAL ANALYSIS

Sendo restrito ao uso interno, os procedimentos de processamento e tractografia do NCA foram utilizados em diversos projetos do Laboratório de Neuroimagem da UNICAMP. O *software* foi utilizado no artigo descrito na sessão **Artigo 1** (pág. 42), além de trabalhos de outros pesquisadores do laboratório^{25,26,27,28}.

4.1.2 UF²C – USER FRIENDLY FUNCTIONAL CONNECTIVITY

Após o compartilhamento online no site do laboratório de Neuroimagem (Fig. 13: Imagem do website do UF²C: <http://www.lni.hc.unicamp.br/app/uf2c/>) da Unicamp e consecutivo compartilhamento e divulgação no site oficial do programa SPM (<http://www.fil.ion.ucl.ac.uk/spm/ext/#UF2C>), o UF²C vem sendo utilizado por centros de pesquisa em todo o mundo (Fig. 14). No laboratório de neuroimagem, além do trabalho apresentando nesta tese (**Artigo 2**, pág. 62), outros dois artigos já foram publicados utilizando o *software* e outros já foram enviados para publicação^{29,30,31}.

Neuroimaging Laboratory
 Department of Neurology - School of Medical Sciences - Unicamp - Brasil

Overview People Software Publications Contact

UF²C - User Friendly Functional Connectivity

[The Software](#) - [Analysis Modalities](#) - [Tools](#) - [Example Images](#) - [UF²C in the world](#) - [How to cite?](#) - [Download](#)

UF²C Introduction

UF²C is an open source software developed by [Brunno M. de Campos](#) at the [Neuroimaging Laboratory](#) at [Unicamp](#) that aims to simplify and organize functional connectivity studies in neuroimaging through a clean and validated methodology, without sacrificing quality. UF²C has a full processing pipeline: The user only needs to select the raw functional and structural NIfTI files from the subjects. The graphical user interface makes the processing and analysis options accessible for neuroscientists, with reasonable choices of default settings. UF²C allows the user to study functional connectivity both through a quantitative view that provides detailed values of average connectivity and through a spatial view that provides statistical maps that can be directly used for further analyses. All results are carefully organized in distinct folder for each subject, and a common folder is generated with a log file reporting the quantitative results of all the analyzed subjects. Several UF²C modalities and tools runs combined with [Statistical Parametric Mapping](#) functions.

UF²C is open source software, distributed under a BSD-style [License](#).

UF²C Requirement

- Windows, Linux or Mac OS X operating system
- [SPM](#) (Statistical Parametric Mapping, version 8 or 12)
- [MATLAB](#) (version R2010a or later, required by SPM)
- MATLAB [Statistics toolbox](#)
- MATLAB [Signal Processing toolbox](#).
- MATLAB [Image Processing toolbox](#).

It is a great effort to make UF²C compatible with all possible combinations of operational systems, Matlab and SPM versions. Some problems can occur in Matlab older than 2010 versions, for example. Please contact me if you find any compatibility problems. Thank you!

Contact the author: brunno@fcm.unicamp.br

Fig. 13: Imagem do website do UF²C: <http://www.lni.hc.unicamp.br/app/uf2c/>.

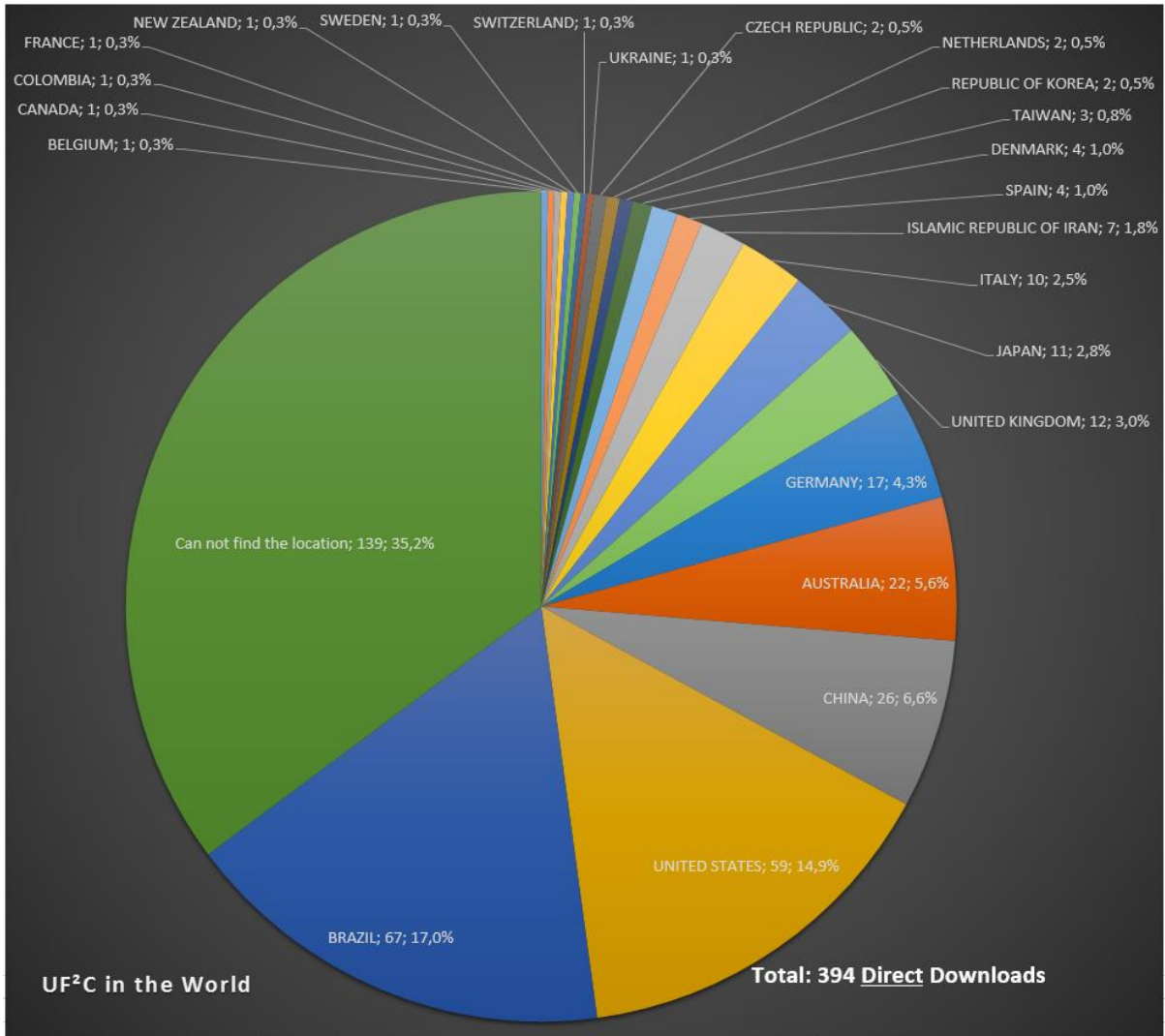
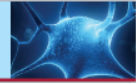


Fig. 14: Dados geográficos rastreáveis dos *downloads* realizados no site. O procedimento exclui *downloads* automáticos realizados por repositórios de arquivos e ainda *downloads* consecutivos de um mesmo usuário.

4.2 ARTIGOS

4.2.1 ARTIGO 1: ANÁLISE DE CONECTIVIDADE ESTRUTURAL



FULL-LENGTH ORIGINAL RESEARCH



White matter abnormalities associate with type and localization of focal epileptogenic lesions

*Brunno M. Campos, *Ana C. Coan, †Guilherme C. Beltramini, ‡Min Liu, *Clarissa L. Yassuda, *Enrico Ghizoni, ‡Christian Beaulieu, §Donald W. Gross, and *Fernando Cendes

Epilepsia, 56(1):125–132, 2015
doi: 10.1111/epi.12871

SUMMARY

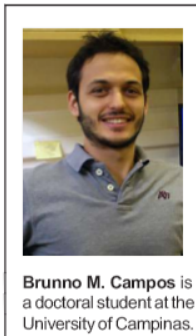
Objective: To evaluate white matter (WM) integrity of distinct groups of patients with antiepileptic drug (AED)-resistant localization-related epilepsies.

Methods: We used diffusion tensor imaging (DTI) fiber-tractography and voxel-based morphometry (VBM) to investigate differences of WM micro- and macrostructural integrity in patients with different drug-resistant localization-related epilepsies: 17 with temporal lobe epilepsy with magnetic resonance imaging (MRI) signs of hippocampal sclerosis (TLE-HS), 17 with TLE and normal MRI (TLE-NL), 14 with frontal lobe epilepsy and subtle MRI signs of focal cortical dysplasia (FLE-FCD), and 112 healthy controls. We performed fiber-tractography using a semiautomatic deterministic method to yield average fractional anisotropy (FA), axial (AD), and radial (RD) diffusivity ipsilateral and contralateral to the epileptogenic zone of the following tracts based on their functional and anatomic relevance: body of fornix (BoF), body of cingulum (BoC), inferior frontal occipital (IFO), and uncinat fasciculi (UF). In addition, we performed VBM of the WM maps to assess macrostructural integrity differences among groups.

Results: TLE-HS had ipsilateral and contralateral decreased FA and increased RD for all tracts. VBM showed WM alterations mainly in the ipsilateral parahippocampal region and contralateral superior temporal gyrus. FLE-FCD showed bilateral FA decreases only in the BoC and ipsilateral RD increases also in the BoC. VBM showed WM reduction mainly in the ipsilateral precuneus and posterior and anterior cingulum. No significant WM alterations were found in the TLE-NL in DTI or VBM analysis.

Significance: WM abnormalities differ in distinct AED-resistant localization-related epilepsies. The diverse distribution of the WM damage in these patients suggests that the localization of the epileptic networks may play a role in the WM burden. However, the distinct degree of this damage, more accentuated in TLE-HS, also suggests that the underlying cause of the epilepsy is probably an additional factor to explain this WM damage.

KEY WORDS: Frontal lobe epilepsy, Temporal lobe epilepsy, Diffusion tensor imaging, Voxel-based morphometry.



Brunno M. Campos is a doctoral student at the University of Campinas.

Accepted October 14, 2014; Early View publication December 26, 2014.

*Neuroimaging Laboratory, Department of Neurology, University of Campinas, Campinas, Brazil; †Neurophysics Group, Gleb Wataghin Physics Institute, University of Campinas, Campinas, Brazil; ‡Department of Biomedical Engineering, Faculty of Medicine and Dentistry, University of Alberta, Edmonton, Alberta, Canada; and §Division of Neurology, Department of Medicine, Faculty of Medicine and Dentistry, University of Alberta, Edmonton, Alberta, Canada

Address correspondence to Fernando Cendes, Departamento de Neurologia, Faculdade de Ciências Médicas – UNICAMP, Cidade Universitária Zeferino Vaz, Campinas SP CEP 13083-970, Brazil. E-mail: fcendes@unicamp.br

Wiley Periodicals, Inc.
© 2014 International League Against Epilepsy

White matter abnormalities associate with type and localization of focal epileptogenic lesions

Brunno M. Campos¹; Ana C. Coan¹; Guilherme C. Beltramini²; Min Liu³; Clarissa L. Yassuda¹; Enrico Ghizoni¹; Christian Beaulieu³; Donald W. Gross⁴; Fernando Cendes¹.

¹Neuroimaging Laboratory, Department of Neurology, University of Campinas, Campinas, SP, Brazil.

²Neurophysics Group, Gleb Wataghin Physics Institute, University of Campinas, Campinas, SP, Brazil.

³Department of Biomedical Engineering, Faculty of Medicine and Dentistry, University of Alberta, Edmonton, Alberta, Canada.

⁴Division of Neurology, Department of Medicine, Faculty of Medicine and Dentistry, University of Alberta, Edmonton, Alberta, Canada.

Correspondence to: Fernando Cendes (Departamento de Neurologia, Faculdade de Ciências Médicas – UNICAMP, Cidade Universitária Zeferino Vaz, Campinas SP, Brazil, CEP 13083-970; Phone: +55 19 35218242; FAX: +55 19 35217711; Email: fcendes@unicamp.br)

Running title: WM integrity in AED-resistant epilepsies

Key words: Frontal lobe epilepsy, Temporal lobe epilepsy, Diffusion tensor image, Voxel based morphometry;

Abstract

Objective: To evaluate white matter (WM) integrity of distinct groups of patients with antiepileptic drug (AED)-resistant localization-related epilepsies.

Methods: We used diffusion tensor imaging (DTI) fiber-tractography and voxel-based morphometry (VBM) to investigate differences of WM micro- and macro-structural integrity in patients with different drug-resistant localization-related epilepsies: 17 with temporal lobe epilepsy with MRI signs of hippocampal sclerosis (TLE-HS), 17 with TLE and normal MRI (TLE-NL), 14 with frontal lobe epilepsy and subtle MRI signs of focal cortical dysplasia (FLE-FCD) and 112 healthy controls. We performed fiber-tractography through a semiautomatic deterministic method to yield average fractional anisotropy (FA), axial (AD) and radial (RD) diffusivity ipsilateral and contralateral to the epileptogenic zone of the following tracts based on their functional and anatomical relevance: body of fornix (BoF), body of cingulum (BoC), inferior frontal occipital (IFO) and uncinate fasciculi (UF). Additionally, we performed VBM of the WM maps to assess macro-structural integrity differences among groups.

Results: TLE-HS had ipsi- and contralateral decreased FA and increased RD for all tracts. VBM showed WM alterations mainly in the ipsilateral parahippocampal region and contralateral superior temporal gyrus. FLE-FCD showed bilateral FA decreases only in the BoC and ipsilateral RD increases also in the BoC. VBM showed WM reduction mainly in the ipsilateral precuneus and posterior and anterior cingulum. No significant WM alterations were found in the TLE-NL in DTI or VBM analysis.

Significance: WM abnormalities differ in distinct AED-resistant localization-related epilepsies. The diverse distribution of the WM damage in these patients suggests that the localization of the epileptic networks may play a role in the WM burden. However, the distinct degree of this damage, more accentuated in TLE-HS, also suggests that the underlying cause of the epilepsy is probably an additional factor to explain this WM damage.

Key words: Frontal lobe epilepsy, Temporal lobe epilepsy, Diffusion tensor imaging, Voxel-based morphometry.

Introduction

Structural neuroimaging studies have shown ample evidence that antiepileptic-drug (AED) resistant epilepsies, especially temporal lobe epilepsy (TLE) with hippocampal sclerosis (HS), have widespread gray matter abnormalities extending beyond the epileptogenic zone^{1, 2}. Moreover, widespread white matter (WM) density abnormalities have also been observed in these patients^{1, 3}. Previous diffusion tensor imaging (DTI) tractography studies reported abnormal WM tracts in various epilepsies^{4, 5, 6, 7}. In TLE-HS, DTI studies show bilateral and diffuse abnormal integrity, while in TLE with normal routine MRI the WM abnormalities are subtler^{8, 9, 10, 11, 12, 13}. These findings are concordant with the results of voxel based morphometry studies^{1, 2}. DTI can also delineate focal WM lesions in patients with focal cortical dysplasia (FCD), and may help explain the ictal spreading^{8, 14, 15}.

So far the causes or the consequences of these WM abnormalities have not been well clarified. Although cross-sectional studies will not definitively solve this question, the comparison of the patterns of WM abnormalities in different epileptic syndromes can improve our knowledge about the possible causes of WM damage. The purpose of the present study was to use voxel based morphometry (VBM), to look for macro-structural WM abnormalities and DTI analysis, to provides inferences of the WM microstructure for the evaluation of three distinct types of AED-resistant localization-related epilepsies: i) TLE associated with HS (TLE-HS); ii) TLE with normal MRI (TLE-NL); and iii) frontal lobe epilepsy with subtle MRI abnormalities suggestive of focal cortical dysplasia (FLE-FCD). We hypothesized that WM damage occurs in AED-resistant localization-related epilepsies irrespective of the epileptic syndrome and that the pattern of WM damage is different according to the localization of the presumed epileptogenic zone and the etiology.

Methods

Subjects

All patients and controls included in this study signed informed consent, approved by the Ethics Committee of the Faculty of Medical Sciences of the University of Campinas.

We included forty-eight patients with AED-resistant localization-related epilepsy followed at the Epilepsy Center of University of Campinas who fulfilled the inclusion

criteria described below. The patients were selected according to one the following characteristics:

- TLE-HS: Clinical and electroencephalographic (EEG) characteristics of TLE and MRI signs of HS (Figure 1-A). There were 17 patients with mean age of 38 years (age range=26-60 years; 77% women). Five of these patients underwent surgical resection due to refractory seizures with HS confirmed by histopathology and all have Engel Ia surgical outcome after an average follow-up of 30 months;
- TLE-NL: Clinical and EEG characteristics of TLE and normal routine MRI (Figure 1-B). There were 17 patients with mean age of 37 years (age range=21-61 years; 65% women). One patient underwent surgery due to refractory seizures with nonspecific findings revealed by histopathology and this patient has Engel Ia surgical outcome after a follow-up of 27 months;
- FLE-FCD: Clinical and EEG characteristics of FLE and subtle MRI abnormalities suggestive of FCD (Figure 1-C). There were 14 patients with mean age of 33 years (age range=22-49 years; 64% women). Two of these patients underwent surgical resection due to refractory seizures with FCD type IIA confirmed by histopathology¹⁶ and all had Engel III surgical outcome after an average follow-up of 24 months. The maintenance of seizures in these patients was attributed to the incomplete resection of the FCD due the proximity of eloquent cortex.

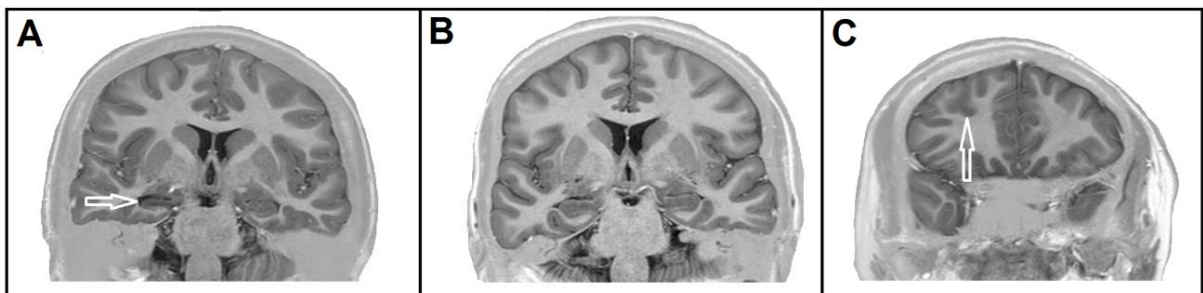


Figure 1: Example of coronal inverse recovery images of patient groups. **(A)** TLE-HS: arrow shows reduced right hippocampal volume compatible with hippocampal sclerosis; **(B)** TLE-NL: no MRI abnormalities detected; **(C)** FLE-FCD: arrow shows deep abnormal sulcus suggestive of focal cortical dysplasia.

Only patients with a clearly defined epileptogenic zone were selected (see Supporting Information for details). The epileptogenic zone of each patient was defined by a panel of specialists based on an extensive workup, which included prolonged scalp EEG

recordings (average of 200 minutes), video-EEG and, when appropriated, FDG-PET or ictal SPECT. All TLE-HS and FLE-FCD patients had the localization of the epileptogenic zone concordant with the MRI abnormality.

After a visual analysis for quality control of the MRI images, we included a group of 112 healthy individuals (mean age=35 years; age range=20-60 years; 68% women) for comparisons in the DTI study and a subset of 72 healthy individuals (mean age=32 years; age range=21-61 years; 56% women) for VBM analysis. Controls subjects were excluded from the VBM analysis due to image movement artifacts or due to different acquisition parameters. In this study, we acquired all MRI data on a 3T Philips Achieva (Best, The Netherlands) at the Neuroimaging Laboratory, University of Campinas-UNICAMP, Campinas, São Paulo, Brazil.

We defined MRI signs of HS as reduced volume and loss of internal structure of hippocampus on coronal T1-weighted images acquired perpendicular to the long axis of hippocampus (T1 "inversion recovery", 3 mm thick, no gap, voxel size=0.75x0.75x3 mm³, TR=3550 ms, TE=15 ms, inversion time=400 ms, matrix=240x229, FOV=180x180 mm², TSE factor=7) and hippocampal signal hyperintensity on T2-weighted and fluid attenuated inversion recovery (FLAIR) images (coronal T2 multi-echo image: 3 mm thick, no gap, voxel size=0.89x1x3 mm³, TR=3300 ms, TE=30/60/90/120/150 ms, matrix=200x180, FOV=180x180 mm², TSE factor=5; EPI factor=5; flip angle=90; FLAIR coronal and axial images: 4 mm thick, slice gap=1 mm, voxel size=0.89x1.12.4 mm³, TR=12000 ms, TE=140 ms, inversion time=2850 ms, matrix=180x440, FOV=200x200 mm²). The presence or absence of MRI signs of HS was also confirmed by automated volumetry and manual T2 signal quantification¹⁷.

We defined MRI signs of FCD as an area of cortical thickening, loss of the sharp interface between white and gray matter, and focal atrophy with or without T2 hyperintense signal^{16,18}. We did not observe transmantle signs in any of these exams. For the patients classified as FLE-FCD, the MRI exams were initially considered normal and the abnormalities were observed after multiplanar reconstruction of T1 and T2 images (T1W with isotropic voxels of 1 mm, acquired in the sagittal plane, 1 mm thick, no gap, flip angle=8°, TR=7.0 ms, TE=3.2 ms, matrix=240x240, FOV=240x240 mm²; T2W with isotropic voxels of 1.5 mm, acquired in the sagittal plane, no gap, TR=1800 ms, TE=340 ms, matrix=140x140, FOV=230x230 mm², Turbo Spin Echo factor= 120; flip angle=90; geometry corrected)¹⁸. Additionally, we carefully evaluated

the MRI images of patients in the TLE-NL group with multiplanar reconstruction and selected only those without signs suggestive of FCD.

DTI Analysis

DTI analysis provides inferences of the WM microstructure non-invasively by measuring the anisotropic water diffusion of the axon tracts. The basic assumption in DTI measurements is that the water diffusion perpendicular to the fiber orientation is constrained by axon membranes and myelination, whereas it is less hindered along the tract^{19, 20}. In this sense, the measures of fractional anisotropy (FA) and diffusion values as axial diffusivity (AD) or diffusivity in the tract direction, and radial diffusivity (RD) or diffusivity perpendicular to the tract direction, can quantify and characterize the water molecules movement, allowing an indirect assessment of the tract “integrity”. DTI tractography also allows the virtual reconstruction of the WM tracts. It provides *in vivo* depiction of large fasciculi and increases the specificity through the definition of pathology-relevant anatomical regions²¹.

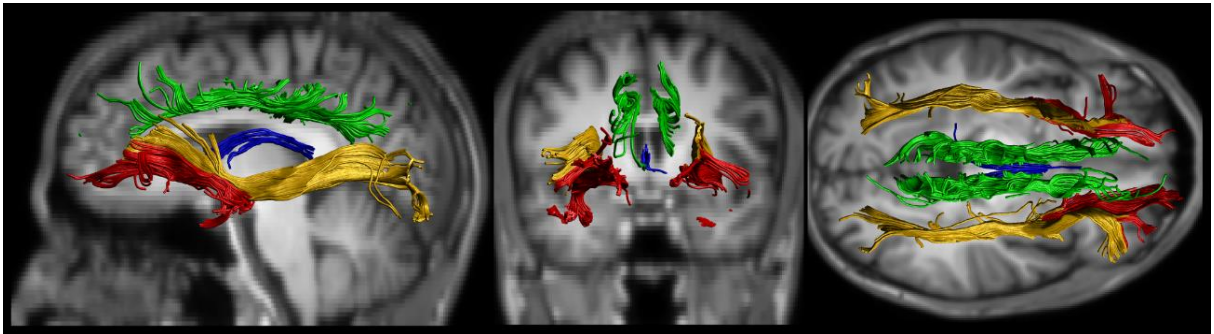


Figure 2: Fiber tractography of the studied tracts in a control subject. In green, the body of cingulum (BoC); in blue, the body of fornix (BoF); in red, the uncinate fasciculi (UF); in yellow, the inferior fronto-occipital fasciculi (IFO).

For tractography analysis, we acquired a spin echo single shot echo planar imaging (2x2x2 mm³ acquiring voxel size, interpolated to 1x1x2 mm³; reconstructed matrix 256x256; 70 slices; TE/TR 61/8500 ms; flip angle 90°; 32 gradient directions; no averages; max b-factor = 1000 s/mm²; six minutes scan).

We chose four tracts based on their functional and anatomical relevance to the spread of focal seizures originating in the temporal and frontal lobes: i) body of the cingulum (BoC); ii) body of the fornix (BoF); iii) uncinate fasciculi (UF); and iv) inferior fronto-occipital (IFO) fasciculi (Figure 2). The tensor calculation of all images was performed

using the ExploreDTI software (A. Leemans, University Medical Center, Utrecht, The Netherlands) and the fiber tractography through a semiautomatic deterministic methodology briefly described below²². Regions of interest (ROIs) to seed each tract were manually drawn on a normalized template. In this study, this template was created with non-diffusion weighted images of 10 local control subjects (mean age=33 years; age range=22-47 years; 50% women) acquired in the same MRI scanner, aiming to improve the anatomical matching to the study sample. Sequentially, the method uses the 3D deformation fields matrix of each subject to apply an inverse normalization operation (SPM8-Deformation fields algorithm), using the variants between native and standardized space to bring the normalized ROIs to that subject specific space. Finally, the adjusted (native space) ROIs were used for the fiber tracking.

The fiber tracking parameters set were the same for all studied fasciculi: minimal FA to start tract=0.25; minimal FA to keep tracking=0.25; maximal tract angle=60°; minimal fiber length=10 mm. We visually checked the resultant tracts and separately calculated the average FA, AD and RD for each hemisphere. The diffusion values were estimated by averaging all voxels in a given tract.

FA, AD and RD values were lateralized as ipsi- or contralateral to the presumed epileptogenic zone as defined by ictal/interictal scalp EEG recordings and concordant lateralized MRI abnormality (due to its interhemispheric positioning, the BoF will be always described without lateralization). The control subjects had their laterality defined randomly with the same proportions of patient groups (37% of the group within the right hemisphere considered as ipsilateral) respecting the gender distribution. The statistical analyses were performed using SPSS version 20 (IBM SPSS Statistics for Windows, Version 20. Armonk, NY: IBM Corp.). Multivariate General Linear Model (mGLM) with Tukey's Honestly-Significant-Difference Post Hoc test was used to evaluate differences between groups. Three distinct mGLM were performed, comparing FA, AD and RD separately whereas in each model, the ipsilateral and contralateral average values of each tract were included. Each mGLM Post Hoc test gave corrected (for multiple comparisons) p values and also, these statistical results were additionally controlled by the false discovery rate (FDR) accounting for the three independent comparisons.

Table 1: Clinical data and demography

	TLE-HS	TLE-NL	FLE-FCD
Gender	4 male/13 female	6 male/11 female	5 male/9 female
Age	38 (26-59) years	36 (21-60) years	33 (21-48) years
First seizure	9 (0.2 -17) years	16 (2-45) years	7 (1-14) years
Epilepsy duration	28 (11-52) years	20 (4-39) years	25 (11-46) years
Family history	6 (35%)	8 (47%)	3 (21.4%)
Laterality (EZ)	5 right/12 left	3 right/14 left	10 right/4 left
SGTCS*	1 (5%)	3 (17%)	7 (50%)

*: History of SGTCS in last year; EZ: Epileptogenic zone; IPI: initial precipitating injuries; TLE-HS: temporal lobe epilepsy with hippocampal sclerosis TLE-NL: non-lesional temporal lobe epilepsy; FLE-FCD: frontal lobe epilepsy - focal cortical dysplasia; SGTCS: secondary generalized tonic clonic seizure

VBM Analysis

For the VBM analysis, we used VBM8 plus DARTEL toolbox (<http://dbm.neuro.unijena.de/vbm8/>). All T1 weighted images were preprocessed using SPM8/VBM8 routines. The images were spatially normalized to the same stereotaxic space (DARTEL algorithm, MNI 152), segmented into WM, grey matter and cerebrospinal fluid, modulated (aiming to correct to locals volume changes during the normalization) and smoothed with an isotropic Gaussian kernel of 10 mm. The post processed WM image homogeneity was checked and finally compared using a voxel-wise statistical analysis. All patients with the epileptogenic zone on the right side had their images lateralized to the left side, so in the following section the left side is referred as ipsilateral and the right as contralateral to the epileptogenic zone. The controls images were randomly flipped in the same proportions (37%). The ANCOVA test was performed to compare the groups of controls and patients using age and gender as covariates. Three different contrasts were designed to separately verify the WM atrophy in each group of patient (family wise error (FWE) correction with $p < 0.05$ and minimum cluster size of five contiguous voxels).

Results

Multivariate analyses of variance (MANOVA) tested the similarity between the three groups of patients. There were no significant differences of the distribution of age ($p=0.39$; mean = 35 years; range = 60-21 years), gender ($p=0.70$), and epilepsy duration ($p=0.09$; mean = 22 years; range = 53-22 years). MANOVA showed significant difference for age of seizure onset with TLE-NL having older mean age at onset ($p=0.01$; Table 1). No difference in age (MANOVA p -value = 0.677; mean = 35 years; range = 60-20 years) and gender (MANOVA $p=0.788$) distribution was observed between the three groups of patients and controls. Additional clinical data is summarized in Table 1.

DTI Analysis

The mGLM performed to test FA between controls and the three epilepsy groups showed significant decrease of FA ipsilateral to the epileptogenic zone for the BoC ($p<0.001$), IFO ($p<0.001$) and UF ($p<0.001$). There was also decreased FA for the BoF ($p=0.003$). The Tukey's Post Hoc pairwise comparisons revealed significant FA decrease for the TLE-HS for all ipsilateral fasciculi (BoC $p=0.003$; IFO $p<0.001$; UF $p<0.001$) and for the BoF ($p=0.002$). Compared to controls, FLE-FCD group showed significant FA decreases in the Post Hoc test only in the BoC ($p=0.011$).

On the contralateral side, mGLM showed significant FA decreases for BoC ($p<0.001$), IFO ($p<0.001$) and UF ($p=0.006$). The Tukey's Post Hoc pairwise comparisons revealed significant FA differences between controls and TLE-HS in all contralateral fasciculi (BoC $p=0.001$; IFO $p<0.001$; UF $p=0.007$). Compared to controls, FLE-FCD group showed contralateral significant decreased FA only in the BoC ($p=0.048$).

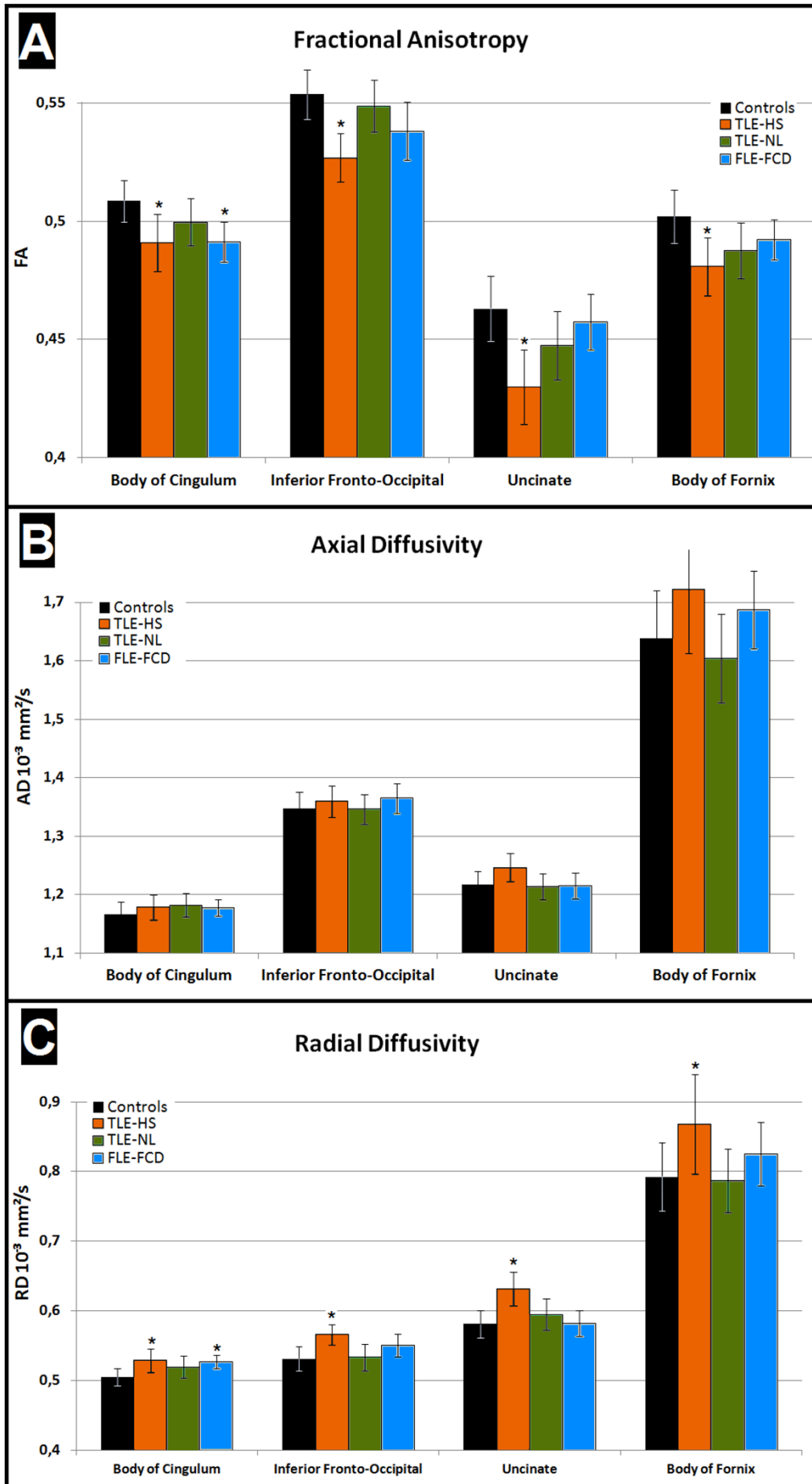


Figure 3: Ipsilateral average diffusion values (and BoF total diffusion values) separated by tracts and groups. TLE-HS patients presented decreased FA ("A") and increase radial diffusivity ("C") for all tracts, while FLE-FCD patients showed decreased FA and increased RD only in the BoC. No abnormalities in axial diffusivity ("B") were found in this study. TLE-NL patients did not have diffusion abnormalities in any of these tracts. .The * indicates parameters with significant difference (mGLM, Tukey's Post Hoc test, $p < 0.05$) when compared to control group.

We found no significant differences between controls and TLE-NL. The average ipsilateral FA values for each tract of all groups with the respective standard deviations are shown in Figure 3-A.

There were no significant differences of AD in the ipsi and contralateral fasciculi or the BoF for each epilepsy groups versus controls. The average ipsilateral AD values of each tract with respective standard deviations are represented in Figure 3-B.

There were significant ipsilateral alterations of RD in all studied tracts: BoC ($p < 0.001$), IFO ($p = 0.001$) and UF ($p < 0.001$) as well as the BoF ($p = 0.031$). The Post Hoc pairwise comparisons showed RD differences between controls and TLE-HS in the ipsilateral BoC ($p = 0.004$), IFO ($p = 0.001$) and UF ($p < 0.001$) and also in the BoF ($p = 0.027$). Furthermore, the Post Hoc test showed ipsilateral decrease of RD in FLE-FCD compared to controls only for the BoC ($p = 0.022$). No significant differences for ipsilateral RD values were found comparing controls and TLE-NL.

There was also differences of RD in the contralateral side for all studied tracts (BoC $p < 0.001$, IFO $p = 0.001$ and UF $p = 0.006$). The Tukey Post Hoc pairwise comparisons revealed significant increases of the RD values on the contralateral side only for the TLE-HS group compared to controls (BoC $p = 0.003$, IFO $p = 0.001$ and UF $p = 0.003$).

VBM Analysis

In comparison with controls, TLE-HS showed extensive mesial temporal WM volumetric decreases including mesial temporal regions thalamic region and posterior cingulum in the hemisphere ipsilateral to the epileptogenic zone but also in the superior temporal gyrus contralateral to the epileptogenic zone (Figure 4-A). For the FLE-FCD group, VBM showed significant WM atrophy exclusively localized in the hemisphere ipsilateral to the epileptogenic zone including the anterior and posterior cingulum and

precuneus (Figure 4-C). No WM volumetric alterations were found in the TLE-NL group (Figure 4-B). All complementary results are presented in Table 2.

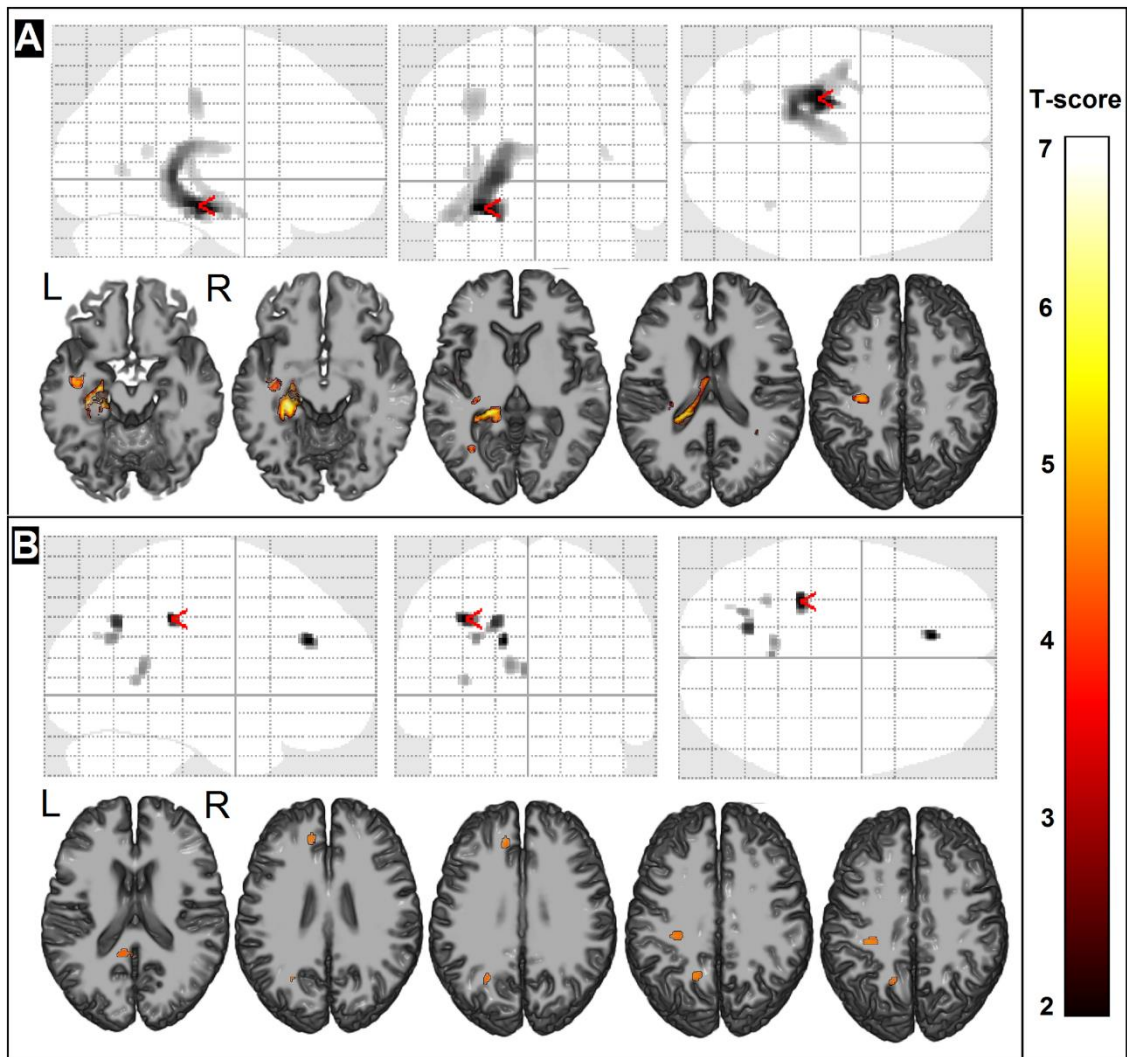


Figure 4: White matter voxel based morphometry results ($p < 0.05$ FWE corrected, cluster with at least 5 voxels). **(A)** temporal lobe epilepsy associated with hippocampus sclerosis: extensive WM atrophy in the ipsilateral parahippocampal gyrus (global maxima). **(B)** frontal lobe epilepsy with MRI signs of focal cortical dysplasia: WM atrophy restricted to the ipsilateral hemisphere and more important in the post central gyrus. Red arrow heads indicate the most statistically significant areas. Temporal lobe epilepsy with normal MRI presented no WM atrophy using this statistical threshold.

Table 2: White Matter Voxel Based Morphometry of T1-weighted MRI

Group	Laterality	Coordinate	N° Voxels	Structure
TLE-HS	Ipsi	-26 -24 -15	1294	Parahippocampal gyrus
	Ipsi	-30 -25 42	212	Postcentral gyrus
	Ipsi	-33 -63 4	30	Middle occipital gyrus
	Contra	36 -51 13	15	Superior temporal gyrus
TLE-NL	--	--	--	--
FLE-FCD	Ipsi	-32 -33 39	64	Postcentral gyrus
	Ipsi	-12 38 28	46	Medial frontal gyrus
	Ipsi	17 -63 37	86	Precuneus
	Ipsi	-2 -49 13	55	Posterior cingulate

TLE-HS: temporal lobe epilepsy with hippocampal sclerosis; TLE-NL: non-lesional temporal lobe epilepsy; FLE-FCD: frontal lobe epilepsy with focal cortical dysplasia; Ipsi: Ipsilateral to the syndrome lateralization; Contra: contralateral to the syndrome lateralization

Discussion

In the current study, WM micro- and macro-structural integrity was evaluated in three groups of AED-resistant localization-related epilepsies. Our results demonstrate that the patterns and the degree of WM abnormalities differ among groups according to the localization of the epileptogenic zone and the presumed etiology. While TLE-HS patients are those with the most diffuse injury, WM damage also occurs in FLE-FCD but could not be detected in TLE-NL by either DTI or VBM.

In this study both DTI and VBM showed that patients with TLE-HS have widespread abnormalities in tract integrity including extra-temporal structures such as cingulum^{11, 23, 24}. Although extra-temporal areas in both hemispheres are also affected in TLE-HS, the most significant damage is observed in the tracts directly connected with the hippocampus ipsilateral to the epileptogenic zone. The diffuse abnormal FA and RD (and the absence of AD abnormalities) observed in these patients suggest that HS pathology co-exists with widespread myelin degeneration, or maldevelopment, affecting the structural connectivity of the hippocampus^{4-7, 23-28}.

In the present study, with the defined statistical parameters and thresholds, no micro or macrostructural WM abnormalities were observed in the TLE-NL group. However,

caution should be taken with this result and we certainly can not affirm that TLE-NL patients have no abnormal tracts. Indeed, a previous study showed significant FA reduction on the posterior part of the cingulum on TLE-NL, suggesting that subtle abnormalities may be diluted by the whole tract analysis¹¹. What is clear with our results, however, is that, if present, the WM abnormalities on TLE-NL patients are subtler than what is observed for both TLE-HS and FLE-FCD. The rationale for this finding could be the different substrate of underlying pathology in TLE-NL or the significant older age of epilepsy when most of the WM maturation has occurred. This hypothesis is supported by a previous study showing that FA increases with age for most of the tracts, more rapidly initially in early ages and reaching a plateau during the late teens or twenties²².

In the FLE-FCD group, FA abnormalities were seen only in the BoC, which is the fasciculus anatomically related to the frontal region. The IFO fasciculi are also related to the frontal regions but possible alterations in the frontal portion of this tract (which is a small portion of the whole tract) could be diluted. In addition, RD abnormalities were found only in the cingulum of FLE-FCD patients. The VBM analysis of the FLE-FCD group showed WM atrophy in areas concordant to the DTI study, including areas ipsilateral to the epileptogenic zone, such as posterior cingulate and medial frontal gyrus. In contrast to the TLE-NL group, the FLE-FCD patients had subtle structural MRI lesions. This information agrees with the hypothesis that focal cortical lesions could widely affect the structural connectivity by a consequent net of axon degeneration.

Considering the other atrophic areas indicated by the VBM in the FLE-FCD group, it is notable the coincidence of the WM alterations with the ipsilateral structures of the default mode network (DMN)²⁹. The DMN concept is based on a set of brain areas that consistently activates in passive control situations and that could be accessed during resting state functional MRI experiments. DMN could be associated with spontaneous cognition, as recounting of recent happenings and expectations about the future³⁰. Furthermore, in the DTI analysis, the only abnormal tract detected in FLE-FCD was the ipsilateral cingulum, which connects the posterior cingulate cortex to the medial frontal cortex, two important components of the DMN³¹. Decreased connectivity in areas of the DMN ipsilateral to the epileptogenic zone has been detected in patients with FLE-FCD³². This pattern of WM disruption was not observed in the two TLE

groups. Although in the TLE-HS group the BoC was also abnormal in the DTI analysis, the VBM analysis demonstrated WM damage only to the anterior portion of the cingulum, which is indeed connected to the limbic system³².

Although we have demonstrated the distinct patterns of WM damage in patients with different AED-resistant epilepsy syndromes, we certainly cannot definitely answer what are the determinants of the occurrence of this injury. One possible mechanism associated to the WM damage is the occurrence of seizures and the pattern of seizure propagation. In this study, all patients were refractory to AEDs. Since this is a cross-sectional study, the number of seizures across life could not be specifically determined. However, we could compare the occurrence or not of secondary generalized tonic-clonic seizures (SGCTS) in the year prior to the MRI acquisition. As expected for clinical cohorts of patients with epilepsy, the group with the lower number of individuals with SGTCS was the TLE-HS group. However, this is exactly the group with the most significant WM abnormalities on both DTI and VBM analysis. Another possible mechanism not thoroughly evaluated so far is the influence of the underlying cause of the epilepsy in the diffuse brain structure damage. TLE-HS is the most studied form of epilepsy and, as observed in our study, this is the epileptic syndrome with the most extensive gray and WM injury². Our study adds the information that patients with subtle MRI signs of FCD also have WM damage, while in those with normal MRI, no significant WM abnormality could be detected. This suggests that the underlying cause of the epilepsy is an important factor that could explain the abnormal WM integrity in patients with focal epilepsy. One limitation of our study is the absence of histological confirmation of HS and FCD for all patients. We have, however, strong neuroimaging evidence that supports the classification of our patients in the three distinct groups. The definition of HS included both visual analysis and MRI quantification measurements confirming decreased volume and hyperintense T2 signal in the hippocampus. For patients with FLE-FCD and TLE-NL, an expert in the field (FC) performed an exhaustive MRI analysis with multiplanar reconstruction before the definition of signs of FCD or normal MRI. Also, the small sample of patients submitted to surgery confirmed the classification in all cases (5 confirmed HS in TLE-HS, 2 confirmed FCD in FLE-FCD and one absence of specific histology findings in TLE-NL). Also, one may argue that this could be a limitation to the accurate lateralization of the epileptogenic zone what could have masked some abnormalities, especially in the

group with normal tracts, TLE-NL. However, the patients included in the present study have undergone a strict selection and only those with clear lateralization of the epileptogenic zone were selected, as described in the methods.

The lateralization of the MRI scans according to the epileptogenic zone in the present study enabled the observation of specific abnormalities of each epilepsy type using a larger number of subjects. However, this methodology does not allow inferences about brain hemispheres particularities. It is known that the epileptogenic hemisphere includes more relevant WM alterations, but previous DTI studies have also shown differences between right and left TLE patients¹⁰. The aim of the present study was to compare epilepsy-specific abnormalities, regardless of side of epileptogenic zone, and side-specific sub analysis should be done in the future with a larger sample size.

As described above, another limitation is the absence of the segmental analysis of the selected tracts. This approach could increase the sensitivity to detect abnormalities especially in the group of patients with TLE-NL and we believe it has its most importance in the analysis of patient specific abnormalities, what was not the aim of the present study. In fact, the statistical approach applied in this study most likely detected abnormalities present in most patients in each group, while it likely missed additional WM abnormalities present in individual patients.

In conclusion, WM integrity is disrupted in AED-resistant localization related epilepsies and this abnormality varies according to the underlying pathological substrate and localization of seizure focus. Although the implications of these WM abnormalities remain unknown, further studies with larger sample size may help to characterize specific focal WM disruptions associated with epileptogenic lesions in individual patients with localization related epilepsies. Whether these WM abnormalities will help in predicting response to clinical and surgical treatment remains to be determined.

Acknowledgements

Study supported by FAPESP (São Paulo Research Foundation), grant 2013/07559-3. ACC was funded by FAPESP, grant 2013/00099-7.

Disclosure of Conflicts of Interest

None of the authors has any conflict of interest to disclose.

We confirm that we have read the Journal's position on issues involved in ethical publication and affirm that this report is consistent with those guidelines.

References:

1. Mueller SG, Laxer KD, Cashdollar N, *et al.*.Voxel-based Optimized Morphometry (VBM) of Gray and White Matter in Temporal Lobe Epilepsy (TLE) with and without Mesial Temporal Sclerosis. *Epilepsia* 2006;47:900-907
2. Coan AC, Campos BM, Yasuda CL, *et al.*. Frequent Seizures Are Associated with a Network of Gray Matter Atrophy in Temporal Lobe Epilepsy with or without Hippocampal Sclerosis. *PLoS ONE* 2014;9:e85843
3. Yasuda CL, Valise C, Saúde AV, *et al.*. Dynamic changes in white and gray matter volume are associated with outcome of surgical treatment in temporal lobe epilepsy. *NeuroImage* 2010;49: 71–79
4. Gross DW, Concha L, Beaulieu C. Extratemporal White Matter Abnormalities in Mesial Temporal Lobe Epilepsy Demonstrated with Diffusion Tensor Imaging. *Epilepsia* 2006;47:1360–1363.
5. Rodrigo S, Oppenheim C, Chassoux F, *et al.*. Unicnate fasciculus fiber tracking in mesialtemporal lobe epilepsy. Initial findings. *European Radiology* 2007;17:1663–1668
6. Concha L, Kim H, Bernasconi A, *et al.*. Spatial patterns of water diffusion along white matter tracts in temporal lobe epilepsy. *Neurology* 2012;79:455-462
7. Liacu D, Idy-Peretti I, Ducreux D, *et al.*. Diffusion Tensor Imaging Tractography Parameters of Limbic System Bundles in Temporal Lobe Epilepsy Patients. *Journal of Magnetic Resonance Imaging* 2012; 36:561–568
8. Gross DW, Bastos A, Beaulieu C. Diffusion Tensor Imaging Abnormalities in Focal Cortical Dysplasia. *Can. J. Neurol. Sci.* 2005;32:477-482
9. Duffau H, Thiebaut de Schotten M, Mandonnet E. White matter functional connectivity as an additional landmark for dominant temporal lobectomy. *J Neurol Neurosurg Psychiatry* 2008;79:492-495
10. Ahmadi ME, Hagler Jr DJ, McDonald CR, *et al.*. Side Matters: Diffusion Tensor Imaging Tractography in Left and Right Temporal Lobe Epilepsy. *AJNR* 2009;30:1740-1747
11. Scanlon C, Mueller SG, Cheong I, *et al.*. Grey and white matter abnormalities in temporal lobe epilepsy with and without mesial temporal sclerosis. *J Neurol* 2013;260:2320–2329

12. Concha L, Beaulieu C, Collins DL *et al.*. White-matter diffusion abnormalities in temporal-lobe epilepsy with and without mesial temporal sclerosis. *Neurol Neurosurg Psychiatry* 2009;80:312-319
13. Liu M, Concha L, Lebel C, *et al.*. Mesial temporal sclerosis is linked with more widespread white matter changes in temporal lobe epilepsy. *NeuroImage: Clinical* 2012;1:99–105
14. Eriksson SH, Rugg-Gunn FJ, Baker GJ, *et al.*. Diffusion Tensor Imaging in Patients with Epilepsy and Malformations of Cortical Development. *Brain* 2001;124:617-626
15. Diehl B, Tkachc I, Piao P, *et al.*. Diffusion tensor imaging in patients with focal epilepsy due to cortical dysplasia in the temporo-occipital region: Electro-clinico-pathological correlations. *Epilepsy Research* 2010;90:178-187
16. Blümcke I, Thom M, Aronica, E, *et al.*. The clinicopathologic spectrum of focal cortical dysplasias: A consensus classification proposed by an ad hoc Task Force of the ILAE Diagnostic Methods Commission. *Epilepsia* 2011;52:158-174.
17. Coan AC, Bergo FPG, Campos BM, *et al.*. 3T MRI Quantification of Hippocampal Volume and Signal in Mesial Temporal Lobe Epilepsy Improves Detection of Hippocampal Sclerosis. *AJNR* 2014;35:77-83
18. Cendes F. Neuroimaging in Investigation of Patients with Epilepsy. *Epilepsy* 2013; 19:623–642
19. Beaulieu C. The Basis of Anisotropic Water Diffusion in the Nervous System - A Technical Review. *NMR In Biomedicine* 2002;15:435–455
20. Parker GJM, Wheeler-Kingshott CAM, Barker GJ. Estimating Distributed Anatomical Connectivity Using Fast Marching Methods and Diffusion Tensor Imaging. *IEEE Transactions on Medical Imaging* 2002;21:505-512
21. Gross DW. Diffusion tensor imaging in temporal lobe epilepsy. *Epilepsia* 2011; 52:32–34
22. Lebel C, Walker L, Leemans A, *et al.*. Microstructural maturation of the human brain from childhood to adulthood. *NeuroImage* 2008;40:1044–1055
23. Focke NK, Yogarajah M, Bonelli SB, *et al.*. Voxel-based diffusion tensor imaging in patients with mesial temporal lobe epilepsy and hippocampal sclerosis; *NeuroImage* 2008; 40:728–737
24. Crespela A, Coubes P, Rousseta MC, *et al.*. Inflammatory reactions in human medial temporal lobe epilepsy with hippocampal sclerosis. *Brain Research* 2002;952:159-169

25. Milesi G, Garbelli R, Zucca I, *et al.*. Assessment of human hippocampal developmental neuroanatomy by means of ex-vivo 7 T magnetic resonance imaging. *Int J Dev Neurosci* 2014;34:33-41
26. Bonilha L, Tabesh A, Dabbs K, *et al.*. Neurodevelopmental alterations of large-scale structural networks in children with new-onset epilepsy. *Hum. Brain Mapp.* 2014;35:3661-3672
27. Amarreh I, Dabbs K, Jackson DC, *et al.*. Cerebral white matter integrity in children with active versus remitted epilepsy 5 years after diagnosis. *Epilepsy Res* 2013;107:263-71
28. Mathern GW, Adelson PD, Cahan LD, *et al.*. Hippocampal neuron damage in human epilepsy: Meyer's hypothesis revisited. *Prog Brain Res* 2002;135:237-51
29. Van den Heuvel M, Mandl R, Luigjes J, *et al.*. Microstructural Organization of the Cingulum Tract and the Level of Default Mode Functional Connectivity. *Journal of Neuroscience* 2008;28:10844-10851
30. Greicius MD, Krasnow B, Reiss AL, *et al.*. Functional connectivity in the resting brain:A network analysis of the default mode hypothesis. *PNAS*;2003;253-258
31. Widjaja E, Zamyadi M, Raybaud C, *et al.*. Abnormal Functional Network Connectivity among Resting-State Networks in Children with Frontal Lobe Epilepsy. *AJNR* 2013;34:2386-2392
32. Concha, L., Gross, D. W., & Beaulieu, C. Diffusion tensor tractography of the limbic system. *American journal of neuroradiology* 2005;26:2267-2274.

4.2.2 ARTIGO 2: ANÁLISE DE CONECTIVIDADE FUNCIONAL

HUMAN BRAIN MAPPING

♦ Human Brain Mapping 37:3137–3152 (2016) ♦

Large-Scale Brain Networks Are Distinctly Affected in Right and Left Mesial Temporal Lobe Epilepsy

Brunno Machado de Campos, Ana Carolina Coan, Clarissa Lin Yasuda, Raphael Fernandes Casseb,* and Fernando Cendes*

Neuroimaging Laboratory, Department of Neurology, University of Campinas, Campinas, São Paulo, Brazil

♦ ————— ♦

Abstract: Mesial temporal lobe epilepsy (MTLE) with hippocampus sclerosis (HS) is associated with functional and structural alterations extending beyond the temporal regions and abnormal pattern of brain resting state networks (RSNs) connectivity. We hypothesized that the interaction of large-scale RSNs is differently affected in patients with right- and left-MTLE with HS compared to controls. We aimed to determine and characterize these alterations through the analysis of 12 RSNs, functionally parceled in 70 regions of interest (ROIs), from resting-state functional-MRIs of 99 subjects (52 controls, 26 right- and 21 left-MTLE patients with HS). Image preprocessing and statistical analysis were performed using UF²C-toolbox, which provided ROI-wise results for intranetwork and internetwork connectivity. Intranetwork abnormalities were observed in the dorsal default mode network (DMN) in both groups of patients and in the posterior salience network in right-MTLE. Both groups showed abnormal correlation between the dorsal-DMN and the posterior salience, as well as between the dorsal-DMN and the executive-control network. Patients with left-MTLE also showed reduced correlation between the dorsal-DMN and visuospatial network and increased correlation between bilateral thalamus and the posterior salience network. The ipsilateral hippocampus stood out as a central area of abnormalities. Alterations on left-MTLE expressed a low cluster coefficient, whereas the altered connections on right-MTLE showed low cluster coefficient in the DMN but high in the posterior salience regions. Both right- and left-MTLE patients with HS have widespread abnormal interactions of large-scale brain networks; however, all parameters evaluated indicate that left-MTLE has a more intricate bihemispheric dysfunction compared to right-MTLE. *Hum Brain Mapp* 37:3137–3152, 2016. © 2016 The Authors Human Brain Mapping Published by Wiley Periodicals, Inc.

Key words: functional connectivity; functional magnetic resonance imaging; default mode network; salience network; hippocampus; visuospatial network

♦ ————— ♦

Contract grant sponsor: FAPESP (São Paulo Research Foundation); Contract grant number: 2013/00099-7, 2013/07559-3, and 2014/15918-6

Correction added on 06 June 2016, after first online publication.

*Correspondence to: Fernando Cendes, Departamento de Neurologia, Faculdade de Ciências Médicas – UNICAMP, Cidade Universitária Zeferino Vaz, Campinas SP, Brazil, CEP 13083-970. E-mail: fcendes@unicamp.br

Conflicts of Interest: None of the authors has any conflict of interest to disclose. We confirm that we have read the Journal's

position on issues involved in ethical publication and affirm that this report is consistent with those guidelines.

Received for publication 14 January 2016; Revised 4 April 2016; Accepted 15 April 2016.

DOI: 10.1002/hbm.23231

Published online 2 May 2016 in Wiley Online Library (wileyonlinelibrary.com).

© 2016 The Authors Human Brain Mapping Published by Wiley Periodicals, Inc.

This is an open access article under the terms of the Creative Commons Attribution NonCommercial License, which permits use, distribution and reproduction in any medium, provided the original work is properly cited and is not used for commercial purposes.

Large-scale brain networks are distinctly affected in right and left mesial temporal lobe epilepsy

Brunno Machado de Campos¹; Ana Carolina Coan¹; Clarissa Lin Yasuda¹; Raphael Fernandes Casseb¹; Fernando Cendes¹.

¹Neuroimaging Laboratory, Department of Neurology, University of Campinas, Campinas, SP, Brazil

Correspondence to:

Fernando Cendes - Departamento de Neurologia,
Faculdade de Ciências Médicas – UNICAMP,
Cidade Universitária Zeferino Vaz, Campinas SP, Brazil,
CEP 13083-970;
Phone: +55 19 35218242;
FAX: +55 19 35217711;
Email: fcendes@unicamp.br

Short Title: Brain networks in right and left MTLE

Key words: functional connectivity; fMRI, default mode network; salience network; hippocampus; visuospatial network

Abstract

Mesial temporal lobe epilepsy (MTLE) with hippocampus sclerosis (HS) is associated with functional and structural alterations extending beyond the temporal regions and abnormal pattern of brain resting state networks (RSNs) connectivity. We hypothesized that the interaction of large-scale RSNs is differently affected in patients with right- and left-MTLE with HS compared to controls. We aimed to determine and characterize these alterations through the analysis of 12 RSNs, functionally parceled in 70 regions of interest (ROIs), from resting-state functional-MRIs of 99 subjects (52 controls, 26 right- and 21 left-MTLE patients with HS). Image preprocessing and statistical analysis were performed using UF²C-toolbox, which provided ROI-wise results for intra- and inter-network connectivity.

Intra-network abnormalities were observed in the dorsal default mode network (DMN) in both groups of patients and in the posterior salience network in right-MTLE. Both groups showed abnormal correlation between the dorsal-DMN and the posterior salience, as well as between the dorsal-DMN and the executive-control network (ECN). Patients with left-MTLE also showed reduced correlation between the dorsal-DMN and visuospatial network and increased correlation between bilateral thalamus and the posterior salience network. The ipsilateral hippocampus stood out as a central area of abnormalities. Alterations on left-MTLE expressed a low cluster coefficient, whereas the altered connections on right-MTLE showed low cluster coefficient in the DMN but high in the posterior salience regions.

Both right- and left-MTLE patients with HS have widespread abnormal interactions of large-scale brain networks; however, all parameters evaluated indicate that left-MTLE has a more intricate bihemispheric dysfunction compared to right-MTLE.

Introduction

Mesial temporal lobe epilepsy (MTLEs) is associated with functional and structural changes that extend beyond the temporal regions (Holmes *et al.*, 2013; Liu *et al.*, 2012). Hippocampus sclerosis (HS) is the hallmark of most MTLE (Cendes *et al.*, 1993) and studies indicate that MTLE with HS involves a complex pattern of brain functional and structural alterations (Holmes *et al.*, 2013; Pittau *et al.*, 2012; Campos *et al.*, 2015). Functional magnetic resonance imaging (fMRI) during task-free conditions has been widely used to portray functional network characteristics in both normal and pathological conditions (Seeley *et al.*, 2009), including MTLE. Different studies have investigated the impact of MTLE on these resting state networks (RSNs) (Bettus *et al.*, 2009; Cataldi *et al.*, 2013; Haneef *et al.*, 2014; Liao *et al.*, 2010), including analysis of specific networks such as the default mode network (DMN) and the salience network. (Zhang *et al.*, 2010).

Other studies have used different approaches (i.e. ICA, seed based connectivity) to explore some specific RSNs such as the DMN (Liao *et al.*, 2011), perceptual (Zhang *et al.*, 2009a) and attention networks (Zhang *et al.*, 2009b). These studies revealed altered networks, compared to controls. The overall activation of DMN in MTLE is apparently reduced, as well as the functional connectivity between its nodes (Liao *et al.*, 2011). Some of these studies also demonstrated that MTLE affects the attention networks and perceptual networks, resulting in significant abnormal impairment between their regions (Cataldi, *et al.*, 2013). These findings could explain the worst performances of these patients on cognitive tasks as memory and language, as well as on auditory and visual naming activities (Alessio *et al.*, 2006; Vannest *et al.*, 2008).

Given the characteristics of a network-level pathology in MTLE (Spencer, 2002), other studies have examined graph-theory properties (Bullmore and Sporns, 2009) of both structural (Bernhardt *et al.*, 2011; Bonilha *et al.*, 2013) and functional data (Liao *et al.*, 2010; Vlooswijk *et al.*, 2011). These studies evaluated the relationships between the syndrome alterations and properties such as degree of connectivity, clustering coefficient and hub distribution, demonstrating alterations in MTLE characterized by reduced specificity and global efficiency (Bernhardt *et al.*, 2011; Liao *et al.*, 2010). Most of the previous graph theory studies in MTLE have applied anatomical parcellation to functional maps and compared differences between right and left MTLE groups in comparison to controls (Bettus *et al.*, 2009; Wang *et al.*, 2009). The use of functional

parcellation aims to improve the access to alterations on the cerebral functional organization. Since we can define the brain functional networks as inherent patterns of areas dynamically correlated during a specific task or at rest (Eguíluz et al., 2005), the direct study of these patterns and the interaction of its sub-areas could improve the identification of changes related to abnormal behavior, or secondary to neurological diseases.

Despite the information about specific RSNs in MTLE, there is no current data about how these networks interact in this condition and whether this interaction differs between patients with right or left HS. As mentioned before, it is well known that patients with left MTLE have worse performance in memory tasks and distinct structural damage of cerebral gray and white matter than patients with right MTLE (Keller et al., 2002; Riederer et al., 2008; Besson et al., 2014). These data put together implies that right and left MTLE could have different pathological mechanisms. Although previous studies have focused on the differences in functional connectivity between these groups of patients, these analyses were restricted to specific brain nodes, more often including the hippocampal region (Zhang et al., 2010; Pereira et al., 2010; Morgan et al., 2012). However, today it is accepted that in order to understand the brain function and its disruptions, we must move forward from looking at specific brain regions and try to understand how the different areas interact and the possible abnormalities of this interaction. Therefore, the study of inter-correlations among RSNs in right and left MTLE might improve the understanding of the underlying mechanisms associated with these conditions.

We hypothesized that inter- and intra-network connectivity of RSNs is differently altered in patients with right and left MTLE compared to controls. In order to investigate that, we studied connectivity between RSNs using regions of interest (ROIs) derived from a functional parcellation in homogeneous groups of MTLE patients with unilateral HS.

Methods

Subjects

All patients and controls included in this study signed an informed consent, approved by the Ethics Committee of the University of Campinas.

We included 47 consecutive adult patients with clinical and electroencephalographic diagnosis of drug-resistant MTLE and MRI signs of unilateral HS followed at the Epilepsy Clinic of the University of Campinas. The clinical diagnosis of MTLE was based on ILAE criteria (Berg et al., 2010). All patients had seizure semiology compatible with seizure onset in the mesial temporal structures and had failed at least two antiepileptic drugs at the moment of the enrollment in this study. All underwent extensive inter-ictal and/or ictal scalp EEG recordings, with epileptiform abnormalities restricted to the anterior and medial temporal electrodes. MRI scans acquired with a protocol for epilepsy were reviewed by two different epileptologists (FC and ACC) looking for signs of HS (clear loss of internal structure and volume reduction on T1 WI and signal hyperintensity on T2 WI/FLAIR). Secondly, MRI signs of HS were confirmed through quantification of volume and T2 signal according to our center protocol (Coan et al., 2014b). In this study, patients classified with bilateral HS were not selected. According to the side of the HS and the ictal/interictal EEG abnormalities, patients were classified as right (R-MTLE) or left (L-MTLE) MTLE. Only patients with concordant laterality on MRI and EEG were selected.

MRI acquisitions

All patients and controls underwent 3-tesla MRI (Philips Achieva) according to the following protocol:

1. Structural images: T1 weighted image (WI) with isotropic voxels of 1 mm, acquired in the sagittal plane, 180 slices, 1 mm thick, no gap, flip angle=8°, TR=7.0 ms, TE=3.2 ms, , FOV=240x240 mm².
2. Functional images: patients and controls were submitted to either one of two distinct functional protocols: P1) echo planar image (EPI) with isotropic voxel of 3 mm, acquired on the axial plane with 32 slices, gap of 0.3 mm, matrix=80x80, flip angle=75°, TR=2 s, TE=30 ms, in a 6 minute scan resulting in 180 dynamics; P2) EPI with isotropic acquisition voxel of 3 mm, acquired on the axial plane with 39 slices, no gap,

matrix=80x80, flip angle=90°, TR=2 s, TE=30 ms in a 6 minute scan resulting in 180 dynamics. The main difference between protocols was the coverage of inferior cerebellar regions. Therefore, we did not include the inferior cerebellum in the analyses as described below.

In total, we selected 99 subjects according to clinical, demographic and MRI parameters (Table I): 52 controls, 26 patients with R-MTLE and 21 patients with L-MTLE.

Table I: Demographic and clinical information

Group	Controls	R-MTLE	L-MTLE
Age (years)	43 (\pm 13)	46 (\pm 7)	47 (\pm 6)
Female	52%	58%	48%
Seizure Onset (years)		12 (\pm 9)	8 (\pm 7)
Epilepsy Duration (years)		33 (\pm 11)	39 (\pm 9)
Familiar History of Epilepsy		50%	45%
Protocol Type (P1/P2)	26/26	20/6	15/6

For “Age”, “Seizure Onset” and “Epilepsy Duration” the values represent the mean and the standard deviation. In the fields “Female” and “Family History” the values represent the percentage of occurrence of these factors in each group.

There was no difference between the groups considering age and gender. Significant differences were observed only between controls and R-MTLE group on the proportion of the protocol types (pairwise Fisher’s Exact Test, two-tailed p-value = 0.028); therefore, this was considered as a covariate on the analysis.

Additionally, we found no differences between patients groups regarding age at seizures onset, duration of epilepsy and family history of epilepsy.

Functional connectivity

The UF²C - User Friendly Functional Connectivity toolbox

The UF²C toolbox (<http://www.lni.hc.unicamp.br/app/uf2c/>) was developed by the author (Campos, BM) aiming to standardize and facilitate connectivity studies through a straightforward graphical user interface and validated preset parameters. The toolbox runs within MATLAB platform (2014b, The MathWorks, Inc. USA) with SPM12 (Statistical Parametric Mapping 12, <http://www.fil.ion.ucl.ac.uk/spm/>) and it is freely available for download.

We preprocessed and performed the statistical analysis (first and second level) according to the UF²C standard pipeline. The preprocessing was based on: fMRIs dynamics realignment (using mean image as reference), images co-registration (fMRI mean image with T1 WI), spatial normalization (MNI-152), smoothing (kernel of 6x6x6 mm³ at FWHM) and T1 WI tissue segmentation (grey matter (GM), white matter (WM) and cerebral spinal fluid (CSF)) and normalization (MNI-152). The segmented GM maps were interpolated to match the functional images and used to mask the analysis, removing non-GM regions. Additionally, we regressed out six head motion parameters (three rotational and three translational) as well as WM and CSF average signals. Finally, we detrended (removed linear trends) and band-pass filtered (0.008-0.1 Hz) the time-series. The Fig.1 is a flowchart representing all the processing steps.

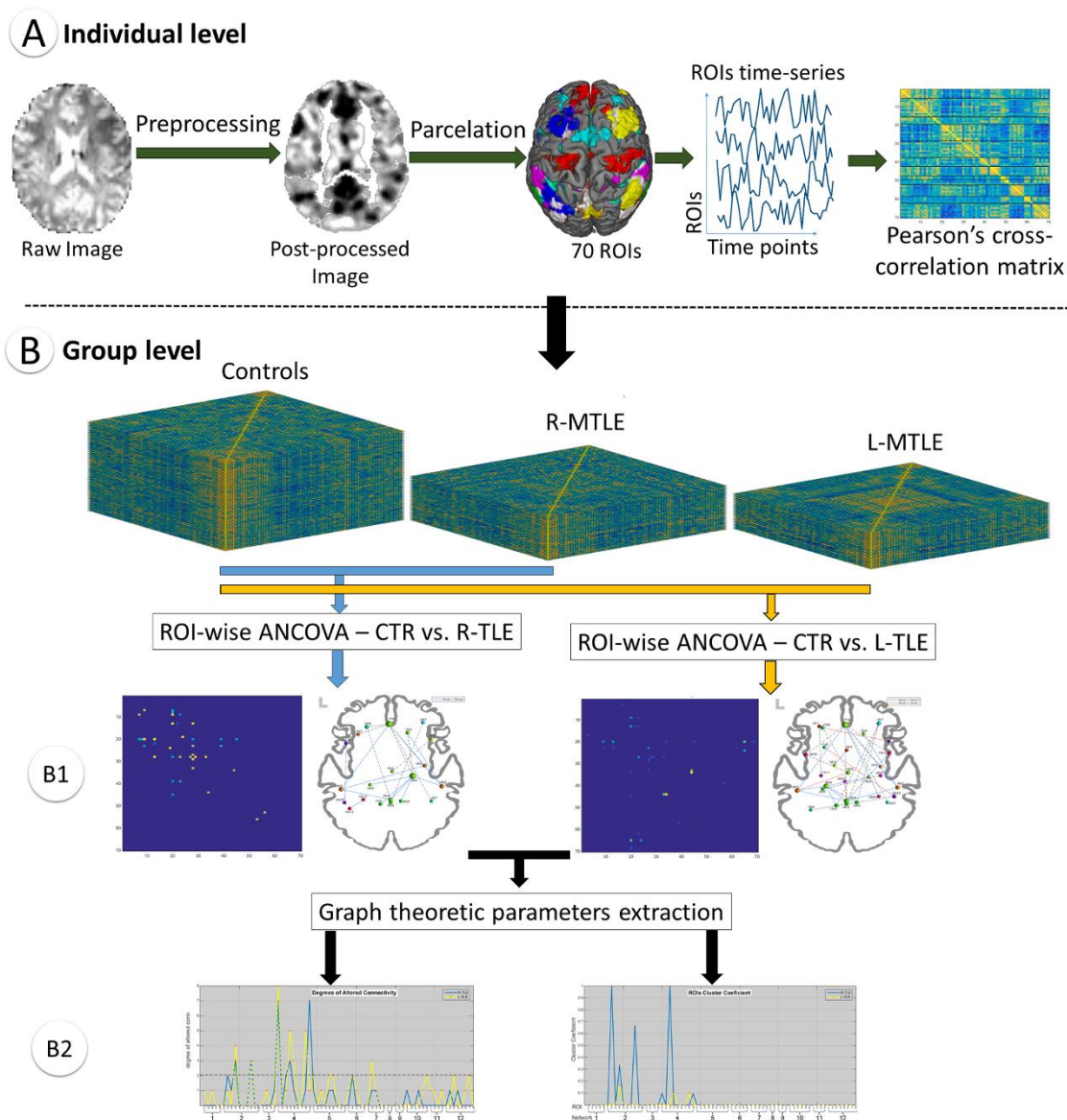


Fig.1: Pre- and post-processing flowchart for first and second statistical levels. The part “A” describes all individual steps included in the first level statistical analysis. The part “B” describes the group level statistical and graph-theory analysis.

ROIs: regions of interest; R-MTLE: right mesial temporal lobe epilepsy; L-MTLE: left mesial temporal lobe epilepsy; CTR: control group.

Regions of interest and cross-correlation matrices

For the first level analysis, we generated individual matrices based on ROIs derived from a functional parcellation. Instead of applying anatomical parcellation as seen in previous studies, we used 70 ROIs from 12 functional networks previously created and described by *Shirer et al (2012)*: *Anterior Salience* (network code=n1, number of ROIs=5), *Posterior Salience* (network code=n2, number of ROIs=10), *Basal Ganglia* (network code=n3, number of ROIs=4), *Dorsal DMN* (network code=n4, number of ROIs=9) *Ventral DMN* (network code=n5, number of ROIs=9) *left ECN* (network code=n6, number of ROIs=5), *right ECN* (network code=n7, number of ROIs=5), *Auditory* (network code=n8, number of ROIs=2), *Visual* (network code=n9, number of ROIs = 3), *Language* (network code=n10, number of ROIs=6), *Sensorimotor* (network code=n11, number of ROIs=4) and *Visuospatial/Dorsal Attention* (network code=n12, number of ROIs=8). We selected these ROIs to evaluate functional connectivity in widespread brain areas considering distributed relevant functional networks. The Visual network in this study is the union of the ROIs from the High and Prime visual networks described by Shirer et al (2012).

As we observed FOV variations between functional protocols in the inferior portion of the cerebellum, no ROIs from this area were included to avoid data from the bottom of the images. Therefore, in our analysis, we excluded the following ROIs due to their positioning on the inferior portion of the cerebellum: two ROIs from the Anterior Salience network (ROIs 6 and 7); two from the Posterior Salience (ROIs 8 and 11); one from Basal Ganglia (ROI 5); one from Language (ROI 7); one from LECN (ROI 5); one from RECN (ROI 5); two from Sensorimotor (ROIs 4 and 6); one from ventral DMN (10); three from Visuospatial (ROIs 9, 10 and 11). Additionally, one ROI was excluded due to its small size: Visual (prime visual 2) with 4 voxels.

Time-series were consistently extracted from each ROI of each subject. For a specific ROI, we used the average time series of all ROI voxels that matched two consecutive criteria:

- a. Being included on the subject GM mask;
- b. The UF²C correlates each single ROI voxel time series with the average ROI time series (GM-masked). The voxel was included (to the average) if its correlation value is within the average \pm standard deviation of all correlations between the between the ROI-masked voxels.

The cross-correlation matrices were created by performing Pearson's correlation tests (2415 tests, pair-wise combination of all the 70 ROIs, removing auto (diagonal) and symmetric correlations). These individual correlation matrices were subsequently converted to z-score (Fisher's Z-transformation) and taken to a second level analysis to investigate differences between controls and patients groups.

Group comparisons

The second level analyses were performed also using an appropriate modality on UF²C toolbox. As a first step, to evaluate confounding effects induced by the two different fMRI acquisition protocols, we performed an additional test, comparing only control subjects, who were divided into two groups with pure protocol types (26 controls with protocol type "P1" and 26 with protocol type "P2"). No significant differences were detected between these groups of control subjects ($\alpha=0.05$, false discovery rate (FDR) corrected).

In order to evaluate and characterize how right or left MTLE functionally affects the RSN behaviors and interactions, we evaluated inter-ROIs connectivity considering the inter- (among ROIs of different networks) and intra-network (among ROIs of a same network) interactions. For that, we performed MANCOVA tests, with a protocol type variable as covariate and $\alpha=0.0375$ (due to the two multiple pair-wise group comparisons – FDR correction). All tests between ROIs (2415 tests) were also corrected for multiple comparisons using the FDR procedure (Benjamini, and Hochberg, 1995) and only corrected sub threshold results ($p<0.0375$) were considered significant.

It is important to highlight and clarify some terms applied in this study. "Relative decreased connectivity" (Fig.2-A and B) and "relative increased connectivity" (Fig.2-C and D) indicate lower or higher absolute Person's correlation scores of patients compared to the control group's respective scores. In this sense, the idea of "decreased" or "increased" means that the Person's correlation values are respectively

farther or closer to zero when compared to controls, regardless of whether the correlation is positive (Fig.2-A and C) or negative (Fig.2-B and D). Interestingly, we also detected some situations in which the correlation scores from patients presented opposite signals compared to controls. Despite the usage of absolute r-score values to define the direction of the differences among groups, the statistical tests were performed with the original values (transformed to z-score, but keeping the original signals), making sure that comparisons among correlations in opposite directions (Fig. 2-E and F) have been considered accordingly in the statistical analysis. For these scenarios, the graphical results (Fig.3) do not show these alterations as decreased or increased, but just indicate them with dashed lines.

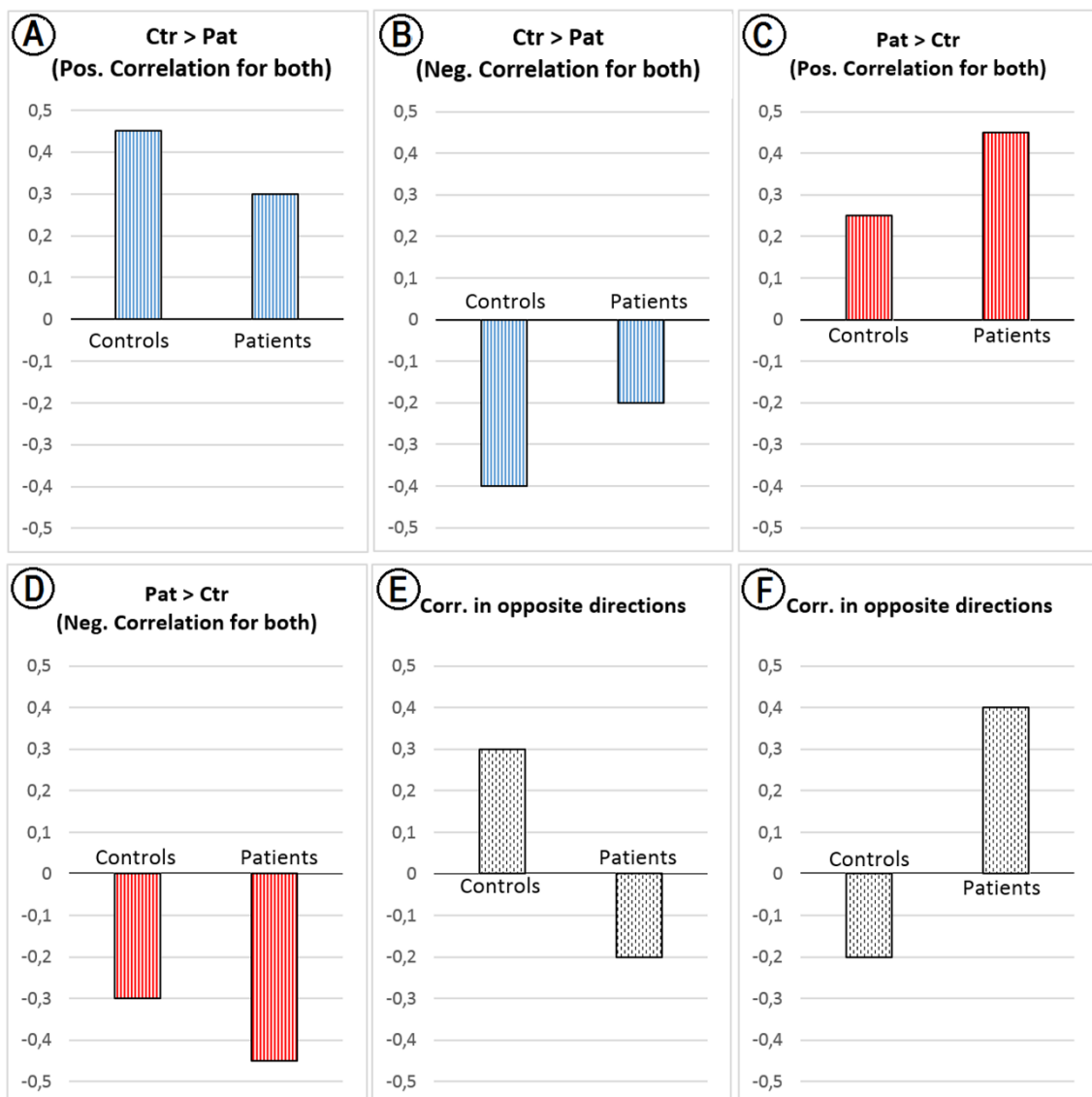


Fig.2: Illustrative examples of possible connectivity results comparing controls and patients average scores. In “A”, controls and patients have positive correlations

between two regions and the control group presents a higher value. In “B”, controls and patients presents negative correlations among two regions and controls showed a higher (absolute) value. The results exemplified in “A” and “B” are represented with blue lines on Fig.3. In “C” and “D” examples similar to “A” and “B”, but in both, patients presented higher absolute correlations values. The results exemplified in “C” and “D” are represented with red lines on Fig.3. Finally, in “E” and “F” we are showing examples of connections with distinct directions (positive for one group and negative to another). The results exemplified in “E” and “F” are represented with dashed lines on Fig.3.

Ctr: control group; Pat: patients; Pos.: positive; Neg.: negative; Corr: correlation.

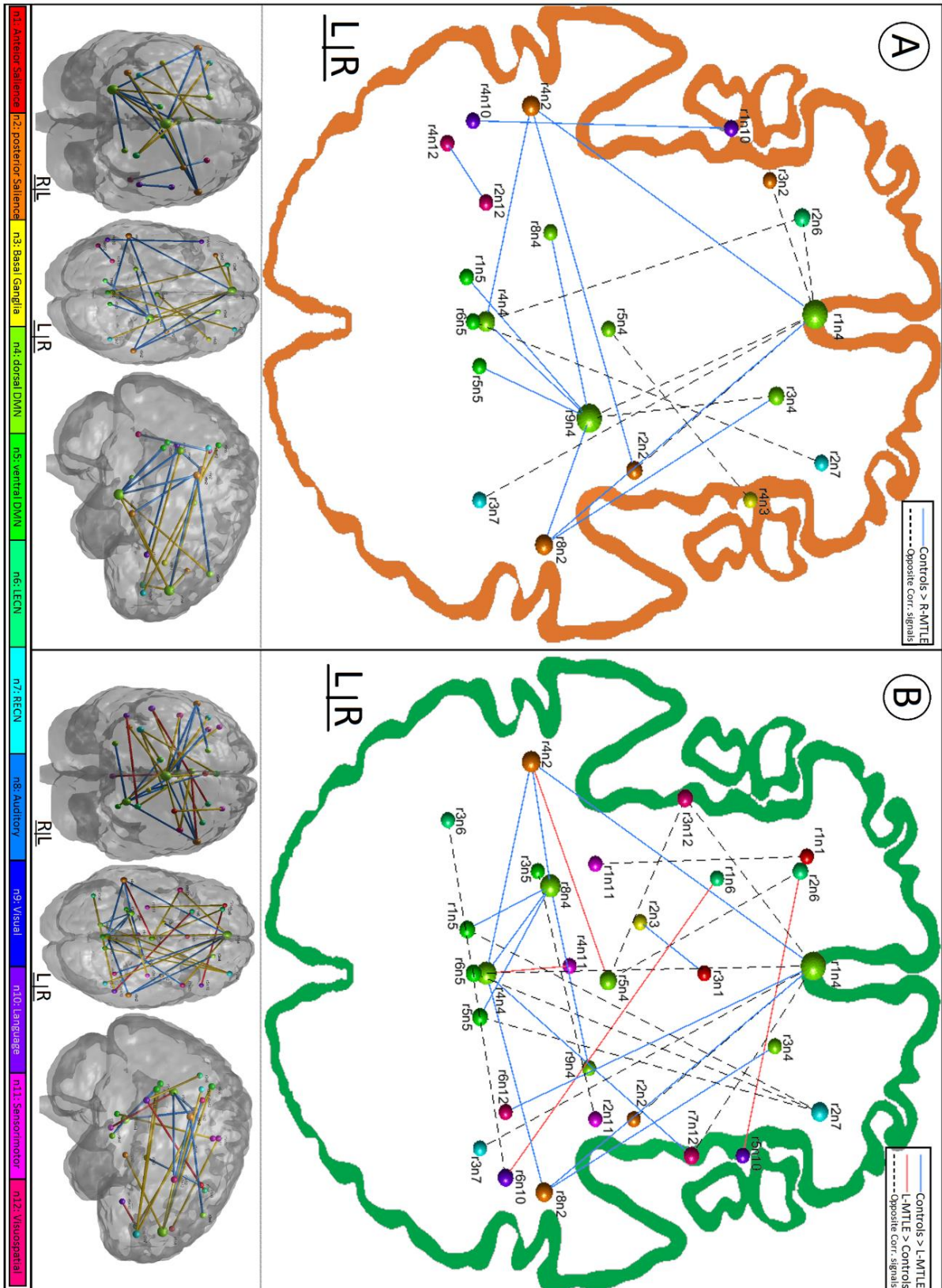


Fig.3: Altered connections on right and left MTLE when compared to control group (ANCOVA test, $p < 0.0375$ false discovery rate (FDR) corrected). A) Altered connections on R-MTLE. The blue lines indicate pairs of ROIs with relative decreased connectivity.

The dashed lines (or yellow on the 3D brain) indicate connections with opposite correlation signal in R-MTLE when compared to controls. B) Altered connections on L-MTLE. The blue lines indicate pairs of ROIs with decreased connectivity. The red lines indicate pairs of ROIs with relative increased connectivity. The dashed lines (or yellow on the 3D brain) indicate connections with opposite correlation signal on L-MTLE when compared to controls. The spheres sizes are in function of the degree of altered connectivity and their colors represent the different networks. R-MTLE: right mesial temporal lobe epilepsy; L-MTLE: left mesial temporal lobe epilepsy; Corr: correlation; L: left side; R: right side; DMN: default mode network; LECN: left executive control network; RECN: right executive control network.

Aiming to characterize how the connectivity alterations are laterally distributed, we calculated a laterality index (LI). We subtracted the number of contralateral altered connections (CAC), from the number of ipsilateral altered connections (IAC) and divided it by the total number of altered connections (Coito et al. 2015):

$$LI = \frac{IAC - CAC}{IAC + CAC}$$

The interpretation of the LI value could be summarized as follows: if the alterations are completely restricted to the ipsilateral side, its LI value is 1. Values between 0 and 1 reveals that the majority of the alterations is ipsilateral and the value oscillates within this range according to the weight (number) of the contralateral alterations. Analogously, the LI is negative if the majority of the alterations is on the contralateral side, varying between -1 and 0 according to the weight (number) of the ipsilateral alterations. If all alterations are restricted to the contralateral side, the LI value would be -1. It is important to clarify that in the case of alterations including a interhemispheric ROI and a non-interhemispheric ROI, we consider the alteration side to be the same as the non-interhemispheric ROI. Another important observation is that since the LI uses the total number of alterations as equation denominator, the resultant LI value quickly decreases (non-linearly) due to the less altered side weight.

Graph Theory Parameters

We performed an additional analysis to extract three graph theory parameters of altered connectivity. We calculated them using the results of the statistical differences between groups, generating graph information related to the connectivity alterations

for R-MTLE and L-MTLE. 1 - The *ROIs degree of altered connectivity (RDAC)*, which means the total number of significant altered connections of each ROI, calculated for each patient group separately. The RDAC provides an overall idea about the significance of a specific altered node, illustrating if it is merely an affected part of a net of alterations (low RDAC) or a center of these alterations (high RDAC). In line with that, the RDAC can be understood as a measure of centrality. 2 - The *average degree of altered connectivity (ADAC)* which considers the RDACs of both patient groups together, calculating an overall average among them:

$$ADAC = \frac{\sum_{i=1}^{n_1} RDAC_i + \sum_{j=1}^{n_2} RDAC_j}{n_1 + n_2},$$

where i and j are the indexes of the ROIs with altered connections for R-MTLE and L-MTLE respectively; and the n_1 and n_2 , the total number of altered ROIs for R-MTLE and L-MTLE respectively. For further reference, we considered a ROI as a hub of alterations, if its RDAC was greater than the ADAC value. 3 - The *clustering coefficient of altered connectivity (CCAC)*:

$$CCAC_i = \frac{t_i}{RDAC_i \times \frac{(RDAC_i - 1)}{2}},$$

where i is the ROI index and t, the total number of triangles (connections between ROI i neighbors'). The CCACs, similarly to the RDACs are calculated for each altered ROI, from each patient group separately. The CCAC indicates how an altered ROI and its neighbors (via altered connections) are segregated (low CCAC) or interlaced (high CCAC) among themselves. It may indicate the existence of a net of alterations. The standard definition of these and other several graph parameters were fully described by Rubinov and Sporns (2010).

Results

Table I shows the detailed clinical characteristics of MTLE patients. No significant differences (alpha=0.03 FDR corrected) were observed between R-MTLE and L-MTLE regarding distribution of gender (p=0.609), age (p=0.675), age of seizure onset (p=0.0798), epilepsy duration (p=0.072) or family history of epilepsy (p=0.743).

Compared to controls, both patients groups (R-MTLE and L-MTLE) presented functional connectivity alterations on the pairwise ROIs analysis (alpha=0.0375 FDR

corrected). From the 12 studied networks, just the auditory and visual networks did not present alterations, although for the R-MTLE group, the anterior salience and sensorimotor networks were also preserved. Tables II to VI show the results organized in hubs of alterations. The ROIs anatomical labelling was performed using xjView toolbox (<http://www.alivelearn.net/xjview>).

Table II: Relative decreased connectivity Hubs on R-MTLE

Hub (ROI/Region)	ROI name	Network	Anatomical regions	ROI (%)	voxel(n)
<u>r4n2</u> L. Supramarginal Gy. L. Inf. Parietal Gy. (Post.Salience)	r1n4	Dorsal DMN	Medial Frontal Gy.	42	2233
			Anterior Cingulate	21	1148
	r4n4	Dorsal DMN	Post. Cingulate	33	525
			Precuneus	31	497
	r2n2	Post.Salience	R. Insula	35	134
		R. Sup. Temporal Gy.	14	19	
<u>r8n2</u> R. Poscentral Gy. R. Supramarginal Gy. (Post.Salience)	r1n4	Dorsal DMN	Medial Frontal Gy.	42	2233
			Anterior Cingulate	21	1148
	r3n4	Dorsal DMN	R. Sup. Frontal Gy.	90	124
	r9n4	Dorsal DMN	R. Hippocampus	97	139
<u>r1n4</u> Sup. Frontal Gy. Medial Frontal Gy. (Dorsal DMN)	r4n2	Post.Salience	L. Supramarginal Gy.	50	660
			L. Inf. Parietal Gy.	32	389
	r8n2	Post.Salience	R. Poscentral Gy.	32	327
			R. Supramarginal Gy.	11	112
<u>r9n4</u> R. Hippocampus (Dorsal DMN)	r8n2	Post.Salience	R. Poscentral Gy.	32	327
			R. Supramarginal Gy.	11	112
	r4n4	Dorsal DMN	Post. Cingulate	33	525
			Precuneus	31	497
	r8n4	Dorsal DMN	L. Hippocampus	87	342
	r1n5	Ventral DMN	Post. Cingulate	54	251
			L. Calcarine	46	214
r5n5	Ventral DMN	Post. Cingulate	58	345	
		R. Precuneus	47	278	

The “voxel (n)” indicates the number of voxels of the respective anatomical region and the “ROI (%)” the percentage of this region within the original ROI mask. R: right; L: left; r: ROI number; n: Network number; Gy: gyrus; DMN: default mode network; Sup: superior; Post: posterior;

R-MTLE connectivity

In total, 21 ROIs linked by 21 connections showed alterations on R-MTLE group when compared to controls. We found significant connectivity decreases in R-MTLE mainly on the right hippocampus (r9n4) connections with dorsal and ventral DMN (n4 and n5) and posterior salience network (n2) (Table II and Fig.3-A in blue lines). Three other

hubs presented relative decreased connectivity, including frontal portion of DMN (r1n4) and right and left posterior salience (r8n2 and r4n2).

Table III: Opposite connectivity Hubs on R-MTLE

Hub (ROI/Region)	ROI name	Network	Anatomical regions	ROI (%)	voxel(n)
r1n4 Sup. Frontal Gy. Medial Frontal Gy. (Dorsal DMN)	r2n2	Post.Salience	R. Insula R. Sup. Temporal Gy.	35 14	134 19
	r3n2	Post.Salience	L. Middle Frontal Gy.	91	93
	r9n4	Dorsal DMN	RT. Hippocampus	97	139
	r2n6	L. ECN	L. Middle Frontal Gy. L. Inf. Frontal Gy.	60 22	264 98
	r3n7	R. ECN	R. Angular Gy. R. Supramarginal Gy.	38 12	715 228
	r1n4	Dorsal DMN	Medial Frontal Gy. Anterior Cingulate	42 21	2233 1148
	r3n4	Dorsal DMN	R. Sup. Frontal Gy.	90	124

The “voxel (n)” indicates the number of voxels of the respective anatomical region and the “ROI (%)” the percentage of this region within the original ROI mask. R: right; L: left; r: ROI number; n: network number; Gy: gyrus; DMN: default mode network; Post: posterior; Sup: superior; Inf: inferior; ECN: executive control network

In summary, by a network perspective, we observed decreased intra-network connectivity between the posterior salience (n2) ROIs and also between dorsal DMN (n4) ROIs. Decreased inter-network connectivity were observed between posterior salience (n2) and dorsal DMN (n4) and also between dorsal DMN (n4) and ventral DMN (n5).

The R-MTLE group also showed opposite connectivity relative to controls including: frontal portion of the dorsal DMN (r1n4), the right hippocampus (r9n4), left and right ECN ROIs (r2n6 and r3n7) and anterior salience (r3n2). By a network perspective, we observed opposite intra-network connectivity only between dorsal DMN (n4) ROIs and opposite inter-network connectivity affecting just the dorsal DMN (n4) and some of its connections with the posterior salience (n2), left ECN (n6) and right ECN (n7) (Table III and Fig.3-A in dashed lines).

Table IV: Relative decreased connectivity Hubs on L-MTLE

Hub (ROI/Region)	ROI name	Network	Anatomical regions	ROI (%)	voxel(n)
r4n2 L. Supramarginal Gy. L. Inf. Parietal Gy. (Post. Saliency)	r1n4	Dorsal DMN	Medial Frontal Gy.	42	2233
			Anterior Cingulate	21	1148
	r4n4	Dorsal DMN	Post. Cingulate	33	525
			Precuneus	31	497
	r8n4	Dorsal DMN	L. Hippocampus	87	342
r8n2 R. Poscentral Gy. R. Supramarginal Gy. (Post. Saliency)	r1n4	Dorsal DMN	Medial Frontal Gy.	42	2233
			Anterior Cingulate	21	1148
	r3n4	Dorsal DMN	R. Sup. Frontal Gy.	90	124
	r4n4	Dorsal DMN	Posterior Cingulate	33	525
			Precuneus	31	497
r1n4 Sup. Frontal Gy. Medial Frontal Gy. (Dorsal DMN)	r4n2	Post.Saliency	L. Supramarginal Gy.	50	660
			L. Inf. Parietal Gy.	32	389
	r8n2	Post.Saliency	R. Poscentral Gy.	32	327
			R. Supramarginal Gy.	11	112
	r6n12	Visuospatial	R. Inf. Parietal lobe	28	329
			R. Sup. Parietal lobe	21	254
r4n4 Post. Cingulate Precuneus (Dorsal DMN)	r4n2	Post.Saliency	L. Supramarginal Gy.	50	660
			L. Inf. Parietal Gy.	32	389
	r8n2	Post.Saliency	R. Poscentral Gy.	32	327
			R. Supramarginal Gy.	11	112
	r8n4	Dorsal DMN	L. Hippocampus	87	342
	r7n12	Visuospatial	R. Inf. Frontal Gy.	61	201
r8n4 L. Hippocampus (Dorsal DMN)	r4n2	Post.Saliency	L. Supramarginal Gy.	50	660
			L. Inf. Parietal Gy.	32	389
	r4n4	Dorsal DMN	Post. Cingulate	33	525
			Precuneus	31	497
	r9n4	Dorsal DMN	R. Hippocampus	97	139
	r1n5	Ventral DMN	Post. Cingulate	54	251
			L. Calcarine	46	214
	r5n5	Ventral DMN	Post. Cingulate	58	345
			R. Precuneus	47	278

The “voxel (n)” indicates the number of voxels of the respective anatomical region and the “ROI (%)” the percentage of this region within the original ROI mask. R: right; L: left; r: ROI number; n: network number; Gy: gyrus; DMN: default mode network; Sup: superior; Inf: inferior; Post: posterior

Table V: Relative increased connectivity Hubs on L-MTLE

Hub (ROI/Region)	ROI name	Network	Anatomical regions	ROI (%)	voxel(n)
<u>r4n2</u> L. Supramarginal Gy. L. Inf. Parietal Gy. (Post.Salience)	r5n4	Dorsal DMN	Bilateral Thalamus	47	105
<u>r4n4</u> Post. Cingulate Precuneus (Dorsal DMN)	r4n11	Sensorimotor	Cerebellum	75	2015
<u>r5n4</u> Bilateral Thalamus (Dorsal DMN)	r4n2	Post.Salience	L. Supramarginal Gy. L. Inf. Parietal Gy.	50 32	660 389

The “voxel (n)” indicates the number of voxels of the respective anatomical region and the “ROI (%)” the percentage of this region within the original ROI mask. R: right; L: left; r: ROI number; n: network number; Gy: gyrus; DMN: default mode network; Sup: superior; Inf: inferior; Post: posterior; L: left; Gy: gyrus; DMN: default mode network; Post: posterior; Inf: inferior;

Graph Theory Properties

On the R-MTLE, the ipsilateral hippocampus and the frontal portion of the DMN (r1n4) presented the highest RDAC (seven connections or 33% of the total number of alterations for each) whereas a relative low CCAC (0.1 for both). On the other hand, posterior salience ROIs (r2n2, r4n2 and r8n2) and the ipsilateral superior frontal gyrus (DMN, r3n4) presented highest CCAC whereas lower RDAC. The LI of the R-MTLE group was 0.190 indicating that the majority of the R-MTLE alterations is ipsilateral, but also there are altered connections on the contralateral side.

L-MTLE connectivity

In total, 29 ROIs linked by 28 connections showed alterations on L-MTLE group when compared to controls. We found five hubs with relative decreased connectivity including left hippocampus (r9n4), affecting connections with ventral and dorsal DMN ROIs (r4n4, r9n4, r1n5 and r5n5) and ipsilateral posterior salience (r4n2). The frontal portion of DMN (r1n4) and the bilateral inferior parietal gyrus of the posterior salience network (r8n2 and r4n2) were also hubs with decreased connections.

Table VI: Opposite connectivity Hubs on L-MTLE

Hub (ROI/Region)	ROI name	Network	Anatomical regions	ROI (%)	voxel(n)
<u>r1n4</u> Sup. Frontal Gy. Medial Frontal Gy. (Dorsal DMN)	r2n2	Post.Salience	R. Insula R. Sup. Temporal Gy.	35 14	134 19
	r6n5	Ventral DMN	Precuneus	88	1703
	r3n7	R. ECN	R. Angular Gy. R. Supramarginal Gy.	38 12	715 228
	r3n12	Visuospatial	L. Inf. Frontal Gy.	67	748
	r7n12	Visuospatial	R. Inf. Frontal Gy.	61	201
	<u>r5n4</u> Bilateral Thalamus (Dorsal DMN)	r2n6	L. ECN	L. Mid. Frontal Gy. L. Inf. Frontal Gy.	60 22
r3n12		Visuospatial	L. Inf. Frontal Gy.	67	748
<u>r2n7</u> R. Mid. Frontal Gy. R. Sup. Frontal Gy. (R. ECN)		r1n5	Ventral DMN	Post. Cingulate L. Calcarine	54 46
	r5n5	Ventral DMN	Post. Cingulate R. Precuneus	58 47	345 278
	r6n5	Ventral DMN	Precuneus	88	1703

The “voxel (n)” indicates the number of voxels of the respective anatomical region and the “ROI (%)” the percentage of this region within the original ROI mask. R: right; L: left; Gy: gyrus; DMN: default mode network; Post: posterior; Inf: inferior; ECN: executive control network Sup: superior; Mid: Middle

By a network perspective, we observed decreased intra-network connectivity only between dorsal DMN (n4) ROIs. We found reductions on inter-network connectivity between posterior salience (n2) and dorsal DMN (n4) ROIs and also between dorsal DMN (n4) with ventral DMN (n5) and visuospatial/dorsal attention network (n12) (Table IV and Fig.3-B in blue lines).

Three hubs presented relative increased connectivity: two dorsal DMN regions, the posterior cingulate (r4n4), bilateral thalamus (r5n4), and the ipsilateral inferior parietal gyrus (r4n2) of posterior salience. We observed increased inter-network connectivity between dorsal DMN (n4) and posterior salience (n2) ROIs and between sensorimotor (n11) and dorsal DMN (n4) ROIs (Table V and Fig.3-B in red lines).

We also observed opposite connectivity (relative to controls) on the L-MTLE group, which included a hub of the right ECN (r2n7) and only its connections with ventral DMN ROIs (r1n5, r5n5 and r6n5). Additionally, we found opposite connectivity on the frontal portion of dorsal DMN (r1n4) with bilateral inferior parietal gyri of the visuospatial/dorsal attention network (r3n12 and r7n12), ventral DMN (r6n5), right ECN (r3n7) and left posterior salience (r2n2). The thalamus (r5n4) was also considered a hub with opposite

connections, which included visuospatial (r3n12) and left ECN (r2n6) networks ROIs (Table VI and Fig.3-B in dashed lines). By a network perspective, we found inter-network opposite connectivity alterations that involved the dorsal DMN (n4) with the posterior salience (n2), ventral DMN (n5), left and right ECN (n6 e n7) and visuospatial (n12). Additionally, we observed alterations between the right ECN (n7) and the ventral DMN (n5). The average connectivity values of all described altered connections are shown on Fig-4.

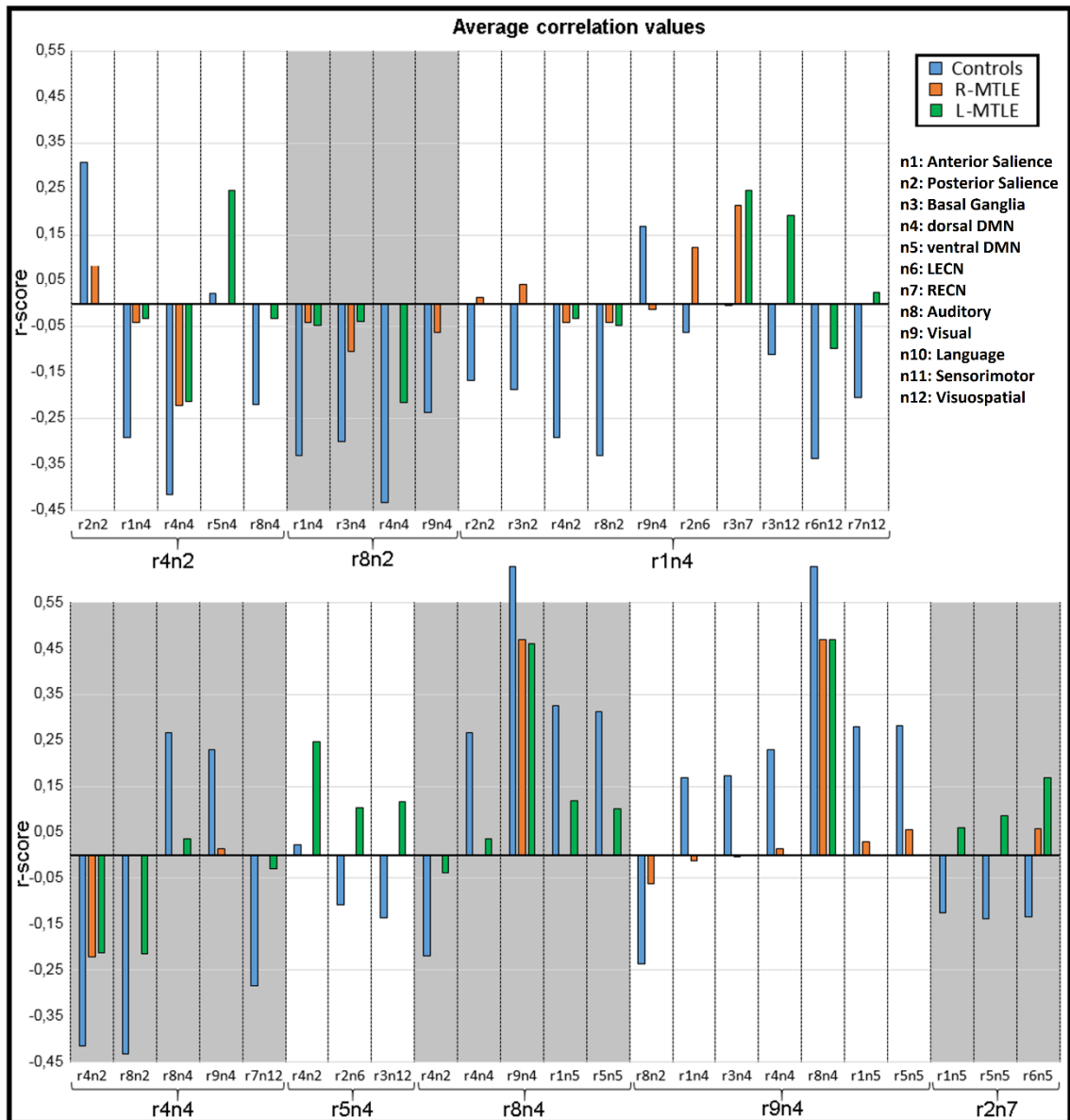


Fig.4: Average correlation values of all (in hubs) altered connections organized by the nine alteration hubs and their existent altered connections.

R-MTLE: right mesial temporal lobe epilepsy; L-MTLE: left mesial temporal lobe epilepsy.

Graph Theory Properties

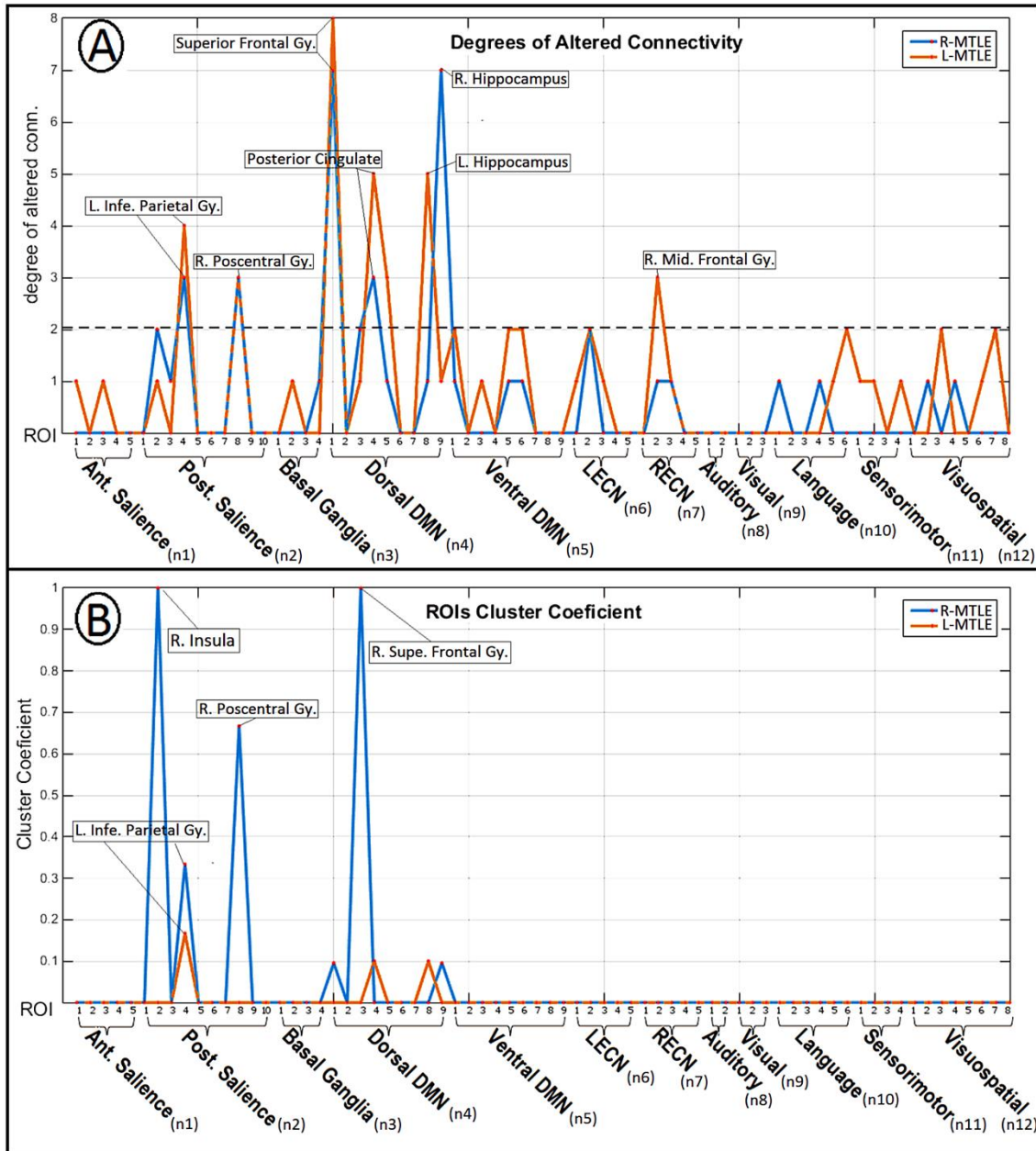


Fig.5: ROIs graph theoretical results. In **A**, the degree of altered connectivity (RDAC) and in **B** the cluster coefficient values (CCAC). The horizontal dashed lines in **A**, represents the average degree of altered connectivity (ADAC) that we used to define a ROIs with higher values as a hub of alterations. The dashed blue and yellow lines were used to indicate overlapping between groups lines.

Conn.: connectivity; R-MTLE: right mesial temporal lobe epilepsy; L-MTLE: left mesial temporal lobe epilepsy; R: right; L: left; Gy: gyrus; Infe: inferior; Mid.: middle; Supe.: superior; Ant.: anterior; Post. Posterior; DMN: default mode network; LECN: left executive control network; RECN: right executive control network.

The L-MTLE group presented relevant RDAC on the frontal portion of the DMN (r1n4), in the posterior cingulate cortex (r4n4) and in the ipsilateral hippocampus (r8n4) (Fig.5–A). The CCAC in this group, revealed low clustering values with the highest score on the ipsilateral inferior parietal lobule (r4n2) (Fig.5–B). The LI for the L-MTLE group was 0.035 indicating that the majority of the L-MTLE alterations is ipsilateral, but with a very similar quantity on the contralateral side.

Discussion

Using resting-state fMRI, we investigated the patterns of connectivity alterations in patients with left and right MTLE. We performed several approaches of validated methodologies to extract clear information about each MTLE type separately. We demonstrated that patients with right and left MTLE have widespread abnormal interactions of large-scale networks. Despite the vast alteration in both patients groups, all evaluated parameters indicates that L-MTLE is a more intricate bilateral functional syndrome than R-MTLE. Moreover, ipsilateral hippocampi of both groups behave as central hubs of decreased functional connectivity.

The large-scale networks interaction abnormalities of L-MTLE and R-MTLE can be summarized as follows: i) both R-MTLE and L-MTLE patients presented decreased connectivity and inversion of the correlation signal between the dorsal DMN and the posterior salience network (compared to controls); ii) both R-MTLE and L-MTLE patients presented inversion of the correlation signal between the dorsal DMN and the ECN; iii) L-MTLE patients presented decreased connectivity and inversion of the correlation signal between the dorsal DMN and the visuospatial/dorsal attention network; iv) in patients with L-MTLE, a relative increased connectivity was observed between the bilateral thalami and the posterior salience network.

Differences on connectivity alterations between left and right MTLE have been previously described in the literature (Haneef et al., 2015; Waites et al., 2006; Pereira et al., 2010). Through diversified methodologies, these studies explored distinct aspects of brain functional connectivity using anatomical or functional relevant ROIs,

independent component analysis and graph theoretical information. Our study unified some of these methodologies, applying consecutive techniques with an unbiased pipeline, providing robust results through an innovative point of view.

Abnormal connectivity in right and left MTLE

For both groups, we found abnormal DMN connections, with the superior and middle frontal gyri as important hubs of alterations. The ipsilateral hippocampi were also highlighted as a central area of abnormalities, as expected due to its dominant importance in MTLE underlying physiopathology.

Differences of abnormal connectivity between right and left MTLE

With the exception of the ipsilateral hippocampi (that are altered according to the group lateralization), all hubs with relative decreased connectivity observed on R-MTLE patients were also observed on L-MTLE. In addition, patients with L-MTLE presented as hubs of relative decreased connectivity the dorsal DMN (r4n4) and the right ECN (r2n7). The idea that the L-MTLE patients are more susceptible to bilateral and diffuse structural alterations was already described in the literature (Ahmadi et al., 2009, Coan et al 2009) and our study suggests that these patterns occurs also with the functional organization, involving contralateral networks. These findings are sustained by the laterality index that showed more ipsilateral-restricted alterations on R-MTLE, while the L-MTLE presented a more bilateral pattern of alterations.

In addition to the diffuse and bilaterally-affected connectivity, the cluster-coefficient on the L-MTLE proved to be lower than in R-MTLE. This finding suggests that despite L-MTLE patients having a higher ADAC and widespread alterations, these abnormal connections presented low interactions between themselves. These facts could be related to the cognitive abnormalities presented in patients with MTLE and in an ineffective attempt to restore these functionalities. On the R-MTLE patients, the ADAC was lower than in L-MTLE, with more restricted pattern of alterations including eight networks. On the other hand, these alterations demonstrated to be integrated between themselves, with higher cluster coefficients and more ipsilaterally distributed as mentioned above. The clinical relevance of these findings, at this point, can only be speculative. Nevertheless, it is widely known that patients with L-MTLE have worse cognitive performance than R-MTLE (Alessio et al., 2006; Hermann et al., 1997). As also suggested by intracranial EEG studies, the abnormal connectivity in the

hemisphere contralateral to the epileptogenic zone in L-MTLE could be an attempt to compensate the functional deficit, as the performance of working memory scores have been correlated to this increased contralateral connectivity (Bettus et al., 2009). However, in our study while regions of increased connectivity were only observed in L-MTLE, the graph theory parameters showed low interactions between these nodes, which could indicate an ineffective connectivity. Therefore, we believe that, at this point, the hypothesis of the occurrence of areas of increased connectivity in L-MTLE as a compensatory mechanism requires further investigation.

The connectivity within DMN ROIs is extensively reduced, with the ipsilateral hippocampus as a main hub of alterations for both groups, differing only on the opposite connectivity with the frontal portion of DMN (r1n4 and r3n) on the R-MTLE. The connectivity reduction between these areas could be secondary to the structural abnormalities as well as both ictal and interictal activities, closely related to the hippocampal damage (Zhang et al. 2010).

We also observed several inter-networks alterations in R-MTLE and L-MTLE. Differently from previous studies, we assessed the inter-networks abnormalities looking at positive and negative correlations and also at the inversion of the correlation directions between patients and controls, providing a full characterization of the abnormal interaction of the different brain regions in MTLE. In our study, both R-MTLE and L-MTLE patients presented altered correlations involving the DMN, the salience network and ECN, showing an inversion of the correlation signal between them in comparison to the control group. The Fig.3-B reveals, for example, that an ECN hub (r2n7) of L-MTLE patients worked positively correlated with the DMN during rest, in opposite to the controls. Accordingly, both inferior frontal gyrus (both sides, r3n12 and r7n12) and the frontal portion of the DMN (r1n4) proved to be positively correlated, also in contrast to controls. The relationship between DMN, salience and ECNs is under investigation, but recent studies defined that DMN and salience work oppositely, meaning that the increase of the first is followed by a decrease in the second, and vice-versa (Balthazar, et al., 2014). Some authors suggest that this mechanism involves a mediation of activity executed by the salience network guiding the focus on internal (DMN) or external (ECN) process and stimulus (Liang et al., 2015).

Other inter-network alterations were observed exclusively in L-MTLE, more specifically between DMN and visuospatial/dorsal attention network, which also presented an

inversion of correlation signal. Previous studies demonstrated that the relation between DMN and visuospatial/dorsal attention network is supposedly anti-correlated (Tomasi et al., 2009), once the DMN should deactivate when the visuospatial is required to focus in a task. Since our study performed the functional acquisitions during rest, we can determine that visuospatial/dorsal attention network regions (r3n12 and r7n12) are misleadingly recruited by DMN, corroborating the evidence of a more disorganized functional behavior on L-MTLE. Additionally, only in patients with L-MTLE an increased connectivity was observed between the bilateral thalami and the posterior salience network, more specifically, the left inferior parietal region.

Although extensively described, the causes of diffuse abnormal functional and structural abnormalities in MTLE are unknown. One possible factor involved on RSN disruption in MTLE patients may be the underlying interictal activity. Although we do not have concomitant EEG recordings to this data, previous studies described the functional alterations caused by interictal spikes (Coan et al., 2014a). However, there is no evidence that the characteristics of interictal epileptiform discharges, including rate, localization or extent, differ between right or left MTLE and, accordingly, these differences were also not observed between our groups of patients. Therefore, while the epileptiform discharges might affect the overall connectivity in MTLE patients, it might not contribute specifically to the differences between right and left MTLE. Similarly, while the chronic use of anti-epileptic drugs (as described for patients in use of topiramate (Yasuda et al., 2013)), as well as the natural disease evolution may also be relevant factors influencing connectivity abnormalities in MTLE, they may not necessarily impact the differences between right and left MTLE described in our study. These characteristics were balanced between the patients groups. Further prospective studies will be necessary to address the influence of these factors on connectivity alterations in MTLE.

Methodological Considerations

ROI based studies applied to diseases with structural alteration such as hippocampal atrophy, should have additional attention during the time-series extractions. Misleading co-registration between the ROI mask and the cortex could include extra cortical tissues or regions with extensively altered cellular constitution that are not functionally representative. Although we did not include an atrophy mask as covariate in our model, the methodology applied for extraction of time series avoided confounding voxels

through the tissue segmented mask and the required homogeneity among time-series from ROIs voxels.

The Fig.4 shows the average correlation values for each altered connection for each group. It is possible to identify means close to values related to noise (or non-significant average correlations: $p > 0.05$ or $r < 0.145$; with 180 degrees of freedom - number of dynamics for each run). Our aim was to include all possible not connected regions in the analysis, since we considered the possibility of the occurrence of conversion of absent connections into significant ones and vice-versa in MTLE. For instance, the connection between regions r1n4 and r3n7 is almost absent in controls subjects but it is consistently present in the R-MTLE and L-MTLE groups.

In this study, we applied established approaches as cross-correlation between series and graph theoretical parameters, but we also quantified these graph properties with the difference between MTLE groups and controls as a third level step. This method characterizes the patterns of alterations directly, avoiding arbitrary successive thresholds commonly applied on graph-theoretical studies.

The networks parcellation and nomination can vary among authors. Since we decided to employ the Shirer's parcellation in our study, we strive to respect that organization with few exceptions (described on the "Methods"). These divergences are usually secondary to chosen parameters during the process to create the functional templates such as, for example, the defined number of components to be determined during an Independent Component Analysis. In our study, the dorsal attention network is represented by the Visuospatial (n12). Differently, a network exclusively composed by ROIs of the Ventral Attention network (VAN) is missing. We concluded that the regions composing the VAN are represented by ROIs included on the perceptual networks (e.g. sensorimotor, auditory). Therefore, despite not including the VAN, the relevant anatomical regions associated to it are considered in our ROI-wise analysis. We understand that the results presented on Tables II to VI, can assist these interpretations, since they 'translate' the functional ROI name to specific anatomical region.

The UF²C toolbox demonstrated to be an efficient and straightforward tool to investigate functional connectivity. The minimalist user interface and the standard

settings enable reliable assessment of functional information through a consistent and validated preprocessing pipeline.

Conclusion

Patients with right and left MTLE have widespread abnormal interactions of large-scale networks. Despite the vast alteration in both patients groups, all evaluated parameters indicates that L-MTLE has a more intense bihemispheric dysfunction compared to right-MTLE.

Acknowledgements

Study supported by FAPESP (São Paulo Research Foundation), grants 2013/00099-7, 2013/07559-3 and 2014/15918-6.

Disclosure of Conflicts of Interest

None of the authors has any conflict of interest to disclose.

We confirm that we have read the Journal's position on issues involved in ethical publication and affirm that this report is consistent with those guidelines.

References

Ahmadi, M.E., Jr, D.J., McDonald, C.R., Tecoma, E.S., Iraguid, V.J., Dale, A.M., Halgren, E., 2009. Side Matters: Diffusion Tensor Imaging Tractography in Left and Right Temporal Lobe Epilepsy. *AJNR* 2009 30: 1740-1747.

Alessio, A., Bonilha, L., Rorden, C., Kobayashi, E., Min, L. L., Damasceno, B. P., & Cendes, F., 2006. Memory and language impairments and their relationships to hippocampal and perirhinal cortex damage in patients with medial temporal lobe epilepsy. *Epilepsy & Behavior*, 8(3), 593-600.

Balthazar, M. L. F., Pereira, F. R. S., Lopes, T. M., da Silva, E. L., Coan, A. C., Campos, B. M., Duncan, N. W., Stella, F., Northoff, G., Damasceno, B. P. and Cendes, F. (2014), Neuropsychiatric symptoms in Alzheimer's disease are related to functional connectivity alterations in the salience network. *Hum. Brain Mapp.*, 35: 1237–1246.

Benjamini, Y. and Hochberg, Y., 1995. Controlling the False Discovery Rate: A Practical and Powerful Approach to Multiple Testing. *Journal of the Royal Statistical Society. Series B (Methodological)*_Vol. 57, No. 1, pp. 289-300

Berg, A. T., Berkovic, S. F., Brodie, M. J., Buchhalter, J., Cross, J. H., Van Emde Boas, W., Engel, J., French, J., Glauser, T. A., Mathern, G. W., Moshé, S. L., Nordli, D., Plouin, P. and Scheffer, I. E., 2010. Revised terminology and concepts for organization of seizures and epilepsies: Report of the ILAE Commission on Classification and Terminology, 2005–2009. *Epilepsia*, 51: 676–685.

Bernhardt, B.C., Chen, Z., He, Y., Evans, A.C., Bernasconi, N., 2011. Graph-theoretical analysis reveals disrupted small-world organization of cortical thickness correlation networks in temporal lobe epilepsy. *Cereb Cortex*. 21, 2147-57.

Besson, P., Dinkelacker, V., Valabregue, R., Thivard, L., Leclerc, X., Baulac, M., Sammler, D., Colliot, O., Lehericy, S., Samson, S., Dupont, S., 2014. Structural connectivity differences in left and right temporal lobe epilepsy. *Neuroimage*. Oct;100 135-144.

Bettus, G., Guedj, E., Joyeux, F., Confort-Gouny, S., Soulier, E., Laguitton, V., Cozzone, P.J., Chauvel, P., Ranjeva, J.P., Bartolomei, F., Guye, M., 2009. Decreased basal fMRI functional connectivity in epileptogenic networks and contralateral compensatory mechanisms. *Hum Brain Mapp*. 30, 1580-91.

Bonilha, L., Helpern, J.A., Sainju, R., Nesland, T., Edwards, J.C., Glazier, S.S., Tabesh, A., 2013. Presurgical connectome and postsurgical seizure control in temporal lobe epilepsy. *Neurology*. 81, 1704-10.

Bullmore, E. and Sporns, O., 2009. Complex brain networks: graph theoretical analysis of structural and functional systems. *Nat Rev Neurosci*. 10, 186-98.

Campos, B.M., Coan, A.C., Beltramini, G.C., Liu, M., Yassuda, C.L., Ghizoni, E., Beaulieu, C., Gross, D.W., Cendes, F., 2015. White matter abnormalities associate with type and localization of focal epileptogenic lesions. *Epilepsia*. 56, 125-32.

Cataldi, M., Avoli, M., de Villers-Sidani, E., 2013. Resting state networks in temporal lobe epilepsy. *Epilepsia*. 54, 2048-59.

Cendes, F., Andermann, F., Gloor, P., Lopes-Cendes, I., Andermann, E., Melanson, D., Jones-Gotman, M., Robitaille, Y., Evans, A., Peters, T., 1993. Atrophy of mesial

structures in patients with temporal lobe epilepsy: cause or consequence of repeated seizures? *Ann Neurol.* 34, 795-801.

Chiang, S., and Haneef, Z., 2014. Graph theory findings in the pathophysiology of temporal lobe epilepsy. *Clin Neurophysiol.* 125, 1295-305.

Coan AC, Appenzeller S, Bonilha L, Li LM, Cendes F. Seizure frequency and lateralization affect progression of atrophy in temporal lobe epilepsy. *Neurology* 2009;73(11):834-42

Coan, A.C., Campos, B.M., Beltramini. G.C., Yasuda, C.L., Covolan R.J.M., Cendes, F., 2014a. Distinct functional and structural MRI abnormalities in mesial temporal lobe epilepsy with and without hippocampal sclerosis. *Epilepsia*, 55(8):1187–1196, 2014.

Coan, A.C., Kubota, B., Bergo, F.P.G., Campos, B.M., Cendes, F., 2014b. 3T MRI Quantification of Hippocampal Volume and Signal in Mesial Temporal Lobe Epilepsy Improves Detection of Hippocampal Sclerosis. *AJNR*, 35: 77-83

Coito, A., Plomp, G., Genetti, M., Abela, E., Wiest, R., Seeck, M., Michel, C. M. and Vulliemoz, S., 2015, Dynamic directed interictal connectivity in left and right temporal lobe epilepsy. *Epilepsia*, 56: 207–217.

Eguíluz, V. M., Chialvo, D. R., Cecchi, G. A., Baliki, M., and Apkarian, A. V., 2005. Scale-Free Brain Functional Networks. *Phys. Rev. Lett.* 94, 018102.

Haneef, Z., Lenartowicz, A., Yeh, H.J., Levin, H.S., Engel, J.Jr., Stern, J.M., 2014. Functional connectivity of hippocampal networks in temporal lobe epilepsy. *Epilepsia*. 55, 137-45.

Haneef, Z., Chiang, S., Yeh, H.J., Engel, J.Jr, Stern, J.M., 2015. Functional connectivity homogeneity correlates with duration of temporal lobe epilepsy. *Epilepsy Behav*; 46:227-33

Hermann, B. P., Seidenberg, M., Schoenfeld, J., Davies, K., 1997. Neuropsychological characteristics of the syndrome of mesial temporal lobe epilepsy. *Archives of Neurology*, 54(4), 369-376.

Holmes, M.J., Yang, X., Landman, B.A., Ding, Z., Kang, H., Abou-Khalil, B., Sonmezturk, H.H., Gore, J.C., Morgan, V.L., 2013. Functional networks in temporal-lobe epilepsy: a voxel-wise study of resting-state functional connectivity and gray-matter concentration. *Brain Connect.* 3, 22-30.

Keller, S. S., Mackay, C. E., Barrick, T. R., Wieshmann, U. C., Howard, M. A., & Roberts, N., 2002. Voxel-based morphometric comparison of hippocampal and extrahippocampal abnormalities in patients with left and right hippocampal atrophy. *Neuroimage*, 16(1), 23-31.

Laufs, H., Hamandi, K., Salek-Haddadi, A., Kleinschmidt, A. K., Duncan, J. S. and Lemieux, L., 2007. Temporal lobe interictal epileptic discharges affect cerebral activity in “default mode” brain regions. *Hum. Brain Mapp.* 28: 1023–1032.

Liang, X., Yong, Z., Yihong, H., Yang, Y., 2015. Topologically Reorganized Connectivity Architecture of Default-Mode, Executive-Control, and Salience Networks across Working Memory Task Loads. *Cereb. Cortex* 10.1093/cercor/bhu316

Liao, W., Zhang, Z., Pan, Z., Mantini, D., Ding, J., Duan, X., Luo, C., Lu, G., Chen, H., 2010. Altered functional connectivity and small-world in mesial temporal lobe epilepsy. *PLoS One.* 5, e8525.

Liao, W., Zhang, Z., Pan, Z., Mantini, D., Ding, J., Duan, X., Luo, C., Wang, Z., Tan, Q., Lu, G., Chen, H., 2011. Default mode network abnormalities in mesial temporal lobe epilepsy: a study combining fMRI and DTI. *Hum Brain Mapp.* 32, 883-95.

Liu, M., Concha, L., Lebel, C., Beaulieu, C., Gross, D.W., 2012. Mesial temporal sclerosis is linked with more widespread white matter changes in temporal lobe epilepsy. *Neuroimage Clin.* 1, 99-105.

Morgan, V.L., Sonmezturk, H.H., Gore, J.C., Abou-Khalil, B., 2012. Lateralization of temporal lobe epilepsy using resting functional magnetic resonance imaging connectivity of hippocampal networks. *Epilepsia*, 53(9), 1628-1635.

Pereira, F. R., Alessio, A., Sercheli, M. S., Pedro, T., Bilevicius, E., Rondina, J. M., ... & Cendes, F., 2010. Asymmetrical hippocampal connectivity in mesial temporal lobe epilepsy: evidence from resting state fMRI. *BMC neuroscience*, 11(1), 66.

Pittau, F., Grova, C., Moeller, F., Dubeau, F., Gotman, J., 2012. Patterns of altered functional connectivity in mesial temporal lobe epilepsy. *Epilepsia*. 53, 1013-23.

Riederer, F., Lanzenberger, R., Kaya, M., Prayer, D., Serles, W., & Baumgartner, C., 2008. Network atrophy in temporal lobe epilepsy A voxel-based morphometry study. *Neurology*, 71(6), 419-425.

Rubinov, M., and Sporns, O., 2010. Complex network measures of brain connectivity: Uses and interpretations. *NeuroImage*, Vol 52, 3, 1059–1069.

Seeley, W.W., Crawford, R.K., Zhou, J., Miller, B.L., Greicius, M.D., 2009. Neurodegenerative diseases target large-scale human brain networks. *Neuron*. 62, 42-52.

Shirer WR, Ryali, S., Rykhlevskaia, E., Menon, V., Greicius, M.D., 2012. Decoding subject-driven cognitive states with whole-brain connectivity patterns. Cereb Cortex.

Spencer, S.S., 2002. Neural networks in human epilepsy: evidence of and implications for treatment. *Epilepsia*. 43, 219-27.

Tomasi D, Volkow ND, Wang R, Telang F, Wang G-J, et al., 2009. Dopamine Transporters in Striatum Correlate with Deactivation in the Default Mode Network during Visuospatial Attention. *PLoS ONE* 4(6): e6102.

Vannest, J., Szaflarski, J.P., Privitera, M.D., Schefft, B.K., Holland, S.K., 2008. Medial temporal fMRI activation reflects memory lateralization and memory performance in patients with epilepsy. *Epilepsy Behav* 12:410–418

Vlooswijk, M.C., Vaessen, M.J., Jansen, J.F., de Krom, M.C., Majoie, H.J., Hofman, P.A., Aldenkamp, A.P., Backes, W.H., 2011. Loss of network efficiency associated with cognitive decline in chronic epilepsy. *Neurology*. 77, 938-44.

Waites, A. B., Briellmann, R. S., Saling, M. M., Abbott, D. F. and Jackson, G. D., 2006. Functional connectivity networks are disrupted in left temporal lobe epilepsy. *Ann Neurol.*, 59: 335–343.

Wang, J., Wang, L., Zang, Y., Yang, H., Tang, H., Gong, Q., Chen, Z., Zhu, C. and He, Y., 2009. Parcellation-dependent small-world brain functional networks: A resting-state fMRI study. *Hum. Brain Mapp.*, 30: 1511–1523.

Yasuda, C.L., Centeno, M., Vollmar, C., Stretton, J., Symms, M., Cendes, F., Mehta, M.A., Thompson, P., Duncan, J.S., Koepp, M.J., 2013. The effect of topiramate on cognitive fMRI, *Epilepsy Research*. 105, 1–2, July, 250-255.

Zhang, Z., Lu, G., Zhong, Y., Tan, Q., Liao, W., Chen, Z., Shi, J., Liu, Y., 2009a. Impaired perceptual networks in temporal lobe epilepsy revealed by resting fMRI. *J Neurol*. 256, 1705-13.

Zhang, Z., Lu, G., Zhong, Y., Tan, Q., Yang, Z., Liao, W., Chen, Z., Shi, J., Liu, Y., 2009b. Impaired attention network in temporal lobe epilepsy: a resting FMRI study. *Neurosci Lett*. 458, 97-101.

Zhang, Z., Lu, G., Zhong, Y., Tan, Q., Liao, W., Wang, Z., Wang, Z., Li, K, Chen, H., Liu, Y., 2010. Altered spontaneous neuronal activity of the default-mode network in mesial temporal lobe epilepsy. *Brain Res*. 1323, 152-60.

5. DISCUSSÃO GERAL

As análises da integridade estrutural demonstraram distintos padrões de alterações micro e macroestruturais em subtipos de epilepsias focais. Os pacientes com ELTM-EH apresentaram danos de SB bilateralmente distribuídos. Por outro lado, pacientes com ELF-DCF demonstraram danos de SB com tendências de serem restritos à região epileptogênica. Pacientes ELT-NL não apresentaram alterações macro- ou micro-estruturais de SB, resultado que apesar de confirmar o diagnóstico clínico e de neuroimagem, pode estar associado a maior inomogeneidade do grupo (individualidade), o que implicaria em pior consistência estatística e consequentes resultados negativos.

Apesar de abrangente, as alterações associadas aos subtipos de epilepsias, seguem padrões específicos e anatomicamente consistentes. A análise quantitativa dos valores de FA, AD e RD indicaram que as alterações encontradas são reflexo do aumento do RD, achado indicativo de desmielinização axonal^{29,32}. Metodologicamente, a definição de regiões de interesse através da seleção de fascículos específicos com a técnica de tractografia semiautomática aprimora a sensibilidade de identificação de alterações, com excelente eficiência metodológica³¹. Nossos resultados também sugerem que estas alterações afetam a organização das redes funcionais³¹.

Os pacientes com E-ELTM apresentaram um padrão difuso e complexo, bilateralmente distribuído que incluía conexões com redução e aumento de conectividade, além de pares de regiões com recrutamento errático (relação invertida em relação aos controles). De forma distinta, os pacientes com D-ELTM, apresentaram alterações mais restritas ao hemisfério ipsilateral ao hipocampo atrófico. O hipocampo direito destacou-se como um hub de alterações (mais conexões alteradas do que a média de alterações de todos os ROIs), mesmo aplicando exigentes mecanismos metodológicos para correção e compensação do fato de atrofia.

Para E- e D-ELTM a DMN é a rede mais alterada (intra-rede)³⁴. Estudo anterior do nosso grupo, demonstrou que alterações da dinâmica da DMN estão relacionadas à atividade interictal em pacientes com ELT^{29,35}. Com exceção do hipocampo (hub sempre alterado no hemisfério ipsilateral), todas as regiões com alterações nos

pacientes com D-ELTM também foram observadas nos E-ELTM. Adicionalmente, os E-ELTM apresentaram alterações associadas a rede de execução motora (ECN) além de áreas adicionais da DMN. Alterações inter-redes são restritas nos pacientes com D-ELTM sendo que a observada diminuição da conectividade da DMN com a salience pode justificar déficits na transição entre estados cognitivos como a introspecção e a execução³⁵.

As alterações inter-redes são vastas e complexas nos pacientes com E-ELTM. Além de alterações entre DMN e salience, o grupo apresenta relevantes alterações entre a DMN com a ECN, a Language e a Visuospatial. Déficits de linguagem são descritos em ELTM e podem ser derivadas de lateralização atípica com representação anatômica da função alterada, sendo mais importante na E-MTLE uma vez que o hemisfério esquerdo é tipicamente associado à linguagem^{37,38}. A interação prejudicada entre a DMN e a rede visuospatial, como mencionado anteriormente pode ser associada a déficits de atenção enquanto, de maneira semelhante, a modulação errônea da relação entre a DMN e a ECN pode resultar em desempenhos ruins em tarefas cognitivas básicas. Os parâmetros de grafos estimados confirmaram a ideia de danos mais difusos em E-ELTM do que D-ELTM. O índice de lateralidade, assim como o coeficiente de cluster, demonstram, respectivamente, maior acometimento bilateral e menor centralidade entre regiões alteradas, sendo que o oposto é visto em pacientes com D-ELTM^{37,38,39,40}.

A metodologia empregada no processamento e análise do estudo de DTI, mostrou-se eficaz, sensível e confiável. O método de tractografia evitou vieses ocasionados por métodos manuais, uma vez que o processamento automático reproduz a relação acerto/erro de forma igual para todos os sujeitos da pesquisa. Além disso, a checagem visual e quantitativa de qualidade dos tratos considerados comprovou grande eficiência, equiparando nosso procedimento adaptado ao descrito na literatura²⁴.

Os métodos aplicados na análise de conectividade funcional, apresentaram o software desenvolvido para este projeto, o UF²C. Utilizando parâmetros definidos através de meta-análise literária, o UF²C busca aplicar o que há de mais novo e estabelecido para análises de conectividade. A interface simplificada e objetiva esconde complexos processos de processamento e verificação dos dados, tornando as análises igualmente factíveis e sofisticadas. Seguindo os padrões literários de

processamento de imagens funcionais para a técnica de conectividade, o UF²C inova e se destaca em diversos pontos como na metodologia robusta de extração das séries temporais e nas representações gráficas e quantitativas únicas que fornece.

Limitações: Utilizando o banco de dados para seleção das imagens, o agrupamento ficou dependente de uma série de fatores como parâmetros de imagem e características clínicas, restringindo o número de sujeitos em alguns grupos. Considerar pacientes com EH direita e esquerda como único grupo no estudo de DTI pode ter mascarado características específicas ao lado do foco epileptogênica. Não foi possível até o momento aplicar a metodologia funcional a outros subtipos de epilepsias focais devido aos parâmetros de imagem definidos. Metodologias secundárias, que utilizam teorias distintas poderiam ser aplicadas para confirmar os achados. No caso das análises de substância branca, métodos de quantificação probabilísticos podem ser aplicados em contrapartida à nossa metodologia determinística de tractografia. Nas avaliações funcionais, análise de componentes independentes (ICA) poderiam ser aplicadas analogamente ao nosso procedimento baseado em sementes, entretanto os ROIs utilizados foram obtidos através deste procedimento.

6. CONCLUSÃO

- Pacientes com lesões focais temporais ou extra temporais apresentaram redes de alterações estruturais de substância branca.
- Os pacientes com ELTM associada a esclerose hipocampal apresentaram piores resultados de alterações estruturais e vasta rede de alterações quando comparados a frontais ou não lesionais
- Sujeitos da pesquisa não lesionais não apresentaram alterações micro ou macroestruturais de substância branca.
- Os grupos com ELTM associada a esclerose hipocampal apresentam complexa rede de alterações funcionais.
- Pacientes com esclerose hipocampal no hemisfério esquerdo (E-ELTM) apresentaram pior padrão de alterações funcionais comparados aos com esclerose hipocampal no hemisfério direito (D-ELTM).
- O desenvolvimento de *softwares* para as modalidades metodológicas propostas, possibilitou a padronização e eficiência na análise dos dados.
- As ferramentas já estão sendo empregadas em outros estudos independentes de forma satisfatória.

REFERÊNCIAS

1. Fisher RS, Boas WVE, Blume W, Elger C, Genton P, Lee P, Engel, J. Epileptic Seizures and Epilepsy: Definitions Proposed by the International League Against Epilepsy (ILAE) and the International Bureau for Epilepsy (IBE). *Epilepsia*. 2005; 46:470–72.
2. Berg AT, Berkovic SF, Brodie MJ, Buchhalter J, Cross JH, Van Emde Boas W, et al. Revised terminology and concepts for organization of seizures and epilepsies: Report of the ILAE Commission on Classification and Terminology, 2005–2009. *Epilepsia*. 2010; 51:676–85.
3. Franzon RC, Montenegro MA, Guimarães AC, Guerreiro CAM, Cendes F, Guerreiro MM. Clinical, Electroencephalographic, and Behavioral Features of Temporal Lobe Epilepsy in Childhood. *J Child Neurol*. 2004; 19:418-43.
4. Blume WT. The Progression of Epilepsy. *Epilepsia*. 2006; 47:71–8.
5. Marchetti RL, Castro APW, Kurcgant D, Cremonese E, Gallucci NJ. Mental disorders associated with epilepsy. *Rev. Psiqu. Clín.* 2005; 32 (3);170-82.
6. Scott RA, Lhatoo SD, Sander JWAS. The treatment of epilepsy in developing countries: where do we go from here?. *Bull World Health Organ*. 2001; 79(4):344-51.
7. Bruton C J. The neuropathology of temporal lobe epilepsy. 31th ed. New York: Oxford University Press; 1988.
8. Riederer F, Lanzenberger R, Kaya M, Prayer D, Serles W, Baumgartner C. Network atrophy in temporal lobe epilepsy: A voxel-based morphometry study. *Neurology*. 2008; 71(6):419-25.
9. Cendes F. Neuroimaging in Investigation of Patients With Epilepsy. *Continuum: Lifelong Learning in Neurology*. 2013; 19(3):623–42.
10. Savoy RL. History and future directions of human brain mapping and functional neuroimaging, *Acta Psychologica*. 2001; 107(1–3):9-42.
11. Buxton RB. Introduction to Functional Magnetic Resonance Imaging: Principles and Techniques. 2nd ed. New York: Cambridge University Press; 2009.
12. Kaiming Li, Lei Guo, Jingxin Nie, *et al.*. Review of methods for functional brain connectivity detection using fMRI. *Computerized Medical Imaging and Graphics*. 2009; 33(2):131-139

13. van den Heuvel MP, Hulshoff PHE. Exploring the brain network: A review on resting-state fMRI functional connectivity, *European Neuropsychopharmacology*. 2010;20(8):519-534
14. Davis KD, Kwan CL, Crawley AP, Mikulis DJ. Functional MRI Study of Thalamic and Cortical Activations Evoked by Cutaneous Heat, Cold, and Tactile Stimuli. *Journal of Neurophysiology*. 1998; 80(3):1533-46.
15. Biswal BB, Resting state fMRI: A personal history, *NeuroImage*. 2012; 62(2):938-44.
16. Moussa MN, Steen MR, Laurienti PJ, Hayasaka S. Consistency of Network Modules in Resting-State fMRI Connectome Data. *PLoS ONE*. 2012; 7(8):e44428.
17. Waites AB, Briellmann RS, Saling MM, Abbott DF, Jackson GD. Functional connectivity networks are disrupted in left temporal lobe epilepsy. *Ann Neurol*. 2006; 59:335–43.
18. Liao W, Zhang Z, Pan Z, Mantini D, Ding J, Duan X, et al. Altered Functional Connectivity and Small-World in Mesial Temporal Lobe Epilepsy. *PLoS ONE*. 2010; 5(1): e8525.
19. Haacke EM, Brown RW, Thompson MR, Venkatesan R. *Magnetic resonance imaging: physical principles and sequence design*. Vol. 82. New York: Wiley-Liss, 1999.
20. Beaulieu C. The basis of anisotropic water diffusion in the nervous system – a technical review. *NMR Biomed*. 2002; 15:435–55.
21. Coan AC. *Diferenças Clínicas e de Alterações Cerebrais Estruturais e Funcionais Entre Epilepsias de Lobo Temporal Mesial com e Sem Sinais de Esclerose Hipocampal [tese]*. Campinas: universidade Estadual de Campinas, Faculdade de Ciências Médicas; 2013.
22. Blümcke I, Thom M, Aronica, E, et al. The clinicopathologic spectrum of focal cortical dysplasias: A consensus classification proposed by an ad hoc Task Force of the ILAE Diagnostic Methods Commission. *Epilepsia* 2011;52:158-174.
23. Concha L, Gross DW, Beaulieu C. Diffusion Tensor Tractography of the Limbic System. *Am J Neuroradiol*. 2005; 26:2267-74.
24. Lebel C, Walker L, Leemans A, Phillips A, Beaulieu C. Microstructural maturation of the human brain from childhood to adulthood. *NeuroImage*. 2008; 40(3):1044-55.

25. Campos BM, Coan AC, Beltramini GC, Liu M, Yassuda CL, Ghizoni E, et al. White matter abnormalities associate with type and localization of focal epileptogenic lesions. *Epilepsia*. 2015; 56:125–32.
26. Weiler M, Campos BM, Nogueira MH, Damasceno BP, Cendes F, Balthazar MLF. Structural connectivity of the default mode network and cognition in Alzheimer's disease, *Psychiatry Research: Neuroimaging*. 2014; 223(1):15-22.
27. Pinheiro GLS, Guimarães RP, Piovesana LG, Campos BM, Campos LS, Azevedo PC, et al. White Matter Microstructure in Idiopathic Craniocervical Dystonia. Louis ED, ed. *Tremor and Other Hyperkinetic Movements*. 2015; 5:tre-5-302.
28. Ghizoni E, Almeida JP, Joaquim AF, Yasuda CL, Campos BM, Tedeschi H, et al. Modified Anterior Temporal Lobectomy: Anatomical Landmarks and Operative Technique. *Journal of Neurological Surgery Part A: Central European Neurosurgery*. 2015; 76(5):407-14.
29. Campos BM, Coan AC, Yasuda CL, Casseb RF, Cendes F. Large-scale brain networks are distinctly affected in right and left mesial temporal lobe epilepsy. *Hum. Brain Mapp*. 2016; 37(9):3137-52.
30. Almeida SRM, Vicentini J, Bonilha L, Campos BM, Casseb RF, Min LL. Brain Connectivity and Functional Recovery in Patients With Ischemic Stroke. *Journal of Neuroimaging*. 2016; Epub 2016 May 31.
31. Vicentini J, Valler L, Weiler M, Almeida SR, Campos BM, Min LL. Depression and anxiety symptoms are associated to disruption of Default Mode Network in subacute ischemic stroke. *Brain Imaging and Behavior*. 2016. Epub 2016 Aug 24.
32. van den Heuvel MP, Stam CJ, Boersma M, Hulshoff HE. Small-world and scale-free organization of voxel-based resting-state functional connectivity in the human brain. *NeuroImage*. 2008; 43(3):528-39.
33. Concha L, Beaulieu C, Collins DL, Gross DW. White-matter diffusion abnormalities in temporal-lobe epilepsy with and without mesial temporal sclerosis. *Neurol Neurosurg Psychiatry*. 2009; 80:312-9.
34. Coan AC, Kubota B, Bergo FPG, Campos BM, Cendes F. 3T MRI Quantification of Hippocampal Volume and Signal in Mesial Temporal Lobe Epilepsy Improves Detection of Hippocampal Sclerosis. *AJNR Am J Neuroradiol*. 2014; 35:77-83.

35. Ahmadi ME, Hagler DJ, McDonald CR, Tecoma ES, Iragui VJ., Dale AM, et al. Side matters: diffusion tensor imaging tractography in left and right temporal lobe epilepsy. *American journal of neuroradiology*. 2009; 30(9): 1740-47.
36. Coan AC, Campos BM, Bergo FPG, Kubota BY, Yasuda CL, Morita ME, et al. Patterns of seizure control in patients with mesial temporal lobe epilepsy with and without hippocampus sclerosis. *Arq. Neuro-Psiquiatr*. 2009; 73(2):79-82.
37. Schubert R. Attention deficit disorder and epilepsy. *Pediatric Neurology*. 2005; 32(1):1-10.
38. Lopes TM, Yasuda CL, Campos BM, Balthazar MLF, Binder JR, Cendes F. Effects of task complexity on activation of language areas in a semantic decision fMRI protocol. *Neuropsychologia*. 2016; 81:140-8.
39. Maulisova A, Korman B, Rey G, Bernal B, Duchowny M, Niederlova M, et al. Atypical language representation in children with intractable temporal lobe epilepsy. *Epilepsy & Behavior*. 2016; 58:91-6 .
40. Wei HL, An J, Zeng LL, Shen H, Qiu SJ, Hu DW. Altered functional connectivity among default, attention, and control networks in idiopathic generalized epilepsy. *Epilepsy & Behavior*. 2015; 46:118-25.

APÊNDICES

APÊNDICE 1: TUTORIAL DO UF²C

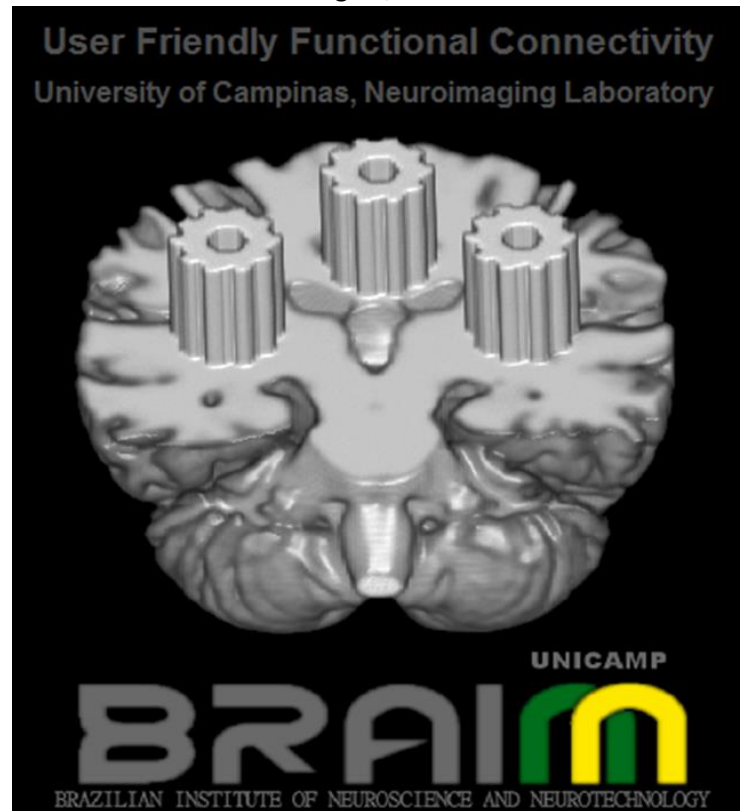
UF²C - User Friendly Functional Connectivity

University of Campinas - Neuroimaging Laboratory

Brunno Machado de Campos

Revised by Elise Facer-Childs (University of Birmingham)

August, 2016



UF²C is an open source software developed by Brunno M. de Campos at the Neuroimaging Laboratory at Unicamp. The aims of UF²C are to simplify and organize functional connectivity studies in neuroimaging through a clean and validated methodology, without sacrificing quality. UF²C has a full processing pipeline in which the user only needs to select the raw functional and structural NIfTI files from the subjects. The graphical user interface makes the processing and analysis options accessible for neuroscientists, with reasonable choices of default settings. UF²C allows the user to study functional connectivity both through a quantitative view that provides detailed values of average connectivity, and through a spatial view that provides statistical maps that can be directly used for further analyses. All results are carefully organized in distinct folders for each subject, and a common folder is generated with a log file reporting the quantitative results of all subjects analyzed.

Index

1. How to Cite.....	105
2. Requirements.....	106
3. Installing UF ² C.....	107
4. Input format.....	108
5. Starting.....	109
6. How to set the anterior commissure as the image origin using SPM12/Display	110
7. Starting to use UF ² C	118
8. Checking compatibilities.....	119
9. Preprocessing only routine.....	122
Band-Pass Filter (low-pass and high-pass filters).....	123
Regression.....	124
Add regressors - instructions	124
10. Modality 1 - Seed Based Functional Connectivity Analysis.....	126
Seed creation and definition.....	128
11. Modality 2 - Seed Based Functional Interactivity.....	130
Brief Introduction:	130
12. Modality 3 – Cross-correlation ROI-to-ROI Analysis	133
a) – First Level analysis (individual)	133
b) – Second Level analysis (Group inference).....	138
13. Modality 3 – Sliding Windows Connectivity	142
14. Some considerations about “time series extraction”	144

1. How to Cite

UF²C was presented to the community with an original research paper at Human Brain Mapping Journal:

- de Campos, B. M., Coan, A. C., Lin Yasuda, C., Casseb, R. F. and Cendes, F. (2016), Large-scale brain networks are distinctly affected in right and left mesial temporal lobe epilepsy. *Hum. Brain Mapp.*, 37: 3137–3152.

Please use this paper for future references or when citing UF²C in your studies.

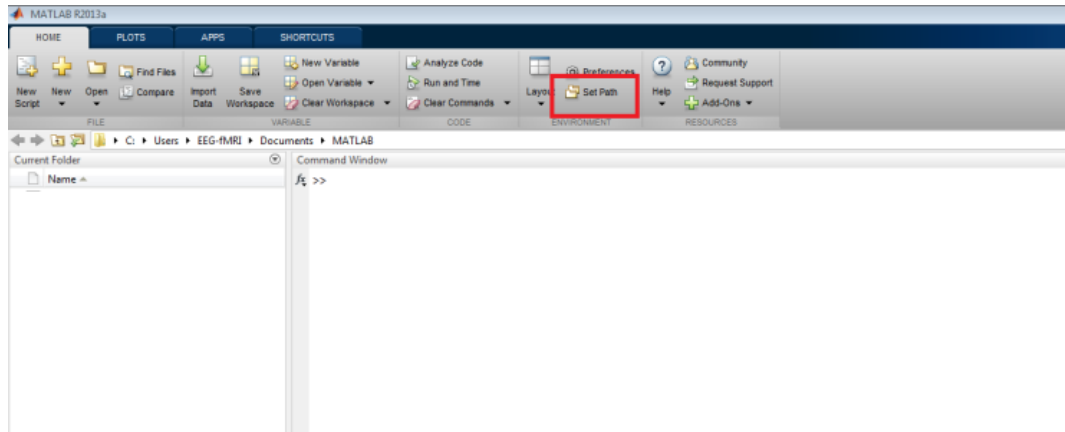
2. Requirements

UF²C is open source software, distributed under a BSD-style License. System requirements for UF²C are:

- Windows, Linux or Mac OS X operational systems
- [SPM8-12](#) (Statistical Parametric Mapping, version 8 or 12)
- [MATLAB](#) (version R2010a or later, required by SPM)
- MATLAB [Statistics toolbox](#)
- MATLAB [Signal Processing toolbox](#)
- MATLAB [Image Processing Toolbox](#) (for advanced graphic results)

3. Installing UF²C

UF²C should to be added to the "**Matlab Path**". The recent versions of Matlab changed the toolbar design and have a direct icon on the main Matlab window:



Click on "**Set Path**" and add the **UF²C** folder extracted from the downloaded Zip file. Use the option "**Add with subfolders**". Now your MATLAB knows that **UF²C** exist in your machine.

If you are using Windows OS, you can run UF²C by running the UF²C.exe file in 'uf2c' folder.

4. Input format

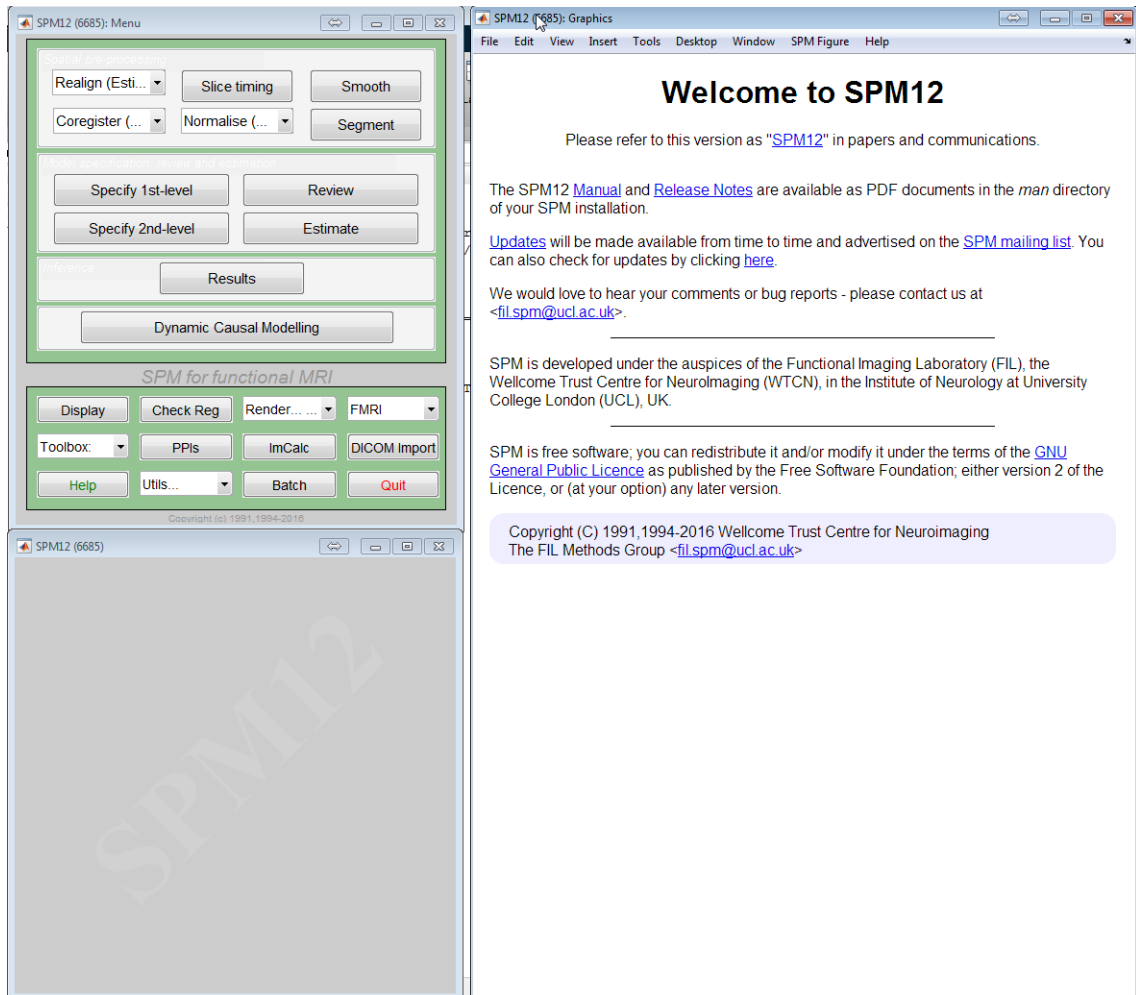
UF²C uses the NIfTI format for input files. You can use the dcm2nii utility (MRICron - www.mccauslandcenter.sc.edu/mricro/mricron/) to convert your files from many formats (e.g.: DICOM, PAR-REC...).

5. Starting

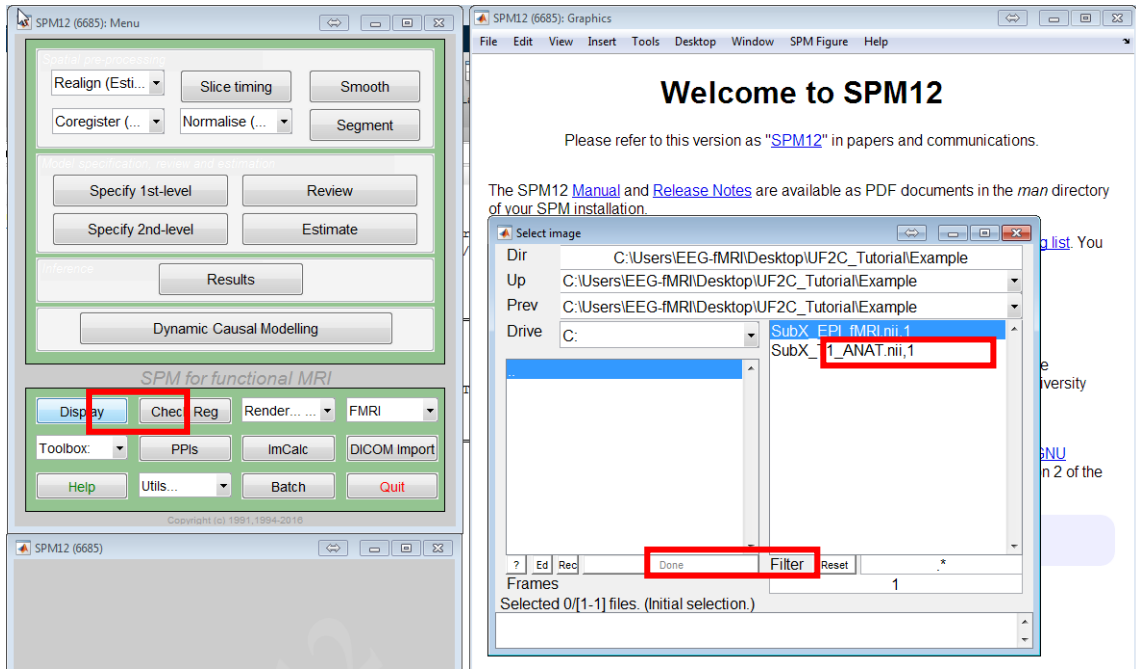
If you have already used SPM, you may know that a pre-preprocessing step improves SPM registration: defining the anterior commissure as the image origin. SPM12 '**Display**' tool is used to perform this tedious step. **UF²C** will probably work without the anterior commissure set as the origin. However, in some cases, when the origin [0,0,0] is too far (more than ~3 cm), the coregistration or normalization could lead to wrong deformations. There are some ways to set the anterior commissure as the origin automatically, but these methodologies need accuracy and repeatability in the FOV positioning during the MRI acquisition and are not recommended if you want to perform a high quality study. Therefore it is suggested that the anterior commissure should be set for each image.

6. How to set the anterior commissure as the image origin using SPM12/Display

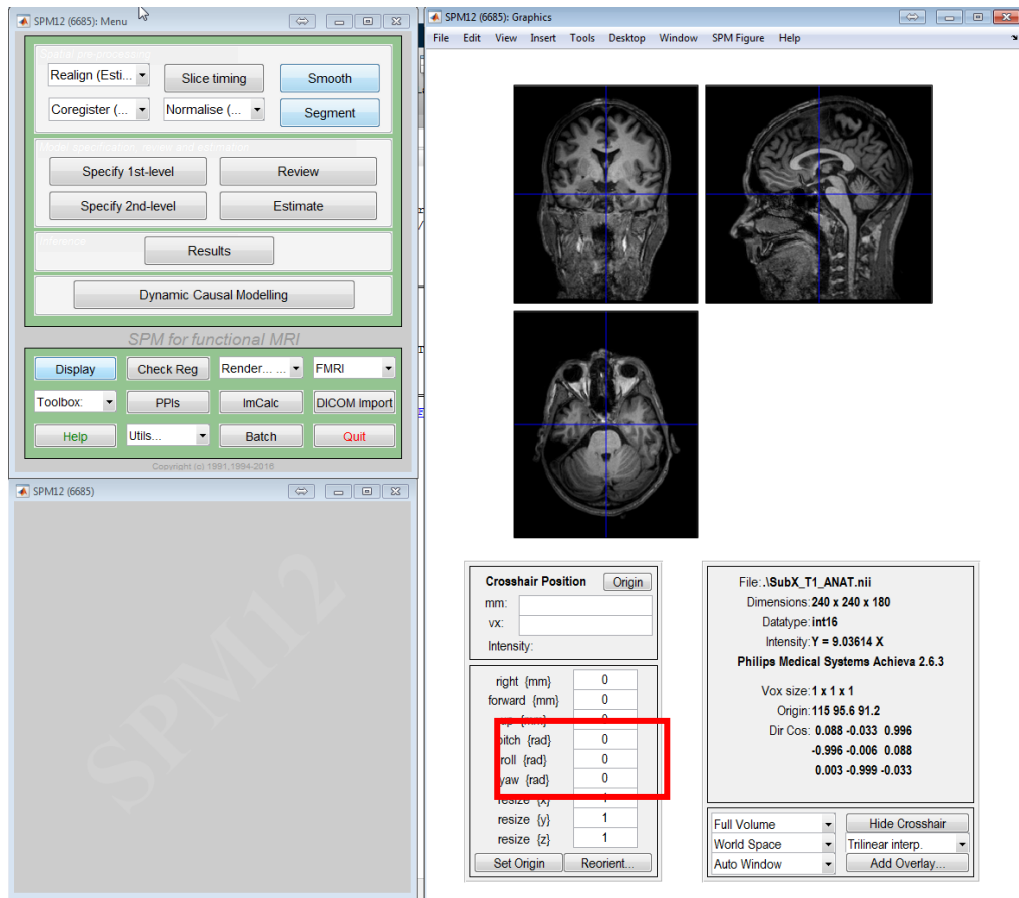
1. Run the Matlab.
2. Run SPM (type "**spm fmri**" on the Matlab command window).



3. On the SPM8 Menu click on "**Display**".



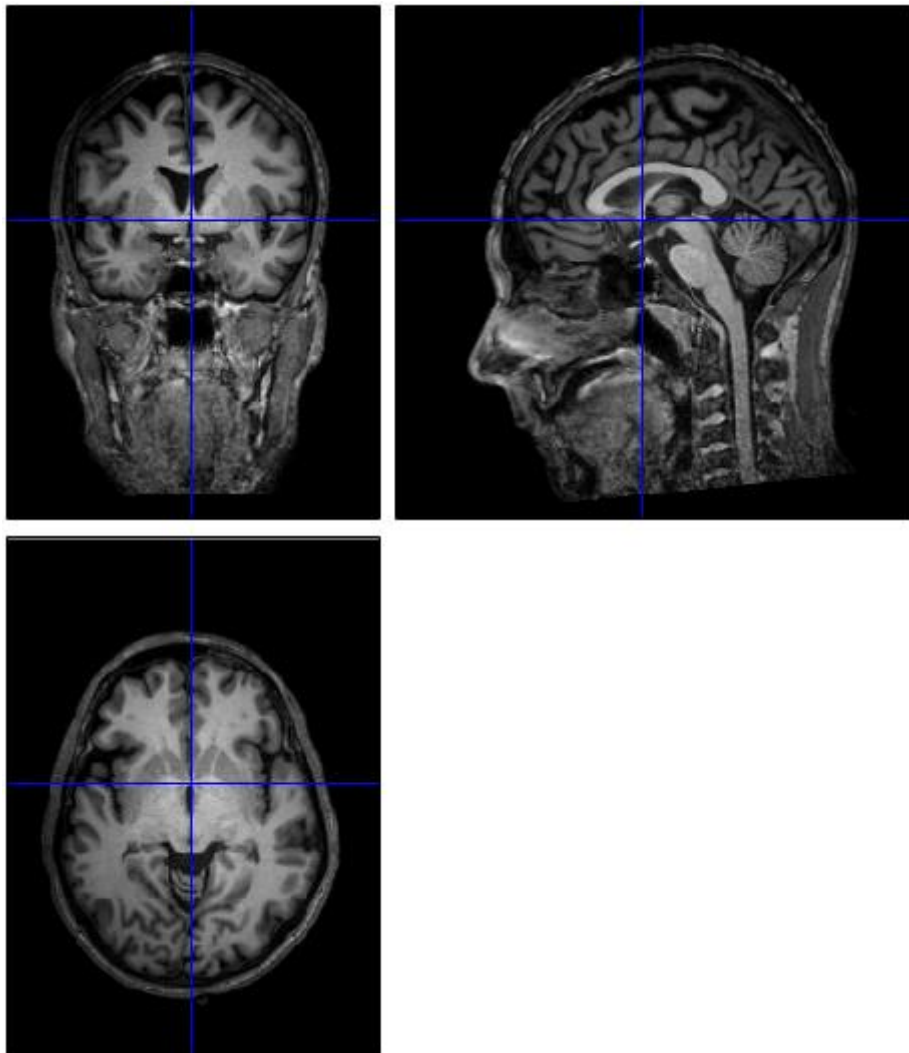
4. You will be asked to add an image. Add a structural (3D) file. Click once of the file of interest, and press “Done”. You can make sure the correct file is selected by looking at the box at the bottom.



5. Now you can use the fields "pitch {rad}", "roll {rad}" and "yaw {rad}" to correct the image orientations and rotations, using the anterior and posterior commissure as the horizontal reference and the inter-hemispheric fissure as the vertical reference.

forward {mm}	0
up {mm}	0
pitch {rad}	0.1
roll {rad}	-0.05
yaw {rad}	0.05
resize {x}	1
resize {y}	1

6. Now, you need to position the crosshairs on the anterior commissure.
7. The numbers inside the first box "Crosshairs Position" are the coordinate offsets between current point, indicated by the crosshairs, and the actual origin.



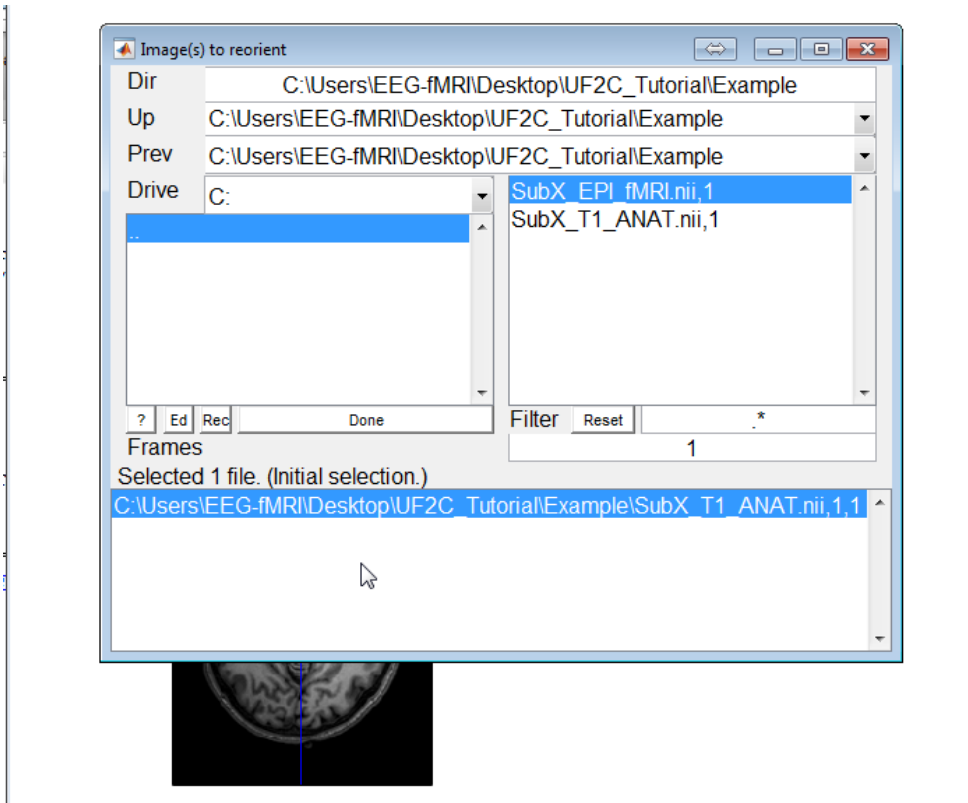
8. Press "Set Origin" and the "right {mm} ", "forward {mm}" and "up {mm}" fields, will be filled with the opposite number from the box above.

Crosshair Position		Origin
mm:	-1.1 -0.5 -2.3	
vx:	115.5 97.9 90.0	
Intensity:	1795.89	
right {mm}	0	
forward {mm}	0	
up {mm}	0	
pitch {rad}	0.1	
roll {rad}	-0.05	
yaw {rad}	0.05	
resize {x}	1	
resize {y}	1	
resize {z}	1	
Set Origin		Reorient...

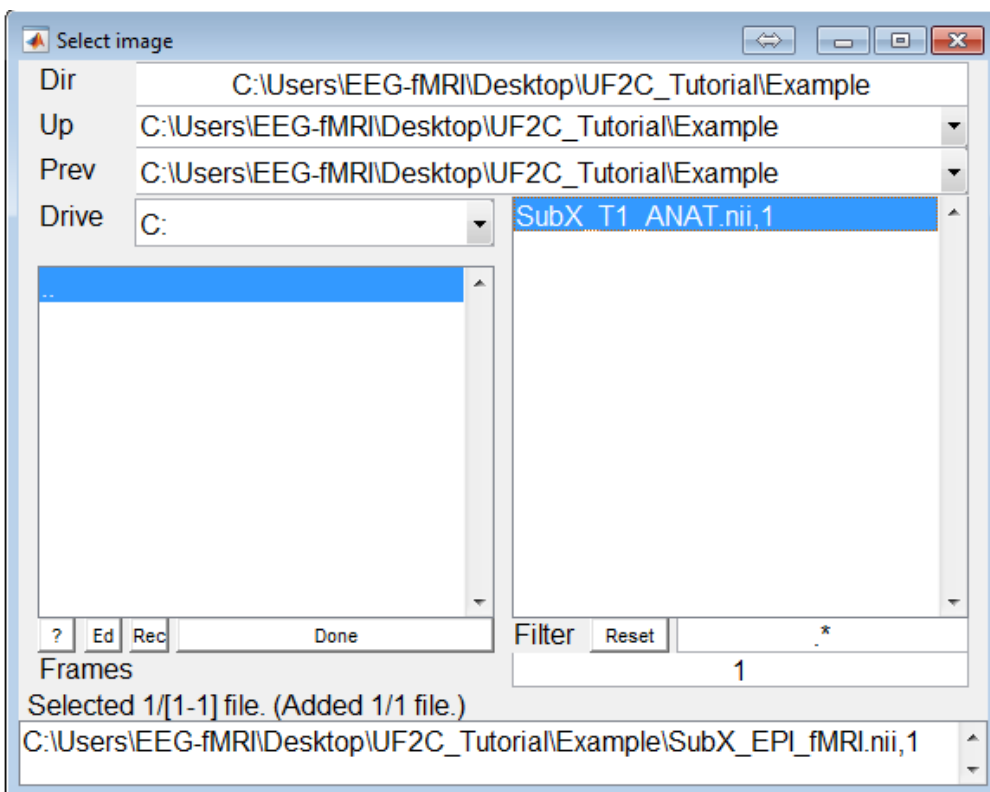
9. Click on the "Reorient..." button.

Crosshair Position		Origin
mm:	0.0 0.0 0.0	
vx:	115.5 97.9 90.0	
Intensity:	1795.89	
right {mm}	1.1398	
forward {mm}	0.47155	
up {mm}	2.2938	
pitch {rad}	0.1	
roll {rad}	-0.05	
yaw {rad}	0.05	
resize {x}	1	
resize {y}	1	
resize {z}	1	
Set Origin		Reorient...

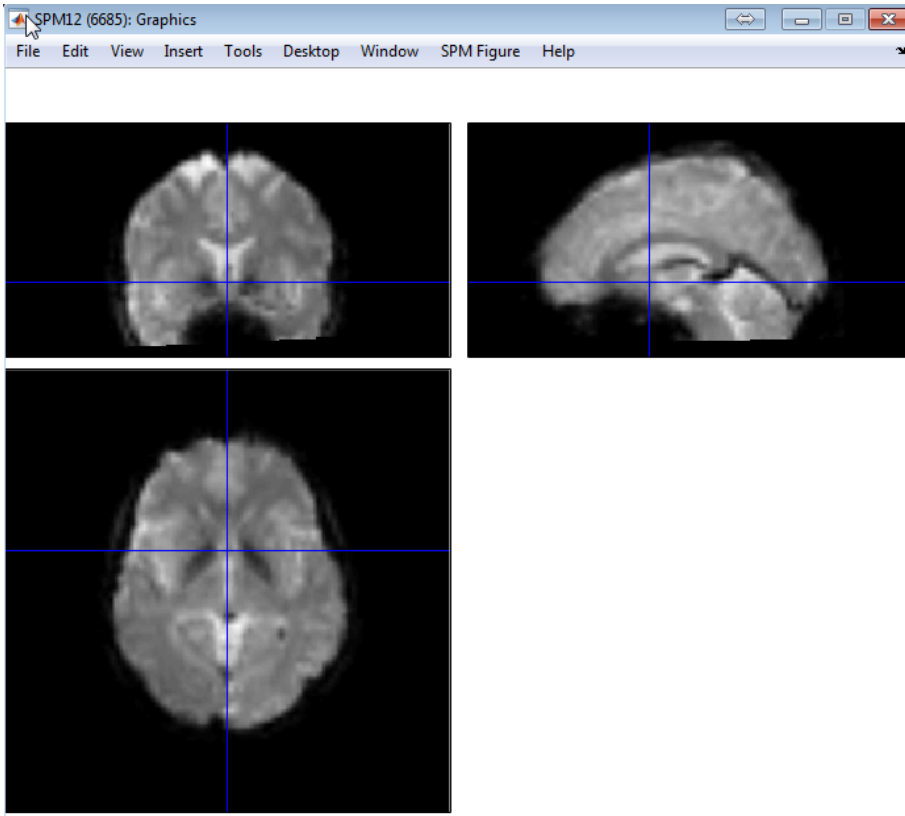
10. You will see the menu on the left hand side of the screen display 'reorienting images' and then the new reoriented image will be displayed. Just click "Done"!



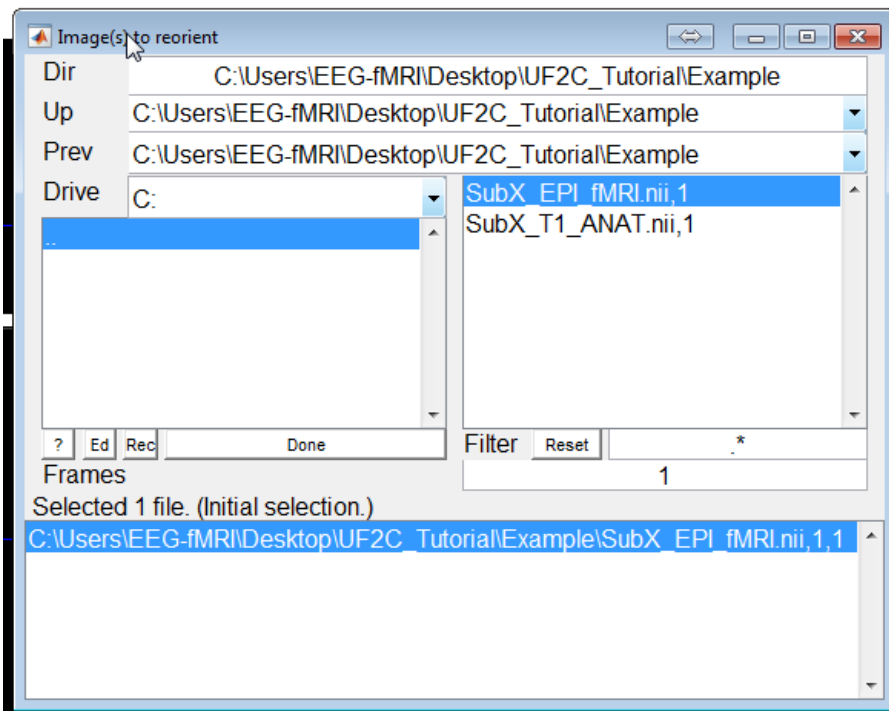
11. You need to repeat these steps for the functional image, but **pay attention: YOU NEED TO APPLY THE COORDINATES FOUND TO ALL VOLUMES (DYNAMICS)**
12. Add the fMRI. Note the “*.nii,1”. This “,1” means that you are adding the first volume ONLY.



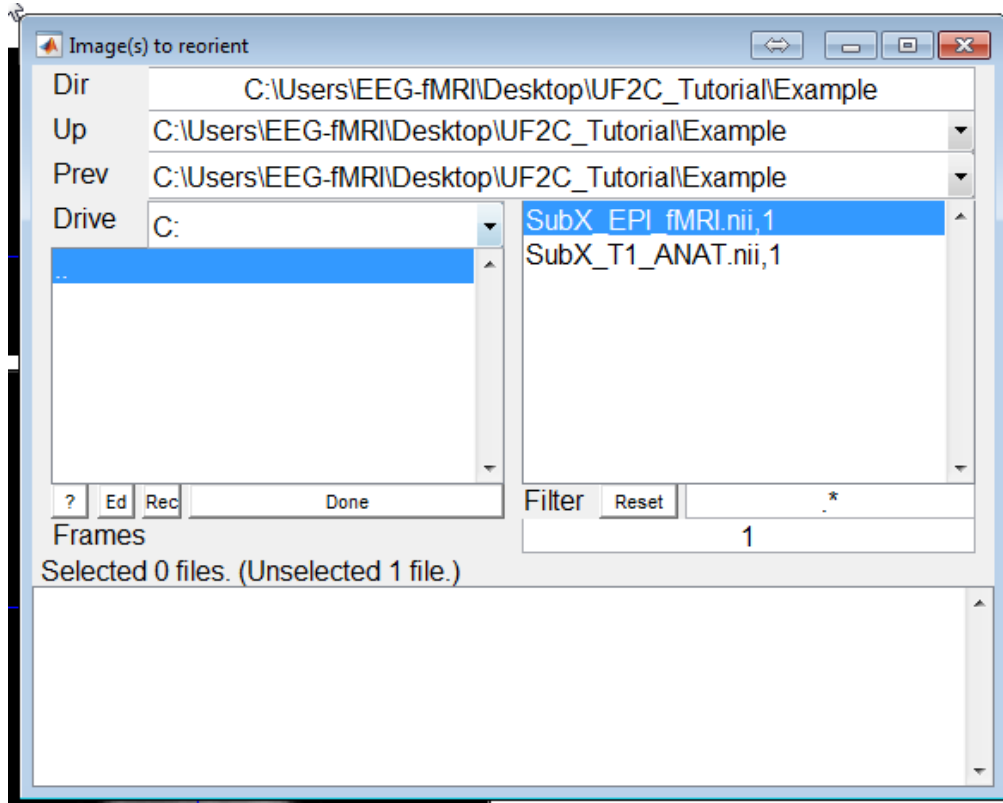
13. Use the same strategy to find the anterior commissure position as best you can. You can use the dark grey corpus callosum and even darker grey fornix as reference:



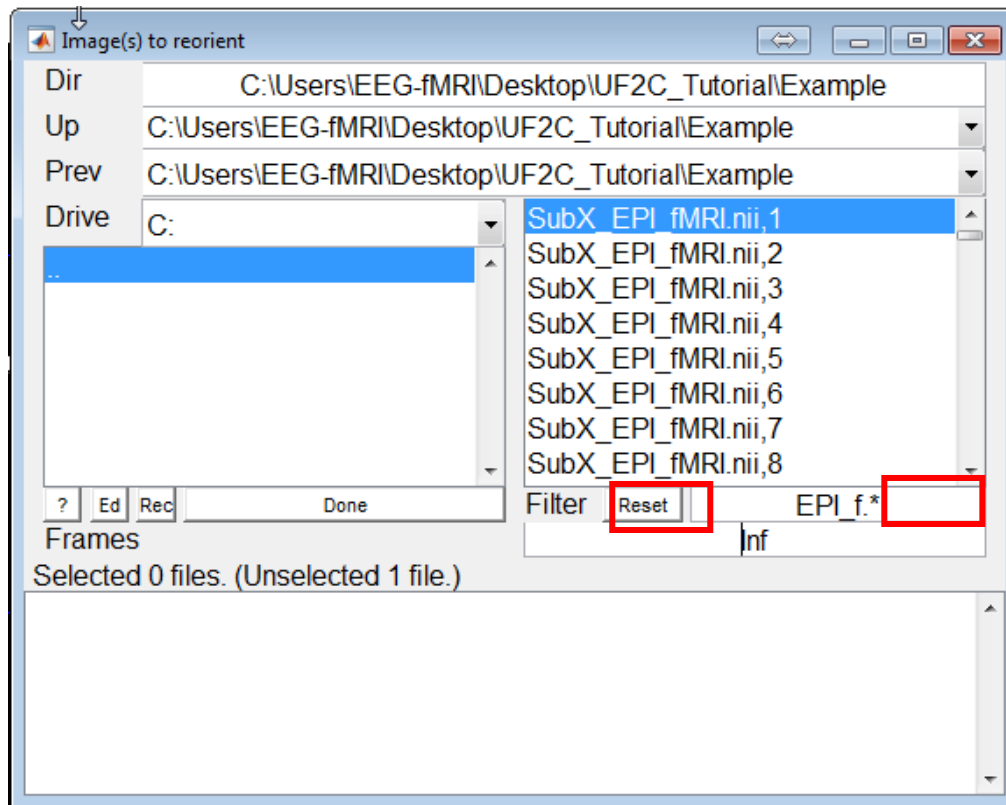
14. Repeat steps 5 to 9.
15. Once this is done you need to apply this reorientation to all dynamics:



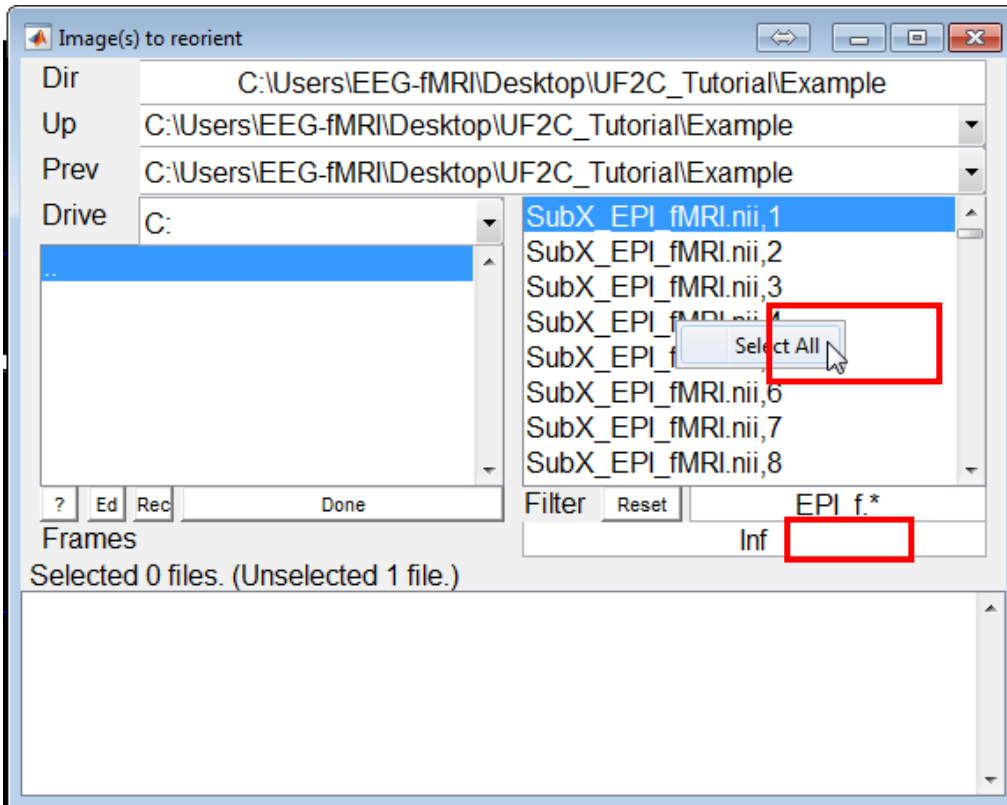
16. Remove the already added “,1” volume (left click on it once).



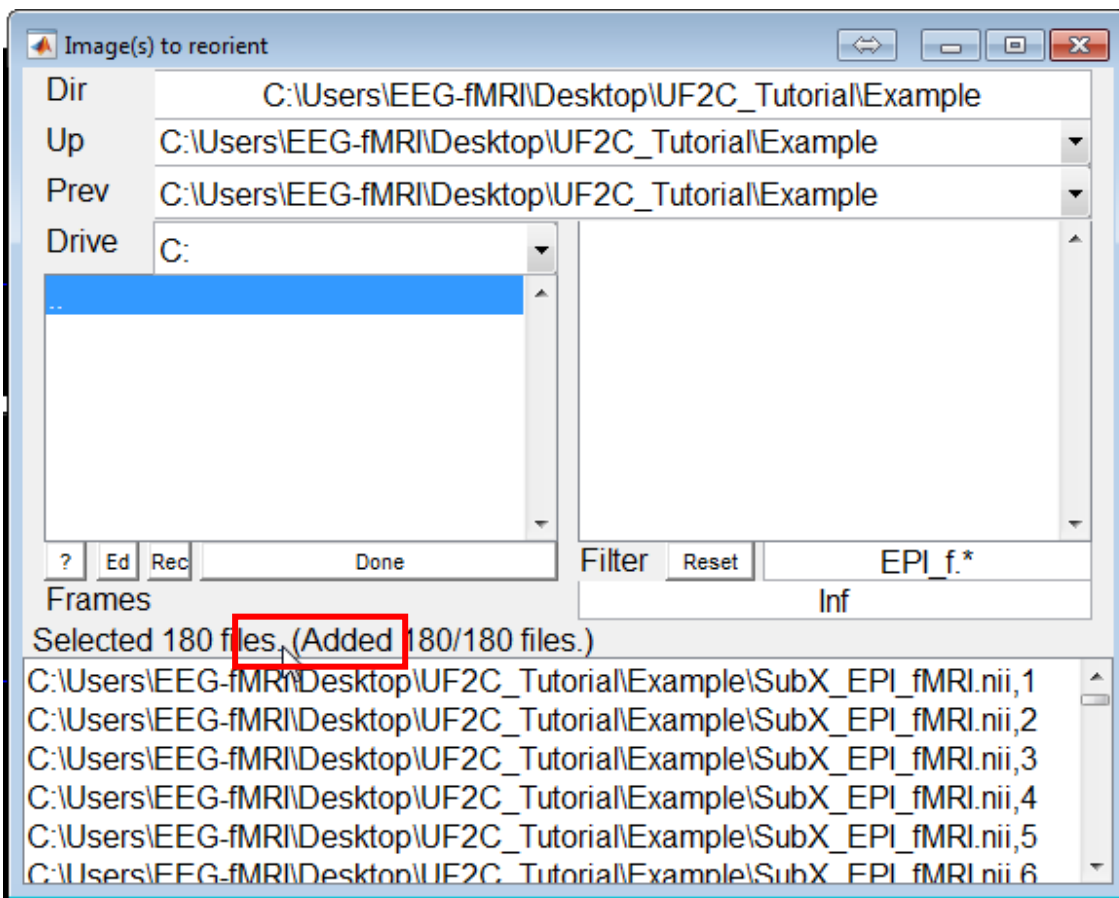
17. Use the field “Filter” to keep only the fMRI that you reoriented:



18. Type “Inf” replacing the number ‘1’. Press “return”. You will see all dynamics listed.



19. With the Right Mouse button, “Select All”:

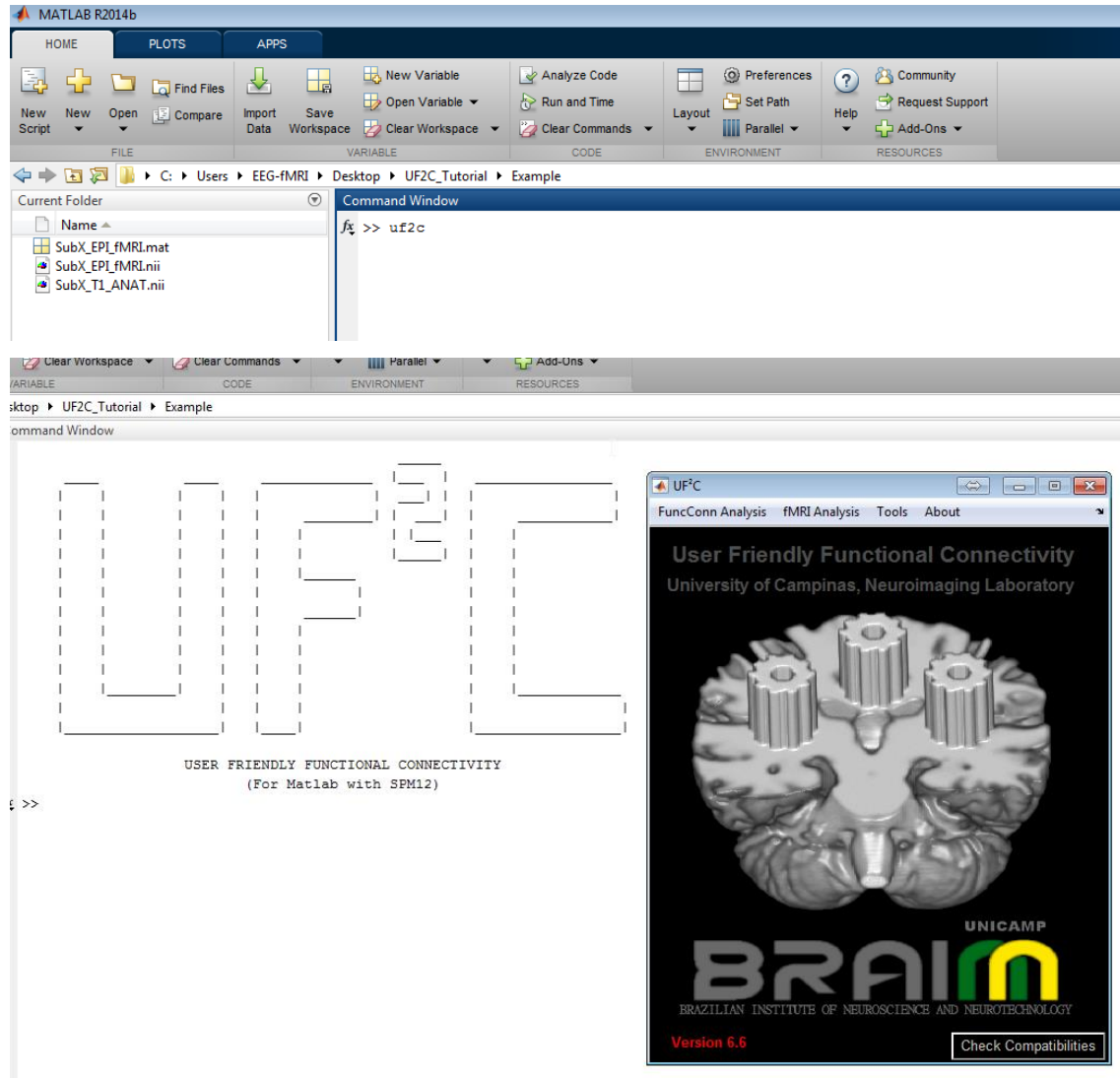


20. Check that the number of files added is correct and then click “Done”.

7. Starting to use UF²C

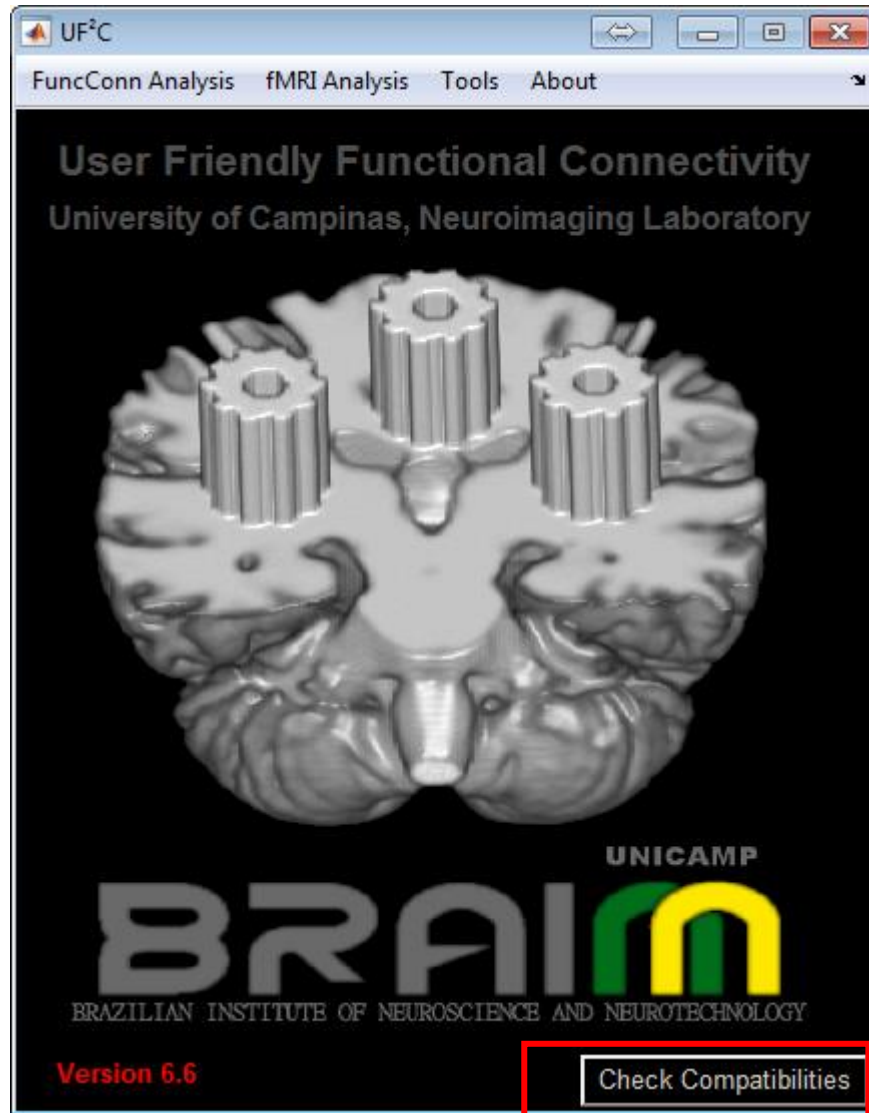
With the UF²C folder added to the Matlab path type `uf2c` in the Matlab command window.

If you are using Windows OS, you can run UF²C running the UF²C.exe file in the u2c folder.

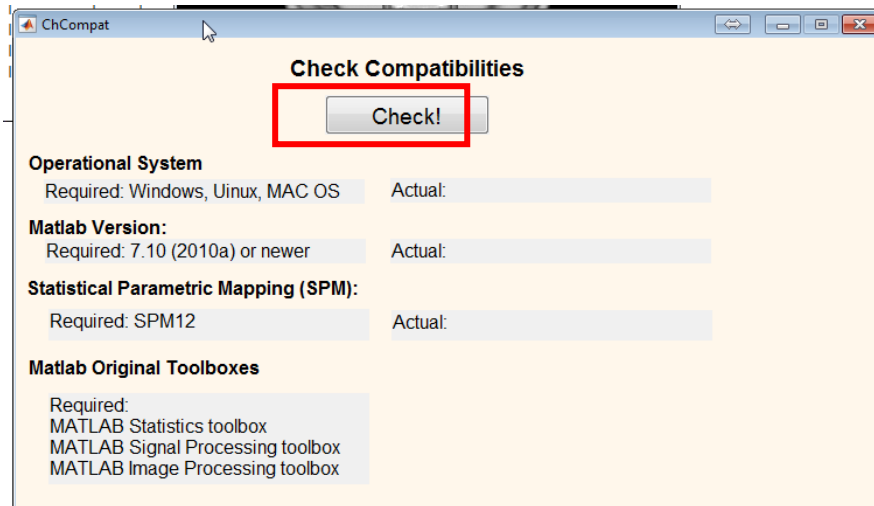


8. Checking compatibilities

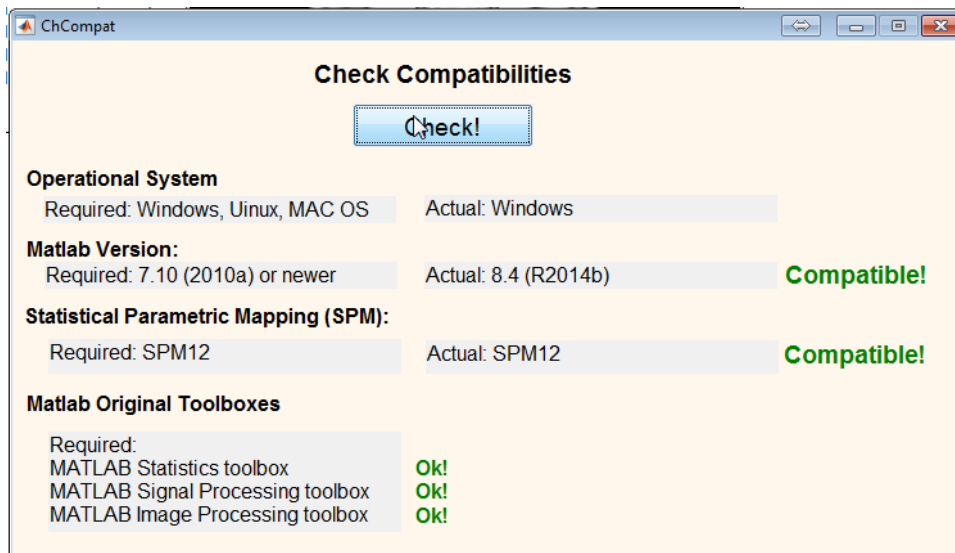
UF²C has a tool to verify the compatibility with your system, Matlab and SPM. Click on the “Check Compatibilities” Button on start screen:



Click on “Check” button.

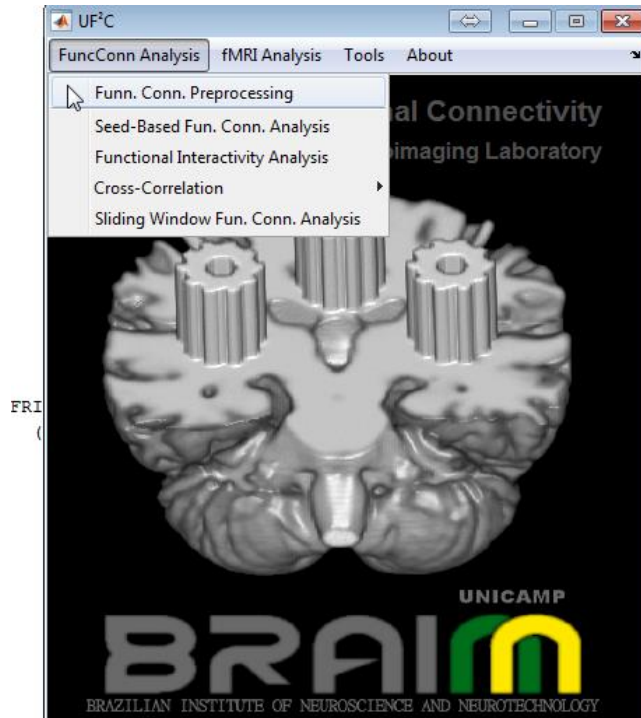


The UF²C will show in green compatible settings and in red if something is wrong or missing:



At this point, UF²C has **four** connectivity analysis modalities and a connectivity-preprocessing tool:

- "Funn. Conn. Preprocessing" (**all following modules can also run this step!**)
- 1. Traditional "Seed-Based Fun. Conn. Analysis (ROI to whole brain)
- 2. The concept analysis "Functional Interactivity Analysis" (ROIs to whole brain)
- 3. The "Cross-Correlation" ROIs connectivity (Inter-ROIs)
 - a. "Cross-Correlation ROI Analysis" (first level)
 - b. "Cross-Corr Second Level" analysis (group inference)
- 4. A sliding windows seed based functional connectivity (ROI to whole brain)



All modalities require functional (EPI) and structural (T1WI) images for all subjects and performs the same SPM preprocessing pipeline:

- 1 - Functional Image Realignment: Realign: Estimate & Reslice
- 2 - Functional – Structural coregistration: Coregister: Estimate
- 3 - Structural image segmentation: Segment
- 4 - Structural image normalization: Normalise: Write
- 5 - Functional image normalization: Normalise: Write
- 6 - Functional image smooth: Smooth

For UF²C specific steps please see below.

All UF²C codes are open so you can check and modify all of the parameters. Otherwise, please respect the UF²C [License](#).

9. Preprocessing only routine

UF²C - Preprocessing only

Check to use SPM-12 standard bonding box (matrix: 53 63 56) and originals voxel sizes

Inputs

Add Functional Files

Add Structural Files

Slice Timing Correction (ascending) Functional Image TR (sec):

Delete residual preprocessing files (Keep the subject folder cleanest)

Image Parameters

Functionals

Number of Dynamics:

Voxel Size (x y x):

Matrix Size:

Anatomicals

Voxel Size (x y x):

Matrix Size:

Filter and Regression Options

Band-Pass Filter

Apply band pass filter

Low-Pass Frequency:

High-pass Frequency:

Stopband attenuation:

Regressors

Movement Regression Save Regs

WM and CSF regression

Add regresors

The Funn. Conn. Preprocessing (Preprocessing only), allows you to preprocess your data, without any statistical or connectivity inference. It is important to highlight that all UF²C analysis modalities are also able to do this process followed by the connectivity analysis. Once you have the post processed functional images (FiltRegrSW_****.nii; obtained from this tool or from any other UF²C modalities) you can quickly perform the connectivity analysis in any modality, skipping the preprocessing (see below for instructions of how to do this).

The option “**Check to use SPM-12 standard bonding box [matrix: 53 63 66] and originals voxels sizes**” allows you to decide between the SPM12 standard matrix and bonding box (smaller, faster, but unique) or the MNI standard parameters (more data, slower, but you can overlap your data with all normalized [MNI-152] images).

With the button "**Add Functional Files**" you can add functional (4D) files of all subjects of your study. It is necessary for all functional files to be in the same folder. With the button "**Add Structural Files**" you will be able to insert all structural (3D) files of all subjects in your study. Obviously, the number of functional and structural files should match. **UF²C will sort files in alphabetic order to match each functional file to their respective structural file, so it is extremely important that both files have similar name structures.** You can use the extra tool "**Filename Changer**" to modify and adjust your filenames, adding prefixes, suffixes or just removing name parts.

After the fMRIs and the T1 WI images are added, you can click on "**Check order**" to verify if the list of functional and structural images are in the same order.

You can include the **slice timing** correction ONLY option when using the "preprocessing only" modality. The slice timing it is optional in FC studies and it is not a default here. We understand that the **slice timing correction** is more relevant in "event-related" analysis, and preferred to avoid more data manipulation.

Define the functional image repetition time (TR). The checkbox "**Delete residual preprocessing files**" gives to you the option to save all the processing files or just the final version of each post processed file. By checking this box the program will save just the realignment parameters (rp_*.txt file), the regressed-filtered-normalized-realigned functional file (FiltRegrSW*.nii) and the modulated-normalized structural file (wm*.nii file).

Image Parameters

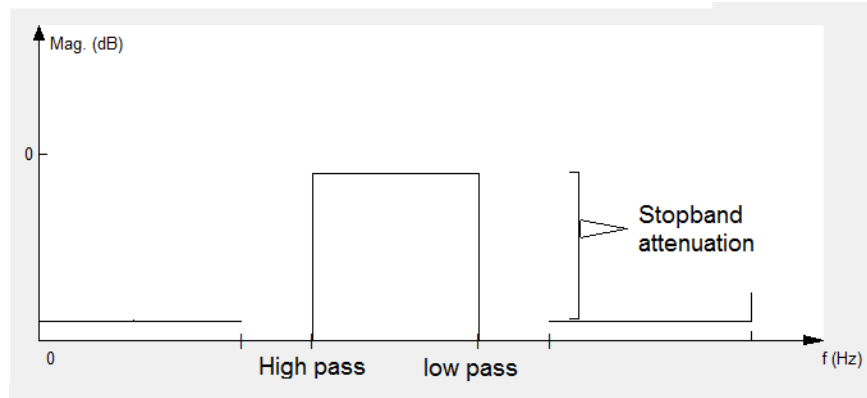
In this panel, relevant information about your functional and structural files will be shown. The first image of each type will be used as reference. **It is extremely important that all files (for different subjects) have the same parameters, such as voxel sizes, FOV, and number of dynamics.**

Filter and Regression Options (same for all UF²C modalities)

Band-Pass Filter (low-pass and high-pass filters)

In the check-box "**Apply band pass filter**", you can choose if you want to apply a filter to your temporal series. If the check box is selected, you will have the option to set low-pass and high pass frequency according to the next figure. The preset values are similar to resting state studies.

The stopband attenuation option defines the value (in dB) of the magnitude difference of the pass band (0dB) and the stop band frequencies.



Regression

UF²C enables the user to perform multiple regressions. By default, the program automatically applies regression to 6 movement parameters (3 rotational and 3 translational). **UF²C also regresses** each time series to average signal fluctuation for white matter (WM) and cerebral spinal fluid (CSF). Both of these options can be disabled.

Additionally, the software allows you to add additional regressors by enabling and clicking the "**Add regressors**" button. This option is activated after adding the functional files.

Add regressors - instructions

In these instructions, we will use an example which included 5 subjects. The functional file will have 15 dynamics (just for illustration). Two additional regressors will be added. For details please see the next figure.

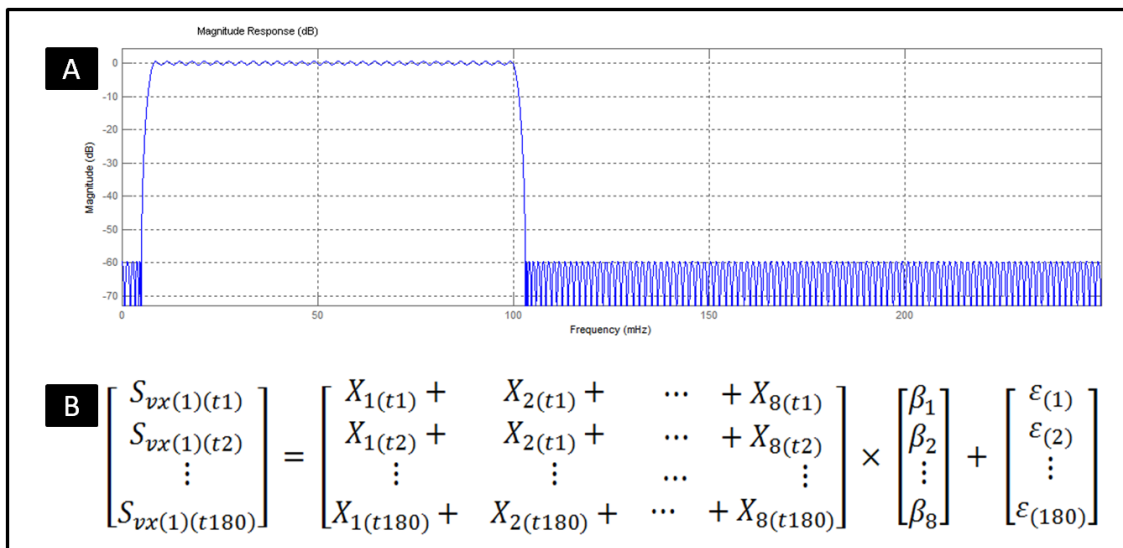
	A	B	C	D	E	F
1	0.8	0.8	0.8	0.8	0.8	
2	0.7	0.7	0.7	0.7	0.7	
3	0.3	0.3	0.3	0.3	0.3	
4	0.8	0.8	0.8	0.8	0.8	
5	0.7	0.7	0.7	0.7	0.7	
6	0.3	0.3	0.3	0.3	0.3	
7	0.8	0.8	0.8	0.8	0.8	
8	0.7	0.7	0.7	0.7	0.7	
9	0.3	0.3	0.3	0.3	0.3	
10	0.8	0.8	0.8	0.8	0.8	
11	0.7	0.7	0.7	0.7	0.7	
12	0.3	0.3	0.3	0.3	0.3	
13	0.8	0.8	0.8	0.8	0.8	
14	0.7	0.7	0.7	0.7	0.7	
15	0.3	0.3	0.3	0.3	0.3	
16	0.8	0.8	0.8	0.8	0.8	
17	0.7	0.7	0.7	0.7	0.7	
18	0.3	0.3	0.3	0.3	0.3	
19	0.8	0.8	0.8	0.8	0.8	
20	0.7	0.7	0.7	0.7	0.7	
21	0.3	0.3	0.3	0.3	0.3	
22	0.8	0.8	0.8	0.8	0.8	
23	0.7	0.7	0.7	0.7	0.7	
24	0.3	0.3	0.3	0.3	0.3	
25	0.8	0.8	0.8	0.8	0.8	
26	0.7	0.7	0.7	0.7	0.7	
27	0.3	0.3	0.3	0.3	0.3	
28	0.8	0.8	0.8	0.8	0.8	
29	0.7	0.7	0.7	0.7	0.7	
30	0.3	0.3	0.3	0.3	0.3	
31						

That is an example of ".xls" file that could be added to **UF²C**.

In this figure, 5 columns are shown, one for each subject (or functional file added). There are also 30 rows. The first 15 rows are from regressor one (shown in grey) and the next 15 rows are from regressor 2 (shown in green). The columns need to be in the same order of the subjects added. To check the subject order, click on the "subject list" button. Add the file on the "**Adreg**" window and click on the "Refresh" button to check if the number of regressors is Ok. Finally, click the "save and close" button to confirm.

The next figure shows the output design of the bandpass filter ("A"). In "B" the figure shows the multiple linear regression equation where:

- "X(n)" are the regressors (in this case we have 8
 - "t(n)" is the temporal variable (in this case, 180 time points)
- "Svx(n)(t)" is the variable that represents each voxel's temporal signal.



10. Modality 1 - Seed Based Functional Connectivity Analysis

The screenshot shows the FuncCon software window titled "UF²C - User Friendly Functional Connectivity". The interface is organized into several sections:

- Check to use SPM-12 standard bonding box (matrix: 53 63 56) and originals voxel sizes:** An unchecked checkbox at the top.
- Inputs:**
 - Check if you want to skip preprocessing
 - Add Functional Files:** A button next to an empty text input field, with a "Check order" button to its right.
 - Add Structural Files:** A button next to an empty text input field, with a "Check order" button to its right.
- Image Parameters:**
 - Functionals:**
 - Number of Dynamics: []
 - Voxel Size (x y x): []
 - Matrix Size: []
 - Anatomicals:**
 - Voxel Size (x y x): []
 - Matrix Size: []
- Experiment Definitions:**
 - Delete residual preprocessing files (Keep the subject folder cleanest)
 - Window Size (dynamics): []
 - Seed Size X Y Z (in voxels): [4 4 4]
 - Seed (ROI) Coordinate (MNI): [0 -51 21]
 - Scan TR (sec.): [2]
 - Add a normalized mask as a seed
- Filter and Regression Options:**
 - Band-Pass Filter:**
 - Apply band pass filter
 - Low-Pass Frequency: [0.1]
 - High-pass Frequency: [0.008]
 - Stopband attenuation: [50]
 - Regressors:**
 - Movement Regression
 - WM and CSF regression
 - Add regresors
 - Refresh

A large "Run" button is centered at the bottom of the window.

The option “**Check to use SPM-12 standard bonding box (matrix: 53 63 66) and originals voxels sizes**” allows you to decide between SPM12 standard matrix and bonding box (smaller, faster, but unique) or the MNI standard parameters (more data, slower, but you can overlay with all normalized (MNI-152) images).

Input Panel

In the "Input" panel, you have the option to "**Check if you want to skip preprocessing**". Click in the box if you already have the normalized post processed functional image that you want to use in your analysis. It is strongly recommended to use only the "FiltRegrSW" images generated by UF²C preprocessing pipelines. By checking this option, all preprocessing parameters and options will be disabled.

Using the button "**Add Functional Files**" you can add raw (reoriented) functional (4D) files of all subjects in your study. With the button "**Add Structural Files**" you can insert all structural (3D) files of all subjects in your study. Obviously, the number of functional and structural files should to match. **UF²C will use alphabetic order to match each functional file to their respective structural file, so it is extremely important that both files have similar name structures, e.g. Subj_XX1_fMRI.nii and Subj_XX1_T1.nii.** You can use the extra tool "**Filename Changer**" to modify and adjust your filenames, adding prefixes, suffixes or removing name parts.

After adding the fMRIs and T1 WI images, you can click on "**Check order**" to verify if the list of function and structural images are in the same order.

Image Parameters

In this panel, relevant information about your functional and structural files will be shown. The first image of each type will be used as reference. **It is extremely important that all files (of different subjects) have the same parameters, such as voxel sizes, FOV, and number of dynamics.**

Experiment Definitions

In this panel, you can define important parameters that are relevant to you experiment. The first checkbox "**Delete residual preprocessing files**" gives you the option to save all the processing files or just the final version of each post processed file. By checking this box the program will just save the:

- realignment parameters (rp_*.txt file)
- modulated-normalized-smoothed functional file (sw*.nii file)
- regressed-filtered functional file (FiltRegrSW*.nii)
- modulated-normalized structural file (wm*.nii file).

By default, the option "**Window Size**" will be filled with the total number of dynamics (volumes or temporal points of your functional file). When looking at dynamic connectivity you can divide your temporal series by setting the size of these windows. For example, if you have functional data with 300 dynamics, and set the Window size to 60, you will divide your temporal series in 5 parts. This option gives information about the temporal variation in the connectivity during the acquisition period. **The window size should be divisible by the number of dynamics.** Remember that the reduction of the

correlation time points, by the addition of a large number of windows, reduce the degrees of freedom of the correlation test and the significance of the r-values.

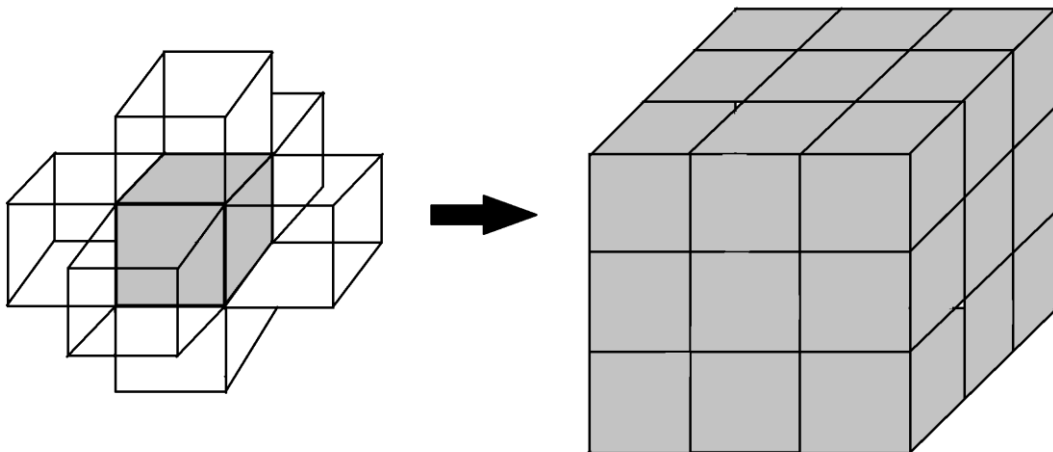
The correlation will be performed separately for each window. As a result, **UF²C** will plot a graph with the connectivity variation during these 5 time points. Also the final connectivity map will be created as a 4D file in which each volume will be the statistical r-map of each window correlations.

Seed creation and definition

In the option "**Seed (ROI) Coordinate**", you should set the MNI (Montreal Neurologic Institute template) coordinate of the region that you want to use as seed. The seed will be the region from where **UF²C** will extract the reference time series. **UF²C** will use the seed's time series to calculate the correlations. In other words, the statistical values in the final map are always the correlation coefficient (r) between the time series of each cortex voxel and the seed's average time series. The coordinate set as default refers to the posterior cingulate cortex, commonly used as seed in Default Mode Network (DMN) studies.

The checkbox "**Add a normalized mask as a seed**" allow you to add a normalized (MNI-152) ROI image (NIfTI) as seed. The average time series will be generated by averaging all ROI voxels time series. In this case, the "**Seed (ROI) Coordinate (MNI)**" option and the "**Seed Size X Y Z (in voxels)**" option would be disabled.

The option "Seed size X Y Z" is used to increase the seed size. For example, 2 2 2 will add 1 voxel (2/2) for each side in each spatial axis. In this case the seed will be a cube with 3 voxels per edge or with 27 voxels total volume (the next figure illustrates this case).



In this situation your seed is a VOI (volume of interest) with 27 voxels, so your reference time series will be the average time series between these voxels. This methodology to set the VOI size may seem unusual, but it is a safe way to keep the defined seed coordinates always in the center of the VOI.

Finally, the field Scan TR is used to define the repetition time (TR) in the functional acquisition. In this option the user needs to set the TR in seconds. The TR is not correct or is missing in most NIfTI headers.

Filter and Regression Option

The same described on the **“Preprocessing Only”** routine.

11. Modality 2 - Seed Based Functional Interactivity

FuncInte

UF²I - User Friendly Functional Interactivity

Check to use SPM standard bonding box (matrix: 53 63 46)

Inputs

Add Functional Files

Add Structural Files

Image Parameters

Functionals

Number of Dynamics:

Voxel Size (x y x):

Matrix Size:

Anatomicals

Voxel Size (x y x):

Matrix Size:

Experiment Definitions

Delete residual preprocessing files (Keep the subject folder cleanest)

Window Size (dynamics):

Seed side increased with: voxel Seed size: voxels³

Scan TR (sec.): Threshold to voxels

Filter and Regression Options

Band-Pass Filter

Apply band pass filter

Low-Pass Frequency:

High-pass Frequency:

Stopband attenuation:

Regressors

Movement Regression

WM and CSF regression

Add regressors Refresh

Run

Brief Introduction:

Functional connectivity (FC) is an fMRI modality able to elucidate brain interactional patterns without cause-effect through the identification of varied functionally cooperative networks related to distinct brain states (Friston *et al.*, 1996). Different methods are used to access FC information from fMRI data, which are divided between seed-based or data-driven methods (Liangsuo Ma; Suresh E. Joel; Kaiming Li). Seed-based FC is a modality that quantifies correlations throughout the whole brain time-series by using a region of interest (ROI) as reference and thereby allows the study of specific networks by controlling the seed position. The method enables an objective and straightforward analysis, although it provides results that depend on a precise initial assumption and are restricted to those defined networks. On the other hand, independent component analysis (ICA) produces more information from the data, providing connectivity patterns without any initial assumption, although could reveal intricate

results, requiring an exhaustive and bias susceptible task to separate study relevant from misleading components (Liangsuo Ma; Calhoun VD, Adali T, Pearlson GD, Pekar JJ). A multi-seed FC analysis keeps the straightforward results provided by seed-based methods but also expands the networks of interest, giving extensive information about connectivity patterns and avoiding a strong initial assumption. The combination of the correlation maps generated for each seed could reveal distinct aspects of the functional networks organization, depending on how these maps were integrated or explored [The future of fMRI connectivity. Stephen M. Smith]. In this sense, the concept of functional interactivity (FI) is based on averaged FC maps to define areas more or less globally integrated, providing an exploratory view of the study and therefore allowing a generalized view of the brain connectivity patterns. [Inf Process Med Imaging. 2007; 20:147-59. Functional interactivity in fMRI using multiple seeds' correlation analyses--novel methods and comparisons. Wang YM1, Xia J.]

Inputs

The same described on the **Preprocessing Routine**.

Image Parameters

The same described on the **Preprocessing Routine**.

Experiment Definitions

The options "**Delete residual preprocessing files**" and "**Window Size (Dynamics)**" have the same functions described on the **modality 1 section**.

The FI analysis uses a cubic seed that varies in position. The option "**Seed side increased with:**" allows you to set your seed side size. For example: If you fill the option "**Seed side increased with:**" **3**, you will define a seed with a 4 voxel side and hence **64** voxels in total. By default, the "**Threshold to sow**" option defines the number of overlapping voxels between the seed and the cortex, to use that seed position as an effective seed in the experiment. In the example, **UF²C** will place the cubic seed in all possible positions that retained at least 42 voxels overlapping with the cortex. For each seed an average time series was extracted and the linear correlation was estimated for all GM voxels, generating a statistical map for each seed position.

You can increase or decrease the "**Threshold to sow**" value → lower values will result in a larger number of seed positions.

Filter and Regression Option

The same described on the "**Preprocessing Only**" Routine.

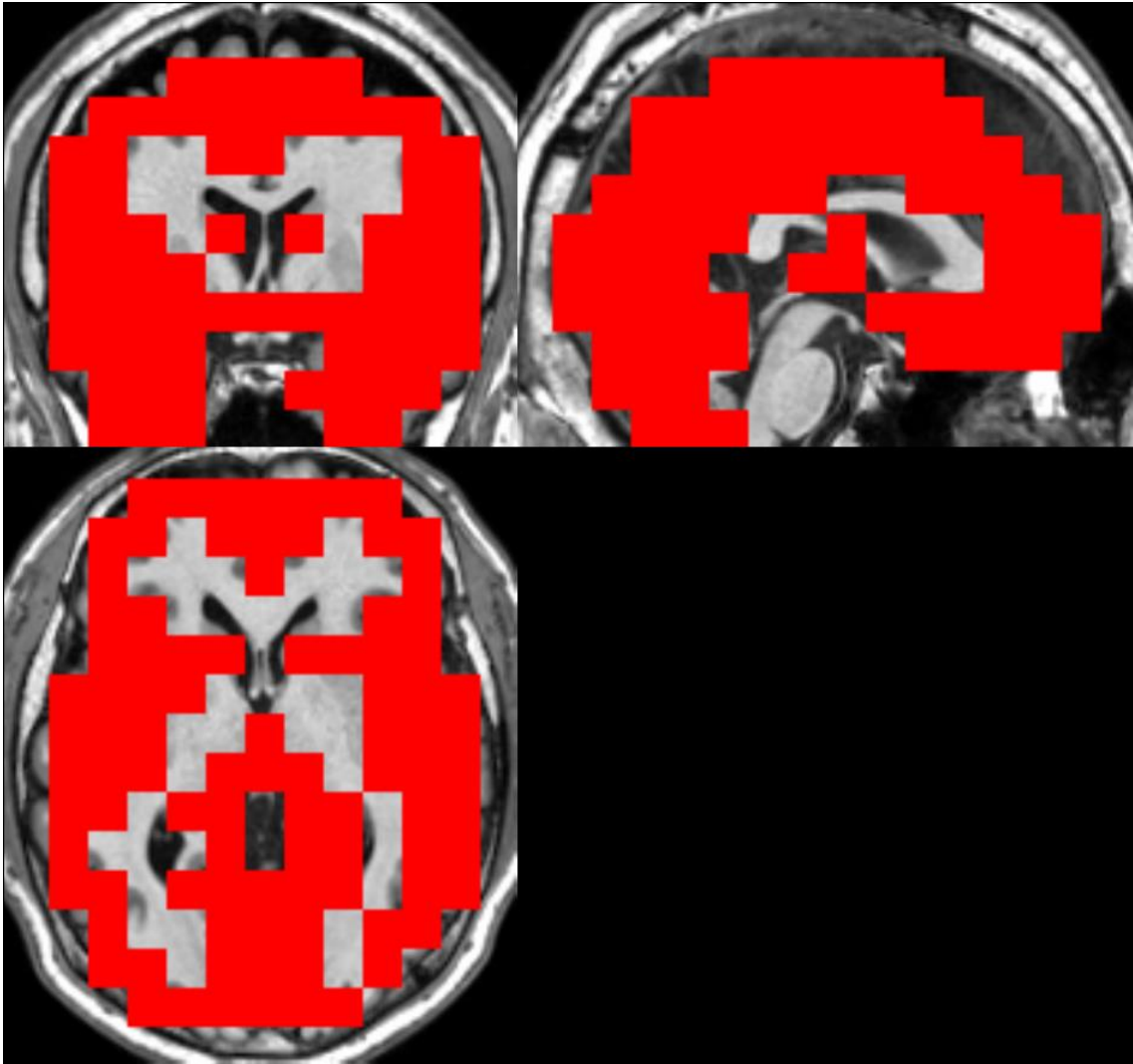


Fig: An example of mask of seeds generated by the code. The red cubes overlays all regions that were used as seed.

12. Modality 3 – Cross-correlation ROI-to-ROI Analysis

a) – First Level analysis (individual)

TS_CrossCor

UF²C - Crosscorrelation ROI-to-ROI analysis

Check to use SPM-12 standard bonding box (matrix: 53 63 56) and original voxel sizes

Inputs

Check if you want to skip preprocessing

Add Functional Files

Add Structural Files

Image Parameters

Functionals

Number of Dynamics:

Voxel Size (x y x):

Matrix Size:

Anatomicals

Voxel Size (x y x):

Matrix Size:

Experiment Definitions

Window Size (dynamics):

Scan TR (sec.):

Images as Seed

Add normalized masks as seeds

Coordinates list

Add a txt file with seeds coordinates

Seed Size X Y Z (in voxels):

Delete residual preprocessing files (Keep the subject folder cleanest)

Plot and save rendered 3D grapho? (requires a good machine)

Filter and Regression Options

1 - Regressors

Movement Regression

WM and CSF regression

Add regresors

2 - Band-Pass Filter

Apply band pass filter

Low-Pass Frequency:

High-pass Frequency:

Stopband attenuation:

The option “**Check to use SPM-12 standard bonding box (matrix: 53 63 66) and originals voxels sizes**” allow you to decide between SPM8 standard matrix and bonding box (smaller, faster, but unique) or the MNI standard parameters (more data, slower, but you will can overlay with all normalized (MNI-152) images).

Input Panel

In the "Input" panel, you have the option **“Check if you want to skip preprocessing”**. Check this option if you already have the normalized post processed functional image that you want to use in your analysis. It is strongly recommended to use only the **“FiltRegrSW”** images generated by UF²C preprocessing pipelines. Checking this option, all preprocessing parameters and options will be disabled.

With the button **"Add Functional Files"** you can add raw (reoriented) functional (4D) files of all subjects of your study. With the button **"Add Structural Files"** you will be able to insert all structural (3D) files of all subjects in your study. Obviously, the number of functional and structural files should to match. **UF²C will use the alphabetic order to match each functional file to their respective structural file, so it is extremely important that both files have similar name structures, e.g.: Subj_XX1_fMRI.nii and Subj_XX1_T1.nii.** You can use the extra tool **"Filename Changer"** to modify and adjust your filenames, adding prefixes, suffixes or removes name parts.

After add the fMRIs and the T1 WI images, you can click on **“Check order”** to verify if the list of function and structural images are in the same order.

Image Parameters

In this panel, relevant information about your functional and structural files will be shown. The first image of each type will be used as reference. **It is extremely important that all files (of different subjects) have the same parameters, such as voxel sizes, FOV, and number of dynamics.**

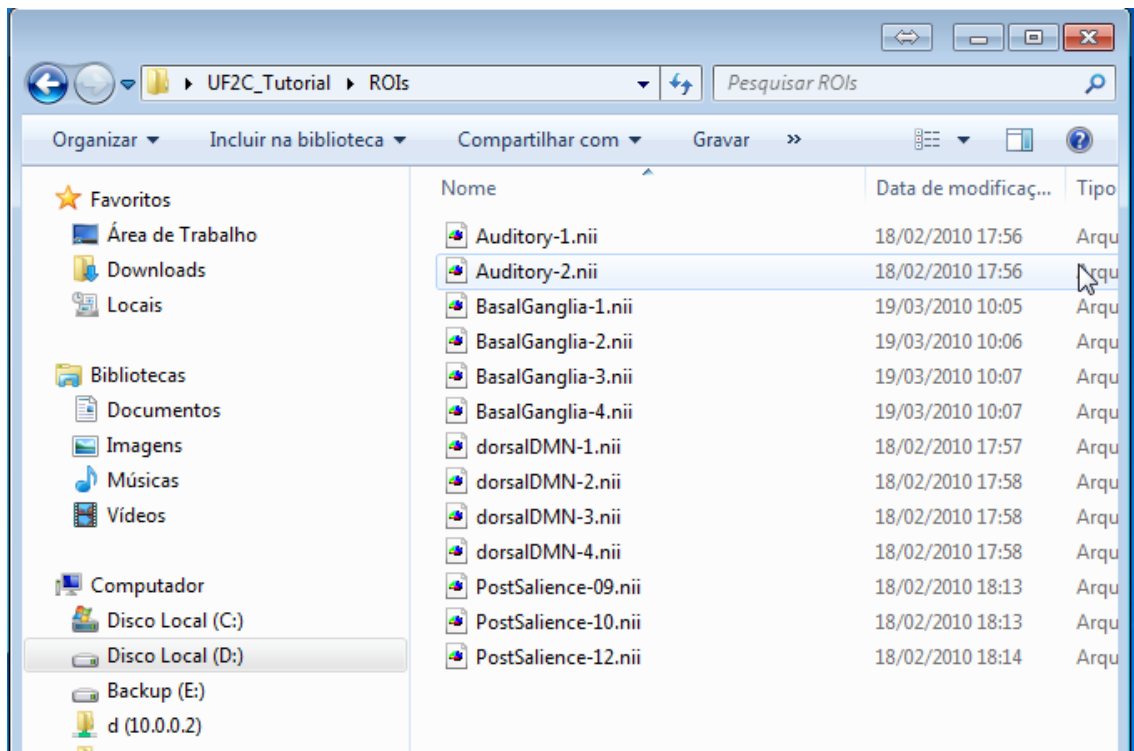
Experiment Definitions

In this panel, you will be able to define important parameters that will be extremely relevant to you experiment. The option **"Window Size"** by default, will be filled with the total number of dynamics (volumes or temporal points of your functional file). You can divide your temporal series by setting the size of these windows. For example, if you have functional data with 300 dynamics, and set the Window size to 60, you will divide your temporal series in 5 parts. This option gives information about the temporal variation in the connectivity during the acquisition period. **The window size should be a divisor of the number of dynamics.** Remember that the reduction of the correlation time points, by the addiction of a large number of windows, reduce the degrees of freedom of the correlation test and the significance of the r-values. The correlation will be performed separately for each window. As a result, **UF²C** will plot a connectivity matrix for each of the five time points.

The field **Scan TR (sec)**, is used to define the repetition time (TR) in the functional acquisition. In this option the user needs to set the TR in seconds. The TR is not correct or is missing in most NIfTI headers. To define the ROIs in which the UF²C will compute the ROI-to-ROI correlations, you have two options. In both options UF²C can identify ROIs from a specific network, and separates them into the analysis

resulting in extra information. The network identification results in the concept of inter (between networks) and Intra (inside ROIs of a same network) connectivity. In the resultant images, like the resultant brain connectome images, the spheres that will represent the ROIs will be colored with respect to the network organization (one color per network).

Option 1 – “**Add normalized masks as seeds**”: By checking this option, an input window will open and you will be able to add ROIs as binary NiftI images. In this option, UF²C will identify the network organization among the files added, using the three first filenames characters:



Considering these ROIs files, UF²C will identify 13 ROIs from 4 networks:

Network 1: Auditory (**Aud**); Network 2: basal Ganglia (**Bas**); Network 3 dorsalDMN (**dor**);

Network 4: PostSalience (**Pos**).

The UF²C GUI will show:

TS_CrossCor

UF²C - Crosscorrelation ROI-to-ROI analysis

Check to use SPM-12 standard bonding box (matrix: 53 63 56) and original voxel sizes

Inputs

Check if you want to skip preprocessing

Add Functional Files: 5 functional image(s) added Check order

Add Structural Files: 5 Structural image(s) added Check order

Image Parameters

Functionals	Anatomicals
Number of Dynamics: 180	Voxel Size (x y x): 1x1x1
Voxel Size (x y x): 3x3x3	Matrix Size: 240x240x180
Matrix Size: 80x80x39	

Experiment Definitions

Window Size (dynamics): 180 Scan TR (sec.): 2

Images as Seed **Coordinates list**

Add normalized masks as seeds Add a txt file with seeds coordinates

13 ROI mask(s) added!
4 network(s) identified! Seed Size X Y Z (in voxels): 4 4 4

Delete residual preprocessing files (Keep the subject folder cleanest)

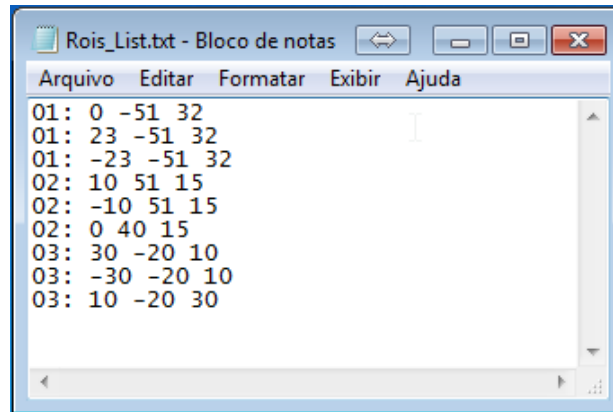
Plot and save rendered 3D grapho? (requires a good machine)

Filter and Regression Options

1 - Regressors	2 - Band-Pass Filter
<input checked="" type="checkbox"/> Movement Regression	<input checked="" type="checkbox"/> Apply band pass filter
<input checked="" type="checkbox"/> WM and CSF regression	Low-Pass Frequency: 0.1
<input type="checkbox"/> Add regresors Refresh 0 added	High-pass Frequency: 0.008
	Stopband attenuation: 50

Run

Option 2 - “Add a txt file with seeds coordinates”: In this option, you will be able to add a text file (*.txt) with MNI coordinates of where you want the seeds. You will be also able to use networks distinction here. For this, you will need to format the text file as follows:



```

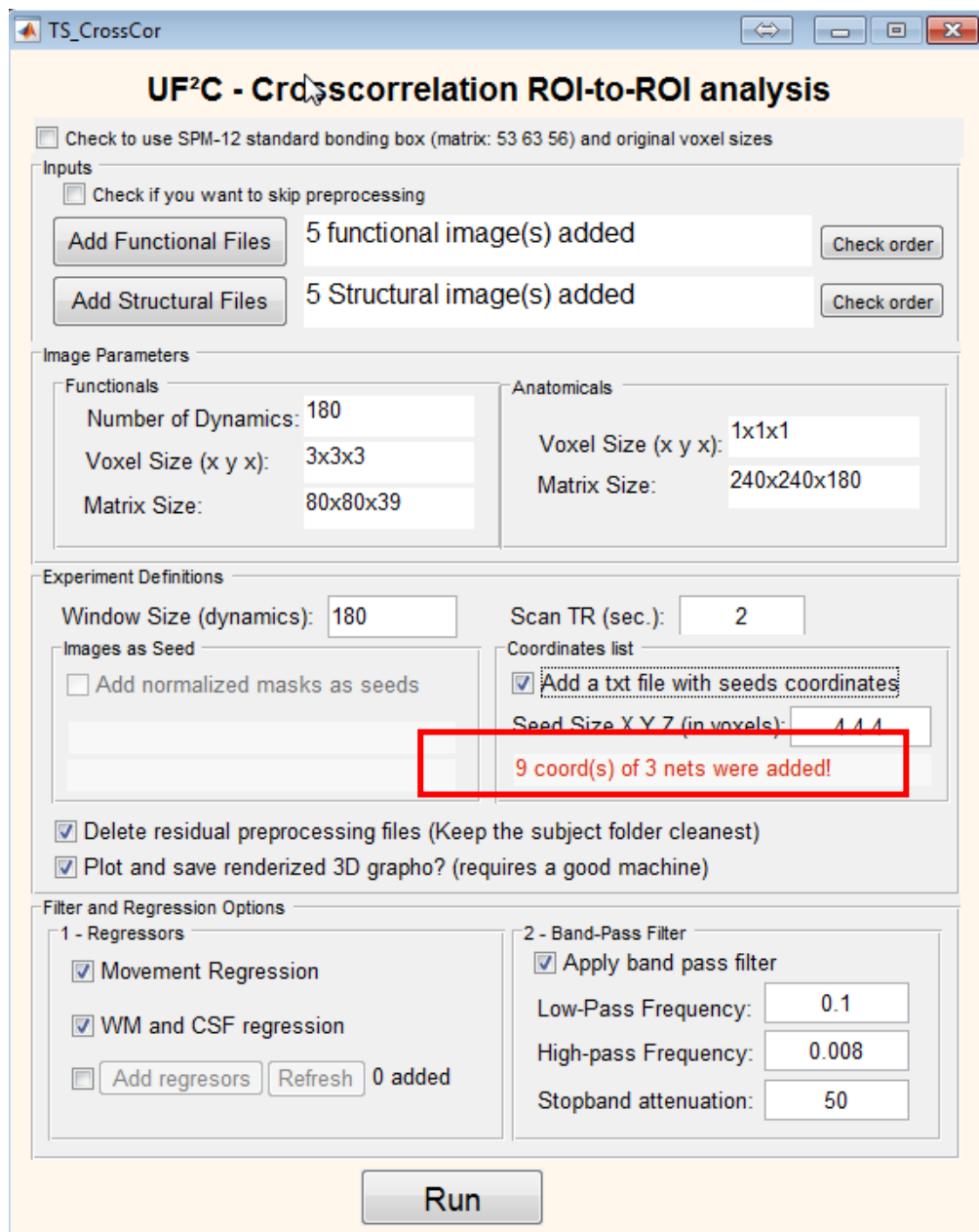
Arquivo  Editar  Formatar  Exibir  Ajuda
01: 0 -51 32
01: 23 -51 32
01: -23 -51 32
02: 10 51 15
02: -10 51 15
02: 0 40 15
03: 30 -20 10
03: -30 -20 10
03: 10 -20 30

```

Considering this coordinate file, UF²C will identify 9 ROIs from 3 networks:

Network 1: 01; Network 2: 02; Network 3: 03.

The UF²C GUI will show:



UF²C - Crosscorrelation ROI-to-ROI analysis

Check to use SPM-12 standard bonding box (matrix: 53 63 56) and original voxel sizes

Inputs

Check if you want to skip preprocessing

Add Functional Files: 5 functional image(s) added [Check order]

Add Structural Files: 5 Structural image(s) added [Check order]

Image Parameters

Functionals

Number of Dynamics: 180

Voxel Size (x y x): 3x3x3

Matrix Size: 80x80x39

Anatomicals

Voxel Size (x y x): 1x1x1

Matrix Size: 240x240x180

Experiment Definitions

Window Size (dynamics): 180

Scan TR (sec.): 2

Images as Seed

Add normalized masks as seeds

Coordinates list

Add a txt file with seeds coordinates

Seed Size X Y Z (in voxels): 4 4 4

9 coord(s) of 3 nets were added!

Delete residual preprocessing files (Keep the subject folder cleanest)

Plot and save rendered 3D grapho? (requires a good machine)

Filter and Regression Options

1 - Regressors

Movement Regression

WM and CSF regression

Add regresors [Refresh] 0 added

2 - Band-Pass Filter

Apply band pass filter

Low-Pass Frequency: 0.1

High-pass Frequency: 0.008

Stopband attenuation: 50

Run

The checkbox "**Delete residual preprocessing files**" gives you the option to save all the processing files or just the final version of each post processed file. By checking this box the program will just save the:

- realignment parameters (rp_*.txt file)
- modulated-normalized-smoothed functional file (sw*.nii file)
- regressed-filtered functional file (FiltRegrSW*.nii)
- modulated-normalized structural file (wm*.nii file).

Filter and Regression Option

The same described on the "Preprocessing Only" Routine.

b) – Second Level analysis (Group inference)

The screenshot shows the 'CrossCorSecLe' software interface for 'UF²C - Crosscorrelation ROI analysis' at the 'Second Level'. The window title is 'CrossCorSecLe'. The main title is 'UF²C - Crosscorrelation ROI analysis' with 'Second Level' in red below it. The interface is divided into several sections:

- Input files:** Contains buttons for 'Add Group 1 file', 'Add Group 2 file', and 'Output Directory'. To the right is a 'Groups Names' table with 'Group 1' and 'Group 2'.
- Nodes:** Contains radio buttons for 'Seeds with ROI files' (selected) and 'Seeds with coordinate list', and an 'Add ROIs images' button.
- Statistical Parameters:** Contains radio buttons for 'Two Sample t-test' (selected) and 'Paired t-test'.
- Corrections:** Contains checkboxes for 'Uncorrected comparison' and 'FDR corrected comparison' (checked), and P-value threshold input fields set to 0.01 and 0.05.
- Outputs (If you add network pair-wise .mat files, uncheck the Graphos outputs):** Contains checkboxes for 'Correlation Matrices', '2D Graphos', and '3D Graphos' (all checked).

A 'Run' button is located at the bottom of the interface.

This modality enables the analysis of group inference with the results of the first level analysis (a).

To do this, some **conditions** should be respected:

1. In the first level analysis (a), you need to add all images (fMRIS and T1s) of a group (Controls group for example) at the same time (running process). This procedure, will create a general (group) resultant file called "**All_Subjs-VAR.mat**" inside the general folder "**Total_Log_*DATE/TIME***". This Matlab file will contain a **NxNxS matrix**, where **N** is the number of ROIs added in the first level analysis and **S** the number of subjects included for this group. **You need to have the All_Subjs-VAR.mat of at least two groups to perform the second level analysis, and these All_Subjs-VAR.mat needs to contain the information of all subjects of each group.**
2. You need to use the same number of ROIs for all groups in the first level analysis to be able to compute the group comparison between them. So, in the **NxNxS matrix, the N should to be the same in both files (same number of ROIs) although the S (number of subjects) may differ between groups.**
3. Before adding the **All_Subjs-VAR.mat** to the second level analysis modality, is strongly recommended to convert the **All_Subjs-VAR.mat** from r-score to z-score. You can use the **UF²C tool R-score to Z-score Transf.** to do that, creating the **Z_Transf_All_Subjs-VAR.mat file** that is ready to be added.

Input Files

In this panel, you can add group 1 and group 2 **Z_Transf_All_Subjs-VAR.mat** files clicking on the buttons "**Add Group 1 file**" and "**Add Group 2 file**". In the text box from the field "**Groups Names**" you can change the name of the groups, modifying how they will be shown in the results.

In the panel "**Nodes**", you should add the same ROIs files ("**Seeds with ROI files**") or the same text file ("**Seeds with coordinate list**") that you used on the first level analysis, respecting the condition

2.

Statistical Parameters

In this panel, you can first choose if your test is transversal ("**two Samples t-test**") or longitudinal ("**Paired t-test**"). In the sub panel corrections, you will be able to set the alpha levels ("**P-value threshold**") of your tests, choosing between "**Uncorrected comparisons**", "**FDR corrected comparison**" or both.

To correct for Bonferroni, you just need to compute the number of multiple comparisons applied and change the uncorrected alpha ("**P-value threshold**").

How to compute the number of dependent tests?

$$\text{NofTests} = \frac{((N \times N) - N)}{2}$$

Where **N** is the number of ROIs used. So, if you used 100 ROIs, the number of multiple tests would be:

$$\text{NofTests} = \frac{((100 \times 100) - 100)}{2}$$

$$\text{NofTests} = \frac{(10000 - 100)}{2}$$

$$\text{NofTests} = \frac{(9900)}{2}$$

$$\text{NofTests} = 4950$$

The alpha to correct by the Bonferroni methodology would be:

$$\text{Bonferroni}_{\text{Alpha}} = \frac{0.05}{4950} = 1,01 \times 10^{-5}$$

Very restrictive!

Add a covariate file

If you selected the “**two Samples t-test**”, you will be able to add covariates to the analysis, converting the statistical approach to an ANCOVA. To do this, you need to create a text file (*.txt) with columns that represent the covariates, and lines that represent the volunteers:

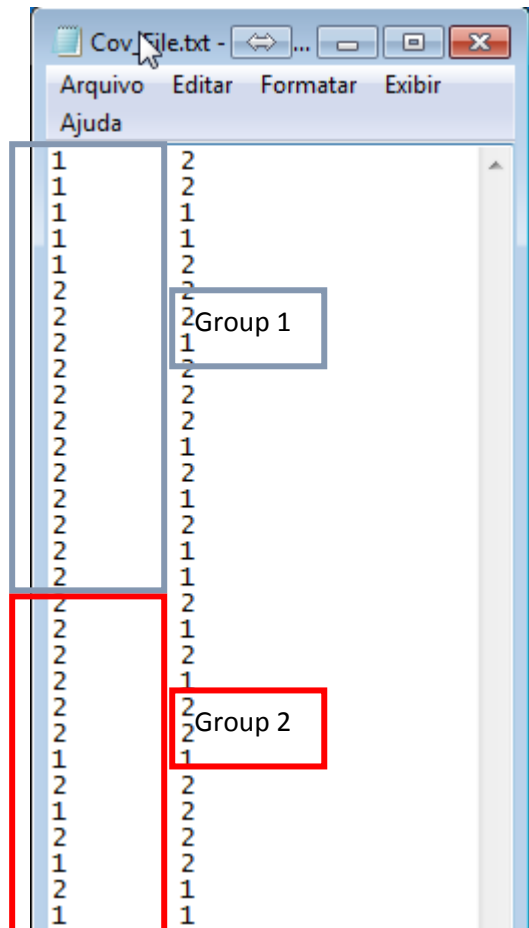


Figure: This figure represents a text file with 2 covariates (2 columns). In this example, we can see 30 rows divided into the two groups.

IMPORTANT: The order of the covariates should be the same as the order of each group added (Group 1 and 2), as well as the subject order inside each group. This is similar to the covariate option on the SPM interface.

13. Modality 3 – Sliding Windows Connectivity

UF²C - User Friendly Functional Connectivity

Inputs

Add Functional Files

Add Structural Files

Image Parameters

Functionals

Number of Dynamics:

Voxel Size (x y x):

Matrix Size:

Anatomicals

Voxel Size (x y x):

Matrix Size:

Experiment Definitions

Delete residual preprocessing files (Keep the subject folder cleanest)

Sliding Window size (dynamics): **Seed Size X Y Z (in voxels):**

Seed (ROI) Coordinate (MNI): **Scan TR (sec.):**

Filter and Regression Options

Band-Pass Filter

Apply band pass filter

Low-Pass Frequency:

High-pass Frequency:

Stopband attenuation:

Regressors

Movement Regression

WM and CSF regression

Add regressors

Inputs

The same described on the **Preprocessing Routine**.

Image Parameters

The same described on the **Preprocessing Routine**.

Experiment Definitions

The options "**Delete residual preprocessing files**" and "**Window Size (Dynamics)**" have the same functions as described on the **modality 1 section**.

The sliding window analysis performs a correlation between a seed defined by a coordinate (“**Seed (ROI) Coordinate (MNI)**”) and all cortical voxels. These correlations are calculated by each windows separately. The windows sizes are define in the “**Sliding Window size (dynamics)**” option. The final number of correlations are found by subtracting from the total number of volumes (dynamics, time points...) and the size of the time window (user defined). UF²C will generate graphics and a 4D image for each volunteer, in which the 4th dimension is the 3D correlation maps of each windows position.

The correlation window moves throughout the time series with a step of 1 time point.

The “**Seed Size**” is implemented equal to what is described in **Modality 1**.

Filter and Regression Option

The same described on the **Preprocessing Routine**.

14. Some considerations about “time series extraction”

15. Time-series are consistently extracted from each ROI of each subject. For a specific ROI, we used the average time series of all ROI voxels that matched two consecutive criteria:

- a. Being included in the subject GM mask;
- b. The UF2C correlates each single ROI voxel time series with the average ROI time series (GM-masked). The voxel will be included on the ROI mask (and to the average) if its correlation value is higher than the average minus the standard deviation of all correlations between the ROI-masked voxels;

16. This methodology was described on “**de Campos, B. M., Coan, A. C., Lin Yasuda, C., Casseb, R. F. and Cendes, F. (2016), Large-scale brain networks are distinctly affected in right and left mesial temporal lobe epilepsy. Hum. Brain Mapp., 37: 3137–3152**”.

17. An example of the effectiveness of this methodology in exclude residual non-GM voxels, or non-functionally representative tissues can be seen in the following example:

18. We performed an analysis using a **left-hippocampus** ROI, from the Shirer ROIs (**Shirer WR, Ryali S, Rykhlevskaia E, Menon V, Greicius MD (2012): Decoding subject-driven cognitive states with wholebrain connectivity patterns. Cereb Cortex. 22(1):158–165**). The subject included was a temporal lobe epilepsy patient, with left-hippocampus sclerosis. The hippocampus sclerosis may results in GM atrophy and gliosis:

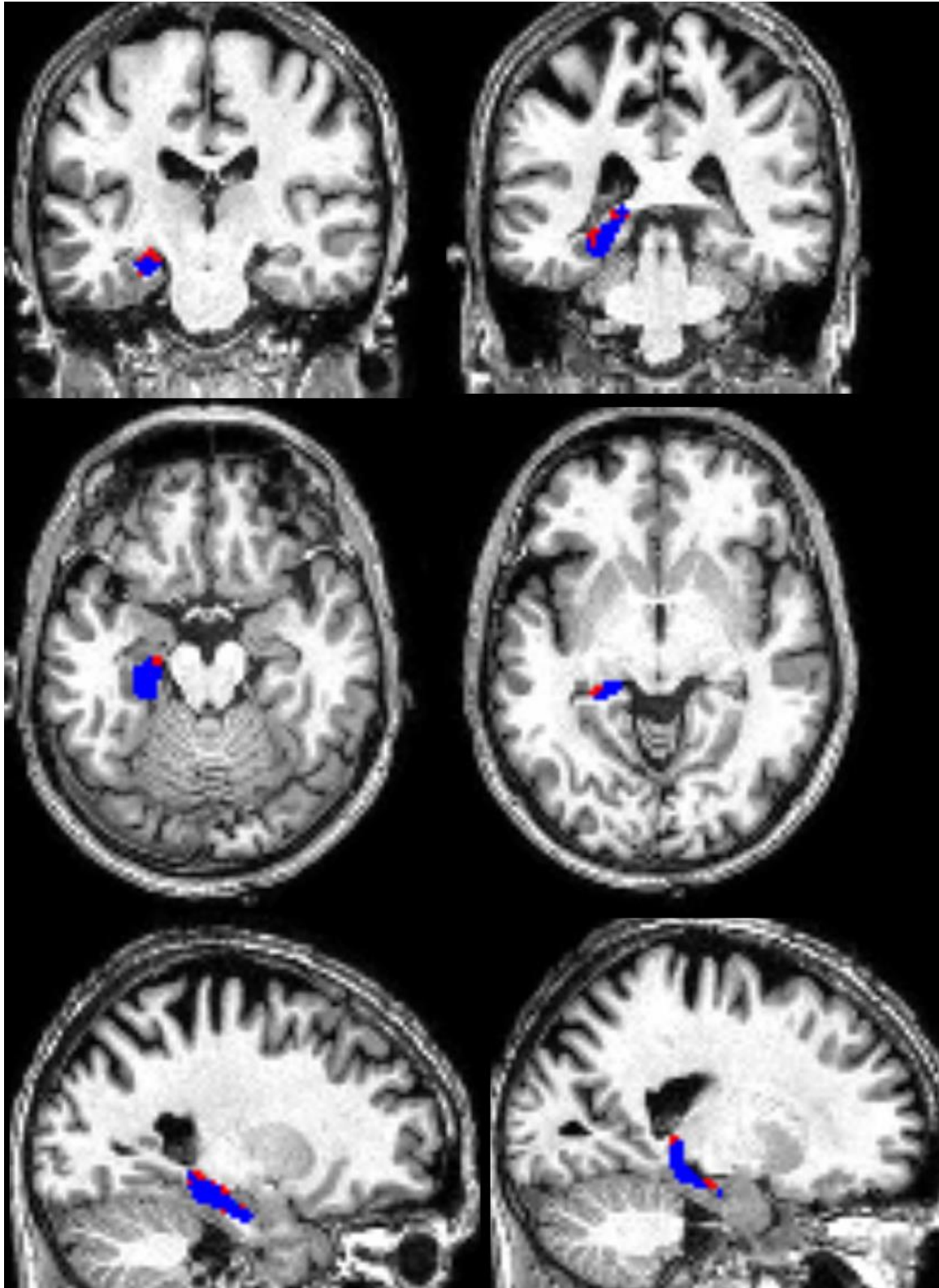


Figure: The ROI regions (shown in blue) that were included on the analysis and the voxels (shown in red) from the ROI (grey matter masked [criteria a.]) that was automatically excluded. The red voxels were excluded AFTER survive to the GM masking (criteria a.), throughout the criteria b. This result shows the effectiveness of the combined criteria a. and b. to provide a refined ROI mask and a consequently a reliable ROI average time series.

ANEXOS

ANEXO 1: OS DOCUMENTOS DE APROVAÇÃO NO COMITÊ DE ÉTICA DA UNICAMP



Universidade Estadual de Campinas
Departamento de Neurologia

Campinas, 28 de abril de 2016

Comitê de Ética em Pesquisa
FCM - UNICAMP

Re: **"Conectividade Funcional e Estrutural em Pacientes com Epilepsia Focal"** – Projeto de Doutorado do aluno **Brunno Machado de Campos**

Prezado Prof. Dr. Marcondes França Júnior,

Este projeto é conduzido em paralelo com o projeto *"Análise da Relação entre Expressão de Vias Inflamatórias Sistêmicas, Epileptogênese e Atrofia Cerebral nas Epilepsias Parciais"* – Prof. Dr. Fernando Cendes.

As análises da RM do projeto de Doutorado acima são realizadas em imagens arquivadas em formato digital para os fins desta pesquisa, conforme Formulário De Consentimento Livre E Esclarecido já aprovado no Comitê de Ética em Pesquisa da UNICAMP (**parecer Nº 1158/2009**).

Desta forma, solicitamos dispensa de solicitação de novo Termo de Consentimento Livre e Esclarecido.

Sem mais no momento, agradeço vossa atenção e subscrevo-me,

Prof. Dr. Fernando Cendes,
Departamento de Neurologia,
Coordenador do Laboratório de Neuroimagem;
Faculdade de Ciências Médicas
UNICAMP



FACULDADE DE CIÊNCIAS MÉDICAS
COMITÊ DE ÉTICA EM PESQUISA

www.fcm.unicamp.br/pesquisa/etica/index.html

CEP, 01/03/10
(Grupo III)

PARECER CEP: N° 1158/2009 (Este n° deve ser citado nas correspondências referente a este projeto)
CAAE: 0893.0.146.000-09

I - IDENTIFICAÇÃO:

PROJETO: “ANÁLISE DA RELAÇÃO ENTRE EXPRESSÃO DE VIAS INFLAMATÓRIAS SISTÊMICAS, EPILEPTOGÊNESE E ATROFIA CEREBRAL NAS EPILEPSIAS PARCIAIS”.

PESQUISADOR RESPONSÁVEL: Fernando Cendes

INSTITUIÇÃO: Hospital das Clínicas/UNICAMP

APRESENTAÇÃO AO CEP: 02/12/2010

II - OBJETIVOS

Desenvolver um estudo multidisciplinar em epilepsia parcial em larga escala, com outras instituições de pesquisa brasileira com um grande número de pacientes que apresenta epilepsia de tipo parcial, para analisar características clínicas, de imagem e perfil inflamatório. A investigação pretende captar as relações entre características clínicas, de imagem e marcadores de inflamação no sangue, chamados citosinas.

III - SUMÁRIO

Trata-se de um estudo prospectivo com inclusão de pacientes com epilepsia submetidos a tratamento clínico e cirúrgico. Para fins de controle, indivíduos assintomáticos, sem doenças clínico-neurológicas, pareados por gênero e idade, serão convidados a participar de uma avaliação clínica e posterior dosagem de marcadores plasmáticos e exame de neuroimagem. Serão incluídos no estudo 350 pacientes acima de 12 anos, com diagnóstico clínico e eletroencefálico de Epilepsia focal temporal ou extratemporal, ELT: RM com atrofia hipocampal unilateral ou bilateral, evidências de patologia estrutural (tumores; lesões vasculares, gliose), ou sem alterações à análise visual. Os pacientes serão recrutados nos Ambulatórios de Epilepsia do Hospital das Clínicas/UNICAMP. Os controles serão recrutados entre funcionários (e seus familiares) da Universidade. Os pacientes serão submetidos ao tratamento cirúrgico conforme rotina de serviço. Serão acompanhados de eletrocorticografia e estimulação cortical quando necessárias. As cirurgias serão realizadas pela equipe de Cirurgia de Epilepsia e o tecido histológico analisado. O tempo de observação de cada paciente será de 12 a 48 meses.

IV - COMENTÁRIOS DOS RELATORES

Projeto com formulação adequada. O Termo de Consentimento Livre e Esclarecido está bem redigido. É necessário esclarecimento em relação às crianças entre 12-18 anos que participarão do projeto. Adequação do Termo de Consentimento Livre e Esclarecido para assinatura do responsável do menor. Na Folha de Rosto/CONEP, onde constam os dados da

Comitê de Ética em Pesquisa - UNICAMP
Rua: Tessália Vieira de Camargo, 126
Caixa Postal 6111
13083-887 Campinas - SP

FONE (019) 3521-8936
FAX (019) 3521-7187
cep@fcm.unicamp.br



**FACULDADE DE CIÊNCIAS MÉDICAS
COMITÊ DE ÉTICA EM PESQUISA**

www.fcm.unicamp.br/pesquisa/etica/index.html

instituição onde serão coletados os dados, está escrito que este projeto não é multicêntrico, mas na descrição do mesmo o pesquisador coloca o projeto como multidisciplinar e inter-institucional. Solicita-se esclarecimento do pesquisador. A Folha de Rosto/CONEP deve ser assinada pelo superintendente do Hospital das Clínicas/UNICAMP e não pelo Diretor da FCM.

V - PARECER DO CEP

O Comitê de Ética em Pesquisa da Faculdade de Ciências Médicas da UNICAMP, de acordo com as atribuições definidas na Resolução CNS 196/96 e suas complementares, manifesta-se por aguardar o atendimento às questões acima para emissão do seu parecer final.

SITUAÇÃO: projeto com pendências

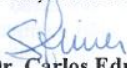
- ✓ *** As pendências deverão ser respondidas preferencialmente no prazo de 10 dias, a partir da data de envio pelo CEP/FCM.**
- ✓ **A resposta deve ser encaminhada pelo Protocolo da FCM em envelope fechado e acompanhado por fora do Formulário de Encaminhamento de Outros Documentos, disponível no site do CEP.**
- ✓ **Projetos de Grupo II e III deverão vir em 01 via e de Grupo I em 02 vias.**

* Quando após 60 dias de ter recebido um parecer pendente, o pesquisador não se manifestar quanto aos quesitos apresentados pelo CEP em seu parecer o projeto será considerado retirado e posteriormente havendo interesse, deverá ser apresentado novo protocolo e reiniciado o processo de registro (Res. CNS 196/96).

O conteúdo e as conclusões aqui apresentados são de responsabilidade exclusiva do CEP/FCM/UNICAMP e não representam a opinião da Universidade Estadual de Campinas nem a comprometem.

VI - DATA DA REUNIÃO

II Reunião Ordinária do CEP/FCM, em 23 de fevereiro de 2010.


Prof. Dr. Carlos Eduardo Steiner
PRESIDENTE DO COMITÊ DE ÉTICA EM PESQUISA
FCM/UNICAMP

ANEXO 2: TERMO DE CONSENTIMENTO LIVRE ESCLARECIDO

FORMULÁRIO DE CONSENTIMENTO PARA PESQUISA MÉDICA, *Página 1 de 3*

Título do projeto: A Neuroimagem nas Epilepsias

Investigador principal: Dr. Fernando Cendes

OBJETIVO DA PESQUISA:

Eu _____ entendo que fui convidado (a) a participar em um projeto de pesquisa envolvendo pacientes com epilepsia. O objetivo geral do estudo é o de determinar a utilidade da Imagem e Espectroscopia por Ressonância Magnética para identificar e quantificar alterações estruturais e metabólicas do sistema nervoso central. A identificação e quantificação dessas anormalidades no cérebro, pode eventualmente melhorar o diagnóstico e levar a um melhor tratamento dessa doença. As informações médicas a meu respeito que forem obtidas para esse estudo, poderão ser compartilhadas com outros pesquisadores que trabalham com epilepsia. Podendo assim ser utilizadas eventualmente para outros fins de pesquisa sobre as epilepsias. O sigilo será mantido em todos os estudos colaborativos através da utilização de um número de código para a identificação dos indivíduos participantes.

A ressonância magnética é uma técnica capaz de produzir imagens de alta qualidade e resolução (nitidez) anatômica, assim como informações sobre a bioquímica dos tecidos. A ressonância magnética produz imagens em cortes que são parecidos com as imagens produzidas pela tomografia computadorizada, porém com maior resolução (nitidez) e sem a exposição aos raios X. Essas imagens também irão produzir informações bioquímicas que serão úteis para melhor definição do diagnóstico e tratamento. O objetivo principal desse estudo é determinar a importância dessas informações bioquímicas e estruturais.

PROCEDIMENTO:

Eu entendo que se concordar em participar desse estudo, os pesquisadores participantes farão perguntas a respeito dos meus antecedentes médicos e de minha família. Eu serei submetido a um exame físico neurológico para estabelecer meu estado clínico. Além disso, poderei ser submetido a um eletroencefalograma (EEG) além dos exames de ressonância magnética. Hospitalização não será necessária.

O procedimento de ressonância magnética é semelhante a uma tomografia. Eu fui informado que eu serei colocado em uma maca e serei movido lentamente para dentro do aparelho de ressonância magnética. Um alto falante dentro do campo magnético possibilita a minha constante comunicação com as pessoas responsáveis pelo exame. Durante todo o tempo o pessoal médico e paramédico pode me ver e ouvir, e eu posso ser removido(a) se for preciso. O procedimento pode durar entre 45 a 90 minutos. Durante a primeira parte do exame eu irei ouvir ruídos, tipo marteladas, por alguns minutos enquanto o aparelho faz as imagens do meu cérebro. O restante do exame será relativamente silencioso.

VANTAGENS:

Eu entendo que não obterei nenhuma vantagem direta com a minha participação nesse estudo e que o meu diagnóstico e o meu tratamento provavelmente não serão modificados. Contudo, os resultados desse estudo podem, a longo prazo, oferecer vantagens para os indivíduos com epilepsia, possibilitando um melhor diagnóstico e um tratamento mais adequado. Os resultados do meu exame de ressonância magnética ficarão a disposição dos médicos responsáveis pelo meu tratamento, e poderão ser úteis no futuro.

FORMULÁRIO DE CONSENTIMENTO PARA PESQUISA MÉDICA, *Página 2 de 3*

Título do projeto: A neuroimagem nas epilepsias parciais.

Investigador principal: Dr. Fernando Cendes

RISCO E DESCONFORTO:

O único desconforto relacionado a este exame é o ruído intermitente durante os primeiros 15 minutos. Depois disso o ruído será muito menor. O pessoal técnico providenciará tapa-ouvidos para me deixar mais confortável.

Uma das principais vantagens da ressonância magnética é que esta não utiliza raios X ou outro tipo de radiação ionizante, ao contrário de outros tipos de exame radiológicos. As imagens são obtidas graças a um campo magnético (imã), um transmissor e receptor de ondas de rádio e um computador que é utilizado para obter as informações bioquímicas e imagens da anatomia interna. Não existem efeitos nocivos associados com a ressonância magnética dentro das condições utilizadas atualmente.

REQUERIMENTOS

É **muito importante** informar aos médicos(as) e técnicos(as) caso eu tenha um **marca-passo cardíaco, um clipe de cirurgia para aneurisma cerebral ou qualquer outro objeto metálico em meu corpo**, que tenha sido implantado durante uma cirurgia ou alojado em meu corpo durante um acidente, pois estes podem parar de funcionar ou causar acidentes devido ao forte campo magnético que funciona como um imã muito forte. Eu também devo remover todos os objetos metálicos que estiverem comigo (relógio, canetas, brincos, colares, anéis, etc), pois estes também podem movimentar ou aquecer dentro do campo magnético.

SIGILO:

Eu entendo que todas as informações médicas decorrentes desse projeto de pesquisa farão parte do meu prontuário médico e serão submetidos aos regulamentos do HC- UNICAMP referentes ao sigilo da informação médica. Se os resultados ou informações fornecidas forem utilizados para fins de publicação científica, nenhum nome será utilizado.

FORNECIMENTO DE INFORMAÇÃO ADICIONAL:

Eu entendo que posso requisitar informações adicionais relativas ao estudo a qualquer momento. O Dr. Fernando Cendes, tel (019) 3521-9217 estará disponível para responder minhas questões e preocupações. Em caso de recurso, dúvidas ou reclamações contactar a secretaria da Comissão de Ética da Faculdade de Ciências Médicas-UNICAMP, tel. (019) 3521-7232.

RECUSA OU DESCONTINUAÇÃO DA PARTICIPAÇÃO:

Eu entendo que a minha participação é voluntária e que eu posso me recusar a participar ou retirar meu consentimento e interromper a minha participação no estudo a qualquer momento sem comprometer os cuidados médicos que recebo atualmente ou receberei no futuro no HC- UNICAMP. Eu reconheço também que o Dr. Fernando Cendes pode interromper a minha participação nesse estudo a qualquer momento que julgar apropriado.

FORMULÁRIO DE CONSENTIMENTO PARA PESQUISA MÉDICA, *Página 3 de 3*

Título do projeto: A neuroimagem nas epilepsias parciais.

Investigador principal: Dr. Fernando Cendes

Eu confirmo que o(a) Dr(a). _____

me explicou o objetivo do estudo, os procedimentos aos quais serei submetido e os riscos, desconforto e possíveis vantagens advindas desse projeto de pesquisa. Eu li e compreendi esse formulário de consentimento e estou de pleno acordo em participar desse estudo.

Nome do participante ou responsável

Assinatura do participante ou responsável

data

Nome da testemunha

Assinatura da testemunha

data

RESPONSABILIDADE DO PESQUISADOR:

Eu expliquei a _____ o objetivo do estudo, os procedimentos requeridos e os possíveis riscos e vantagens que poderão advir do estudo, usando o melhor do meu conhecimento. Eu me comprometo a fornecer uma cópia desse formulário de consentimento ao participante ou responsável.

Nome do pesquisador ou associado

Assinatura do pesquisador ou associado

data

ANEXO 3: PERMISSÕES EDITORIAIS

ARTIGO 1

JOHN WILEY AND SONS LICENSE TERMS AND CONDITIONS

Aug 23, 2016

This Agreement between Brunno M. de Campos ("You") and John Wiley and Sons ("John Wiley and Sons") consists of your license details and the terms and conditions provided by John Wiley and Sons and Copyright Clearance Center.

License Number 3934810509476
 License date Aug 23, 2016
 Licensed Content Publisher John Wiley and Sons
 Licensed Content Publication Epilepsia

Licensed Content Title White matter abnormalities associate with type and localization of focal epileptogenic lesions

Licensed Content Author Brunno M. Campos, Ana C. Coan, Guilherme C. Beltramini, Min Liu, Clarissa L. Yassuda, Enrico Ghizoni, Christian Beaulieu, Donald W.

Licensed Content Date Gross, Fernando Cendes
Dec 26, 2014

Licensed Content Pages 8

Type of use Dissertation/Thesis

Requestor type Author of this Wiley article

Format Print and electronic

Portion Full article

Will you be translating? No

Title of your thesis / dissertation CONECTIVIDADE FUNCIONAL E ESTRUTURAL EM PACIENTES COM EPILEPSIA FOCAL

Expected completion date Nov 2016

Expected size (number of pages) 150

Requestor Location Brunno M. de Campos
Cidade Universitária Zeferino Vaz
R. Vital Brasil, 251
Campinas, São Paulo 13083-888, Brazil
Attn: Brunno M. de Campos

Publisher Tax ID EU826007151

Billing Type Invoice

Billing Address Brunno M. de Campos
Cidade Universitária Zeferino Vaz
R. Vital Brasil, 251
Campinas, Brazil 13083-888
Attn: Brunno M. de Campos

Total 0.00 USD
[Terms and Conditions](#)

TERMS AND CONDITIONS

This copyrighted material is owned by or exclusively licensed to John Wiley & Sons, Inc. or one of its group companies (each a "Wiley Company") or handled on behalf of a society with which a Wiley Company has exclusive publishing rights in relation to a particular work (collectively "WILEY"). By clicking "accept" in connection with completing this licensing transaction, you agree that the following terms and conditions apply to this transaction (along with the billing and payment terms and conditions established by the Copyright Clearance Center Inc., ("CCC's Billing and Payment terms and conditions"), at the time that you opened your RightsLink account (these are available at any time at <http://myaccount.copyright.com>).

Terms and Conditions

- The materials you have requested permission to reproduce or reuse (the "Wiley Materials") are protected by copyright.
- You are hereby granted a personal, non-exclusive, non-sub licensable (on a standalone basis), non-transferable, worldwide, limited license to reproduce the Wiley Materials for the purpose specified in the licensing process. This license, and any CONTENT (PDF or image file) purchased as part of your order, is for a one-time use only and limited to any maximum distribution number specified in the license. The first instance of republication or reuse granted by this license must be completed within two years of the date of the grant of this license (although copies prepared before the end date may be distributed thereafter). The Wiley Materials shall not be used in any other manner or for any other purpose, beyond what is granted in the license. Permission is granted subject to an appropriate acknowledgement given to the author, title of the material/book/journal and the publisher. You shall also duplicate the copyright notice that appears in the Wiley publication in your use of the Wiley Material. Permission is also granted on the understanding that nowhere in the text is a previously published source acknowledged for all or part of this Wiley Material. Any third party content is expressly excluded from this permission.
- With respect to the Wiley Materials, all rights are reserved. Except as expressly granted by the terms of the license, no part of the Wiley Materials may be copied, modified, adapted (except for minor reformatting required by the new Publication), translated, reproduced, transferred or distributed, in any form or by any means, and no derivative works may be made based on the Wiley Materials without the prior permission of the respective copyright owner. For STM Signatory Publishers clearing permission under the terms of the STM Permissions Guidelines only, the terms of the license are extended to include subsequent editions and for editions in other languages, provided such editions are for the work as a whole in situ and does not involve the separate exploitation of the permitted figures or extracts, You may not alter, remove or suppress in any manner any copyright, trademark or other notices displayed by the Wiley Materials. You may not license, rent, sell, loan, lease, pledge, offer as security, transfer or assign the Wiley Materials on a stand-alone basis, or any of the rights granted to you hereunder to any other person.
- The Wiley Materials and all of the intellectual property rights therein shall at all times remain the exclusive property of John Wiley & Sons Inc, the Wiley Companies, or their respective licensors, and your interest therein is only that of having possession of and the right to reproduce the Wiley Materials pursuant to Section 2 herein during the continuance of this Agreement. You agree that you own no

right, title or interest in or to the Wiley Materials or any of the intellectual property rights therein. You shall have no rights hereunder other than the license as provided for above in Section 2. No right, license or interest to any trademark, trade name, service mark or other branding ("Marks") of WILEY or its licensors is granted hereunder, and you agree that you shall not assert any such right, license or interest with respect thereto

- NEITHER WILEY NOR ITS LICENSORS MAKES ANY WARRANTY OR REPRESENTATION OF ANY KIND TO YOU OR ANY THIRD PARTY, EXPRESS, IMPLIED OR STATUTORY, WITH RESPECT TO THE MATERIALS OR THE ACCURACY OF ANY INFORMATION CONTAINED IN THE MATERIALS, INCLUDING, WITHOUT LIMITATION, ANY IMPLIED WARRANTY OF MERCHANTABILITY, ACCURACY, SATISFACTORY QUALITY, FITNESS FOR A PARTICULAR PURPOSE, USABILITY, INTEGRATION OR NON-INFRINGEMENT AND ALL SUCH WARRANTIES ARE HEREBY EXCLUDED BY WILEY AND ITS LICENSORS AND WAIVED BY YOU.
- WILEY shall have the right to terminate this Agreement immediately upon breach of this Agreement by you.
- You shall indemnify, defend and hold harmless WILEY, its Licensors and their respective directors, officers, agents and employees, from and against any actual or threatened claims, demands, causes of action or proceedings arising from any breach of this Agreement by you.
- IN NO EVENT SHALL WILEY OR ITS LICENSORS BE LIABLE TO YOU OR ANY OTHER PARTY OR ANY OTHER PERSON OR ENTITY FOR ANY SPECIAL, CONSEQUENTIAL, INCIDENTAL, INDIRECT, EXEMPLARY OR PUNITIVE DAMAGES, HOWEVER CAUSED, ARISING OUT OF OR IN CONNECTION WITH THE DOWNLOADING, PROVISIONING, VIEWING OR USE OF THE MATERIALS REGARDLESS OF THE FORM OF ACTION, WHETHER FOR BREACH OF CONTRACT, BREACH OF WARRANTY, TORT, NEGLIGENCE, INFRINGEMENT OR OTHERWISE (INCLUDING, WITHOUT LIMITATION, DAMAGES BASED ON LOSS OF PROFITS, DATA, FILES, USE, BUSINESS OPPORTUNITY OR CLAIMS OF THIRD PARTIES), AND WHETHER OR NOT THE PARTY HAS BEEN ADVISED OF THE POSSIBILITY OF SUCH DAMAGES. THIS LIMITATION SHALL APPLY NOTWITHSTANDING ANY FAILURE OF ESSENTIAL PURPOSE OF ANY LIMITED REMEDY PROVIDED HEREIN.
- Should any provision of this Agreement be held by a court of competent jurisdiction to be illegal, invalid, or unenforceable, that provision shall be deemed amended to achieve as nearly as possible the same economic effect as the original provision, and the legality, validity and enforceability of the remaining provisions of this Agreement shall not be affected or impaired thereby.
- The failure of either party to enforce any term or condition of this Agreement shall not constitute a waiver of either party's right to enforce each and every term and condition of this Agreement. No breach under this agreement shall be deemed waived or excused by either party unless such waiver or consent is in writing signed by the party granting such waiver or consent. The waiver by or consent of a party to a breach of any provision of this Agreement shall not operate or be construed as a waiver of or consent to any other or subsequent breach by such other party.
- This Agreement may not be assigned (including by operation of law or otherwise) by you without WILEY's prior written consent.
- Any fee required for this permission shall be non-refundable after thirty (30) days from receipt by the CCC.
- These terms and conditions together with CCC's Billing and Payment terms and conditions (which are incorporated herein) form the entire agreement between you and WILEY concerning this licensing transaction and (in the absence of fraud) supersedes all prior agreements and representations of the parties, oral or written. This Agreement may not be amended except in writing signed by both parties. This Agreement shall be binding upon and inure to the benefit of the parties' successors, legal representatives, and authorized assigns.

- In the event of any conflict between your obligations established by these terms and conditions and those established by CCC's Billing and Payment terms and conditions, these terms and conditions shall prevail.
- WILEY expressly reserves all rights not specifically granted in the combination of (i) the license details provided by you and accepted in the course of this licensing transaction, (ii) these terms and conditions and (iii) CCC's Billing and Payment terms and conditions.
- This Agreement will be void if the Type of Use, Format, Circulation, or Requestor Type was misrepresented during the licensing process.
- This Agreement shall be governed by and construed in accordance with the laws of the State of New York, USA, without regards to such state's conflict of law rules. Any legal action, suit or proceeding arising out of or relating to these Terms and Conditions or the breach thereof shall be instituted in a court of competent jurisdiction in New York County in the State of New York in the United States of America and each party hereby consents and submits to the personal jurisdiction of such court, waives any objection to venue in such court and consents to service of process by registered or certified mail, return receipt requested, at the last known address of such party.

WILEY OPEN ACCESS TERMS AND CONDITIONS

Wiley Publishes Open Access Articles in fully Open Access Journals and in Subscription journals offering Online Open. Although most of the fully Open Access journals publish open access articles under the terms of the Creative Commons Attribution (CC BY) License only, the subscription journals and a few of the Open Access Journals offer a choice of Creative Commons Licenses. The license type is clearly identified on the article.

The Creative Commons Attribution License

The Creative Commons Attribution License (CC-BY) allows users to copy, distribute and transmit an article, adapt the article and make commercial use of the article. The CC-BY license permits commercial and non-

Creative Commons Attribution Non-Commercial License

The Creative Commons Attribution Non-Commercial (CC-BY-NC) License permits use, distribution and reproduction in any medium, provided the original work is properly cited and is not used for commercial purposes. (see below)

Creative Commons Attribution-Non-Commercial-NoDerivs License

The Creative Commons Attribution Non-Commercial-NoDerivs License (CC-BY-NC-ND) permits use, distribution and reproduction in any medium, provided the original work is properly cited, is not used for commercial purposes and no modifications or adaptations are made. (see below)

Use by commercial "for-profit" organizations

Use of Wiley Open Access articles for commercial, promotional, or marketing purposes requires further explicit permission from Wiley and will be subject to a fee. Further details can be found on Wiley Online Library <http://olabout.wiley.com/WileyCDA/Section/id-410895.html> Other Terms and Conditions: v1.10 Last updated September 2015

Questions? customercare@copyright.com or +1-855-239-3415 (toll free in the US) or +1-978-646-2777.

ARTIGO 2

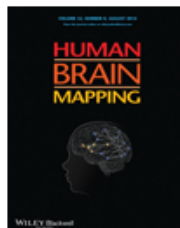


RightsLink®

Home

Account
Info

Help



Title: Large-scale brain networks are distinctly affected in right and left mesial temporal lobe epilepsy

Author: Brunno Machado de Campos, Ana Carolina Coan, Clarissa Lin Yasuda, Raphael Fernandes Casseb, Fernando Cendes

Publication: Human Brain Mapping

Publisher: John Wiley and Sons

Date: May 2, 2016

© 2016 The Authors Human Brain Mapping Published by Wiley Periodicals, Inc.

Logged in as:
Brunno M. de Campos

LOGOUT

Open Access Article

This article is available under the terms of the Creative Commons Attribution Non-Commercial License CC BY-NC (which may be updated from time to time) and permits [non-commercial](#) use, distribution and reproduction in any medium, provided the original work is properly cited.

For an understanding of what is meant by the terms of the Creative Commons License, please refer to [Wiley's Open Access Terms and Conditions](#).

Permission is not required for [non-commercial](#) reuse. For [commercial](#) reuse, please hit the "back" button and select the most appropriate [commercial](#) requestor type before completing your order.

BACK

CLOSE WINDOW

Copyright © 2016 [Copyright Clearance Center, Inc.](#) All Rights Reserved. [Privacy statement](#). [Terms and Conditions](#). Comments? We would like to hear from you. E-mail us at customer-care@copyright.com

ANEXO 4: DECLARAÇÃO

Eu, Brunno Machado de Campos, declaro não estar infringindo os direitos autorais transferidos às editoras e referentes aos artigos, figuras e tabelas incluídas nesta tese.